Fakultät für Medizin

Institut für Virologie

# Characterization of fluorescently-labeled hepatitis C virus genomes and their application to visualize the intracellular transport of viral particles

Karen Bayer

Vollständiger Abdruck der von der Fakultät für Medizin

der Technischen Universität München zur Erlangung des akademischen Grades eines

Doktors der Naturwissenschaften

genehmigten Dissertation.

Vorsitzender: Univ.-Prof. Dr. Dr. Stefan Engelhardt

Prüfer der Dissertation:

1. Univ.-Prof. Dr. Ulrike Protzer
2. apl. Prof. Dr. Johannes Beckers

Die Dissertation wurde am 24.04.2014 bei der Technischen Universität München eingereicht und durch die Fakultät für Medizin am 09.07.2014 angenommen.

# Contents

# Zusammenfassung

Ca. 150 Millionen Menschen sind chronisch mit dem Hepatitis C Virus infiziert, weshalb es eine globale gesundheitsökonomische Bedeutung hat. HCV ist ein RNA Virus mit einzelstrang Genom in positiv Orientierung, welches dem Genus *Hepacivirus* der Familie der *Flaviviridae* zugeordnet wird. Die Übertragung findet hauptsächlich über Blutkontakt statt und kann zu chronischer Leberentzündung, Fibrose und dem tödlichen Leberzellkarzinom führen. Seit der Entdeckung des Virus im Jahr 1989 hat es in der HCV Forschung bedeutende Fortschritte gegeben und vor allem die frühen Phasen der Virusvermehrung wurden intensiv untersucht. Mehrere Eintritts- und Wirtszellfaktoren wurden gefunden, die den strikten Leberzelltropismus von HCV erklären. HCV Partikel in Patientenseren und Zellkulturüberständen sind mit Lipoproteinen und Lipiden vor allem ApoE assoziiert. Aufgrund dessen sind für die HCV Anlagerung an Zellen Lipid- und Lipoprotein-spezifische Rezeptoren, wie HSPG, LDLR und SR-BI wichtig. Anschließend wird durch E2-spezifische Interaktionen mit den Rezeptoren CD81, Claudin 1 und Occludin die Aufnahme in die Zelle initiiert. Die IRES-abhängige Proteintranslation wird sofort eingeleitet und die Nichtstrukturproteine reorganisieren Membranen des ERs zum *membranous web*, in dem die Replikation stattfindet. Wo die finalen Schritte der Virusassemblierung und -ausschleusung stattfinden ist noch umstritten; einzig bekannt ist, dass sogenannte „Lipid Droplets“ eine wichtige Rolle spielen und die Umhüllung der Viruspartikel im ER stattfindet.

In dieser Arbeit wurden der Zusammenbau und der intrazelluläre Transport von HCV mit Hilfe verschiedener HCV Genome untersucht, die ein mit mCherry fluoreszenz-markiertes Oberflächenprotein E1 exprimieren (HCV JC1-E1-mCherry). Eine umfangreiche Charakterisierung dieser Konstrukte zeigte, dass die physiologische Funktion der Proteine durch den E1-mCherry-Tag nicht beeinträchtigt wird. Sowohl die Konstrukte mit den unmarkierten, wie auch die mit markierten E1-Proteinen wiesen eine ähnliche Proteinexpression und intrazelluläre Verteilung sowie vergleichbare Replikationskinetiken und Virusfreisetzung auf. Auch der korrekte Partikelzusammenbau und die Ausschleusung wurden durch Gradientenzentrifugation bestätigt. Sowohl die Strukturproteine als auch die virale RNA und ApolipoproteinE sind in derselben Fraktion angereichert, die charakteristisch für zell-freie HCV Partikel ist. Dennoch ist die Infektiosität durch das Fluorophor im E1 stark reduziert.

Durch die zusätzliche Insertion eines GFP-markierten NS5A in das HCV JC1-E1-mCherry Genom können gleichzeitig die viralen Nichtstrukturproteine und die Strukturproteine in Echtzeit mikroskopisch untersucht werden. Um die späte Phase des HCV Lebenszyklus zu untersuchen wurden HCV exprimierende Zellen über vier Tage beobachtet. Dabei wurde im Besonderen auf die

Proteinlokalisation, -assoziation und -bewegung geachtet. Die Daten zeigen, dass die Initiation der Translation in Replikationskomplexen unmittelbar nach Einschleusung des HCV RNA Genoms in die Zelle beginnt, jedoch im weiteren Zeitverlauf wieder abnimmt. Im Gegensatz dazu wird E1-mCherry kontinuierlich über die Zeit exprimiert und akkumuliert zu Komplexen die assemblierten Viruspartikeln entsprechen könnten. Im Einklang mit dieser Hypothese ist, dass die Interaktion zwischen den Strukturproteinen E1, Core und E2 im Verlauf der Replikation kontinuierlich zunimmt und mit den E1-mCherry Akkumulationen überlappt. Zudem konnte gezeigt werden, dass sich zu späteren Zeitpunkten die Struktur- und Nichtstrukturproteine voneinander trennen was dem intrazellulären Zusammenbau und Transport von Viruspartikeln entsprechen könnte.

Um den intrazellulären Partikeltransport von HCV durch *spinning disc* Mikroskopie zu untersuchen, wurde das HCV JC1-E1-mCherry Genom mit verschiedenen fluoreszenz-markierten Proteinen coexprimiert, die spezifisch für bestimmte zelluläre Kompartimente sind. E1-mCherry lokalisierte nicht im *trans*-Golgi, was darauf hindeutet dass HCV Partikel nicht über den sekretorischen Transit sezerniert werden. Um diese Hypothese zu überprüfen, wurde eine biochemische Charakterisierung der beiden viralen Oberflächenproteine aus Zelllysaten und Viruspartikeln im Überstand durchgeführt. Dabei zeigte sich, dass E1 und E2 ausschließlich EndoH-sensitive Glykosylierungen aufweisen. Dies ist ein weiterer deutlicher Hinweis darauf, dass weder E1 noch E2 während der Ausschleusung im Golgi prozessiert werden. Im Gegensatz dazu segregierte intrazelluläres E1-mCherry zusammen mit verschiedenen Rab-Proteinen. Daraus lässt sich schließen, dass der endosomale Transport eine wichtige Rolle bei der Freisetzung von HCV spielt.

In dieser Arbeit konnte gezeigt werden, dass der HCV Lebenszyklus zeitlich streng organisiert ist. Nachdem zunächst die Replikation eingeleitet wird, kommt es zu späteren Zeitpunkten zur Akkumulation von Strukturproteinen und dem Zusammenbau von Viruspartikeln. Die Strukturproteinakkumulationen, welche wahrscheinlich assemblierten Virionen entsprechen, trennen sich anschließend von den Orten der Virusreplikation und Proteintranslation. Dann erfolgt deren Freisetzung unter Ausschluss des sekretorischen Transits, vermutlich in endosomalen Kompartimenten. Somit wurden in dieser Arbeit neue Erkenntnisse zur Freisetzung und zum intrazellulären Transport von HCV gewonnen. Des Weiteren deuten die Daten darauf hin, dass es einen sekretorischen zellulären Transport vom ER zur Plasma Membran unter Ausschluss des Golgi Apparats gibt.

# Summary

Infection with the hepatitis C virus is a global health burden with approximately 150 million people chronically infected worldwide. The hepatitis C virus is an enveloped single-stranded RNA virus that is a member of the *Hepacivirus* genus in the *Flaviviridae* family. It is mainly transmitted by blood-blood contact and can lead to chronic infection, liver fibrosis and severe hepatocellular carcinoma. From the year of its discovery in 1989 to the first cell culture model with the complete infectious cycle a decade ago, great progress has been made in elucidating early steps of viral entry and replication. HCV particles in patients' serum and cell culture supernatant are closely associated with lipoproteins, especially ApoE, leading to an unconventional low density. Due to this association of viral particles with lipids, lipoprotein-specific receptors like the HSPG, LDLR and SR-BI also contribute to HCV cell-attachment. These receptors bring the virus particle's surface protein E2 in close proximity to the binding partners necessary for the actual entry step, like CD81, claudin 1 and occludin. After internalization and IRES-mediated protein translation, replication is initiated by HCV non-structural proteins in a so-called membranous web. To date, it is hypothesized that HCV assembles on the surface of lipid droplets and buds into ER-derived membranes. In contrast, the intracellular routes and pathways HCV uses for release remain still poorly understood.

In this thesis, virus assembly and intracellular pathways involved in HCV release were examined by utilizing different HCV genomes that encode a mCherry-labeled E1 surface protein. The physiological properties of the virus were not impaired by the tag, as HCV genomes expressing labeled or unlabeled viral proteins revealed similar protein expression and intracellular protein distribution, comparable replication kinetics and virus release. Furthermore, correct virus particle assembly and release was confirmed by showing that all structural proteins, together with the viral RNA and the HCV-associated ApoE are enriched in the same density fraction characteristic for infectious cell-free HCV particles. However, infectivity of mCherry-labeled HCV was highly attenuated.

The HCV JC1 genome expressing E1-mCherry and NS5A-GFP allowed the visualization and discrimination of viral non-structural and structural proteins within living cells throughout the whole replication cycle. To analyze the late steps of viral replication, HCV expressing cells were monitored over a four-day period, while protein localization, association and movement were carefully observed. Our studies revealed a tightly regulated appearance and accumulation of NS5A replication complexes increasing quickly after RNA delivery, while decreasing at later time points. On the other hand, structural protein E1 complexes accumulated over time, possibly representing upcoming

assembly sites or assembled viral particle. This observation was supported by a coinciding increase in the interaction between the structural proteins E1, Core and E2, which additionally colocalized at E1-mCherry positive accumulations, again most likely depicting assembly sites or viral particles. Furthermore, at later time-points structural protein E1-mCherry accumulations were separated from NS5A-GFP translational sites, suggesting virus particles within transport compartments.

Further, this thesis addressed the nature of intracellular HCV trafficking and release by spinning disc microscopy and the coexpression of HCV with different fluorescently-tagged proteins specific for certain cellular compartments. Altogether, E1-mCherry did not colocalize with the *trans*-Golgi compartment and the investigation of both viral surface proteins E1 and E2 within the cell and in released viral particles revealed an overall EndoH-sensitive glycosylation pattern. These data strongly indicate that HCV is not processed in the Golgi compartments during release. Rather HCV accumulations cotrafficked with specific Rab proteins supporting the idea that endosomal compartments are used by HCV for its transport to the cell membrane.

To summarize, the HCV life cycle is strictly organized in a time-dependent manner. After RNA-entry, replication is directly initiated. At later time points structural protein accumulates when viral particle assembly takes place. Then the data suggests that virus particles separate from the sites of translation and are transported through endosomal compartments towards the cell membrane in a Golgi independent manner. These findings help towards the understanding of hepatitis C virus particle assembly and release. Furthermore, the data implies the existence of a non-yet discovered direct secretory ER to plasma membrane pathway bypassing the Golgi apparatus.

# 1 Abbreviations

| | | | |
|---|---|---|---|
| (+)ssRNA | positive, single-stranded RNA | LD | lipid droplet |
| µ | micro | LDL(R) | low density lipoprotein (receptor) |
| α | alpha, or anti- | LVP | lipo-viro-particles |
| aa | aminoacid | m | milliliter |
| ab | antibody | M | molar |
| Apo | Apolipoprotein | Man | mannose |
| APS | ammoniumperoxdisulfate | $MgCl_2$ | magnesium chloride |
| β | beta | min | minutes |
| CD81 | cluster of differentiation 81 | miRNA | micro RNA |
| CHV | canine hepacivirus | MTP | microsomal triglyceride transfer protein |
| CLDN1 | claudin 1 | n | nano |
| coIP | Coimmunoprecipitation | NaCl | sodium chloride |
| Δ | delta | NCR | noncoding region |
| DAA | direct-acting antivirals | NPC1L1 | Niemann-Pick C1-like 1 |
| DGATI | diacylglycerol acetyltransferase I | NPHV | non-primate hepacivirus |
| $dH_2O$ | distilled water | NS | non-structural protein |
| DNA, RNA | deoxy-, ribonucleic acid | NTPase | RNA nucleoside triphosphatases |
| ds | double strand | OCLN | occludin |
| e.g. | *exempli gratia* | ORF | open reading frame |
| EEA1 | early endosome antigen 1 | PBS | phosphate buffered saline |
| EndoH | Endoglycosidase H | PCR | Polymerase chain reaction |
| ER | endoplasmic reticulum | PEG-IFN | pegylated interferon-α |
| ESCRT | endosomal sorting complex required for transport | pEP | post electroporation |
| EtOH | ethanol | PFA | Paraformaldehyde |

| | | | |
|---|---|---|---|
| FACS | fluorescence activated cell sorting | PLA | Proximity Ligation Assay |
| FCS | forward scatter | PNGaseF | Peptide-N-Glycosidase F |
| FRAP | Fluorescence Recovery after Photobleaching | qRT-PCR | quantitative reverse-transcription polymerase chain reaction |
| g | gram | r | Pearson's correlation coefficient |
| GalT | β-1,4-galactosyltransferase | RdRp | RNA-dependent RNA polymerase |
| Gaussia | Gaussia luciferase | rpm | round per minute |
| GFP | green fluorescent protein | RT | room temperature |
| Glc | glucose | s | seconds |
| GlcNAc | N-acetylglucosamin | SDS-PAGE | sodium dodecyl sulfate-polyacrylamide-gel electrophoresis |
| HBV | hepatitis B virus | SOE | splicing by overlap extension |
| HCC | hepatocellular carcinoma | SR-BI | scavenger receptor BI |
| HCV | hepatitis C virus | SVR | sustained virological response |
| HIV | human immunodeficiency virus | TEMED | N,N,N',N'-Tetramethylethylenediamine |
| HSPG | heparan sulfate proteoglycans | v or w/v | volume or weight per volume |
| IRES | internal ribosomal entry site | VLDL | very low density lipoproteins |
| L | liter | VSV | vesicular stomatitis Indiana virus |

# 2 Introduction

## 2.1 Hepatitis C

Hepatitis is defined as an inflammation of the liver with the potential of progression to liver fibrosis and cirrhosis. Multiple causes are responsible for the disease. Besides the impact of toxins like alcohol, drugs or a fatty liver, virus infections are the most common cause for chronic hepatitis, liver cirrhosis and hepatocellular carcinoma (HCC) worldwide.

### 2.1.1 History and epidemiology

In 1989 hepatitis C virus (HCV) was initially discovered and characterized as the source for chronic non-A, non-B hepatitis (Choo et al. 1989). Until then, numerous patients had suffered from an unknown disease that was transmitted by blood transfusion and other blood products (Alter et al. 1975, Feinstone et al. 1975). With the discovery of HCV and the subsequent development of diagnostic tests, a new global health problem was revealed. 150 million people (2-3% of the world's population) are chronically infected to date, with 350 000 deaths and four million new infections annually (Hoofnagle 2002, Lavanchy 2011, Shepard, Finelli, and Alter 2005). With a high prevalence in the Eastern Mediterranean region and Africa (Fig. 1) (Shepard, Finelli, and Alter 2005).

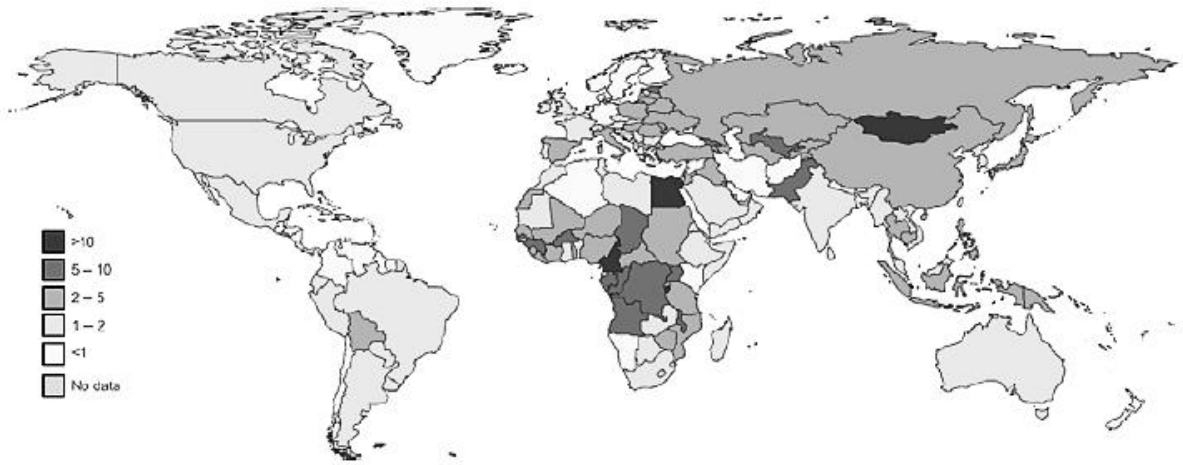


**Figure 1: Global prevalence of hepatits C in 2010** [%]. (Lavanchy 2011)

### 2.1.2 Transmission and pathogenesis

Before the discovery and identification of HCV in blood supplies, the main route of viral transfer was through blood transfusions and unsterilized needles during medical treatments (Nelson et al. 2011). But since the introduction of blood donor screening and inactivation, the most common mode of

transmission has been needle-sharing among drug users (Drucker, Alcabes, and Marx 2001). Thus, in the last decade, efforts to curb further spread of the virus have focused on programs for needle and syringe exchange. While sexual intercourse has also been considered, it seems to be an inefficient and therefore, very unlikely mode for transmission (Thomas 2000, Vandelli et al. 2004).

HCV is one of the major causes of progressive liver disease worldwide and by extension, of liver transplantation in developed countries. 75 to 90% of infected patients develop chronicity and of these, 10 to 40% develop liver cirrhosis (Roche and Samuel 2012). Inflammation-associated growth factors, chemokines and cytokines in the liver lead to the expansion of extracellular matrix, thereby triggering fibrosis (Hernandez-Gea and Friedman 2011). Additionally, HCV proteins are thought to promote fibrogenesis via the transcription factor NF-κB. It is activated by pattern recognition receptor signaling, direct activation (Saito et al. 2008, Sato et al. 2006, Waris et al. 2003) or by the induction of oxidative stress (Fujita et al. 2008). As a result, alcohol abuse as well as co-infection with the human immunodeficiency virus (HIV) or hepatitis B virus (HBV) can lead to facilitated progression (Gitto et al. 2009, Shepard, Finelli, and Alter 2005). Hepatic steatosis, with its characteristic accumulation of lipid droplets in the cell cytoplasm, insulin resistance and type 2 diabetes mellitus are also linked with the infection, increasing the risk of fibrosis and HCC (D'Souza, Sabin, and Foster 2005, Ohata et al. 2003, Veldt et al. 2008). 1 to 5% of the patients progress to HCC (Perz et al. 2006). Genomic mutations facilitating carcinogenesis could be driven by oxidative stress, inflammation, regenerative proliferation within the liver and immune response- or directly HCV-induced cell death (Deng et al. 2008). Furthermore, it has been shown that HCV proteins act on cell cycle regulation and tumor suppressors like p53 and the retinoblastoma tumor suppressor protein (Rb), which likely hinders DNA damage response and supports viral replication (McGivern and Lemon 2009).

### 2.1.3 Prophylaxis and therapy

At this point, there is no HCV vaccine available. In the last decade, chronic hepatitis C has been treated with a combination of pegylated interferon-α (PEG-IFN) and ribavirin therapy. Polyethylene glycol (PEG) increases the half-life of IFN-α in the patient's body while IFN activates the innate and adaptive immune response against viral infection by triggering RNA degradation and generation of MHC class I molecules. Ribavirin, a broad-spectrum antiviral, acts as nucleoside analog for guanosine and thus interferes with RNA synthesis. Medication is administered for 24 or 48 weeks till sustained virological response (SVR) is reached. SVR is defined as undetectable viral RNA 24 weeks after therapy termination. In addition to only curing 80% of genotype 2 and 3 patients and 40 to 50% of genotype 1 patients, the current treatment of HCV has major side effects, including the loss of neutrophils, insomnia, depression and anemia (Andriulli et al. 2008, Janssen et al. 1994, Reddy et al.

2007). As a result, combination therapies of direct-acting antivirals (DAA) are promising for future therapy.

DAAs target HCV proteins specifically, thereby reducing side effects on the patient's body. Two protease inhibitors against NS3/4A, known as telaprevir (Vertex Pharmaceuticals/Johnson&Johnson) and boceprevir (Merck), passed the clinical phase 3 in 2012. In combination with PEG-IFN and ribavirin, these inhibitors have cured up to 80% of patients with treatment-resistant HCV genotype 1 (Fontaine and Pol 2011).

Nevertheless, interferon-free therapies are still absent and DAAs with broad genotype activity and less probability for developing viral resistance have to be developed. In line with these demands, new drugs targeting the viral protease NS3/4A, the NS5A protein and the viral RNA-dependent RNA polymerase NS5B are in clinical phases (Manns and von Hahn 2013). In addition, the viral ion channel p7 and the replication supporting protein NS4B show potential for drug targeting (Bryson et al. 2010, Griffin et al. 2003). Furthermore, agents that target host proteins, like microRNA-122 antagonistis and cyclophilin A inhibitors (Coelmont et al. 2009, Janssen et al. 2013), have been reported. Recently sofosbuvir (Gilead Sciences) (Sofia et al. 2010) was approved by the FDA. This drug targets the viral polymerase NS5B by serving as a defective substrate, thereby hindering RNA synthesis. The dual interferon-free regimen of sofosbuvir with ribavirin showed 100% responses in patients with genotype 2 and 3 (Gane et al. 2013). In triple regimen of ribavirin and sofosbuvir with other DAAs like the NS5A inhibitor daclatasvir (Bristol-Myers Squibb) or ledipasvir (Gilead Sciences), cure rates of patients with genotype 1 also reach up to 100% (Lawitz et al. 2014, Sulkowski et al. 2014). Taken together, very efficient treatment options have been discovered that cure patients with all genotypes regardless treatment history and with fewer adverse events. Current research is addressing second-generation inhibitors in different combinations with the goal of finding the most efficient combination therapy and to broaden the repertoire of antivirals to prevent resistance mutation (Manns and von Hahn 2013).

## 2.2 Hepatitis C virus

### 2.2.1 Taxonomy and morphology

The hepatitis C virus belongs to the *Hepacivirus* genus within the F*laviviridae* family (Bukh, Miller, and Purcell 1995, Simmonds et al. 1993). Its sequence divergence, mainly caused by the non-proof reading RNA-polymerase, divides HCV into seven genotypes (Smith et al. 2014). Within these genotypes several subtypes are endemic in different parts of the world. In Europe and Asia, genotypes 1b, 2a and 2b are widely distributed, whereas genotype 4a is more frequently discovered

in the Middle East and 3a among injecting drug users (Simmonds 2013). This variance challenges the research on vaccination and therapy.

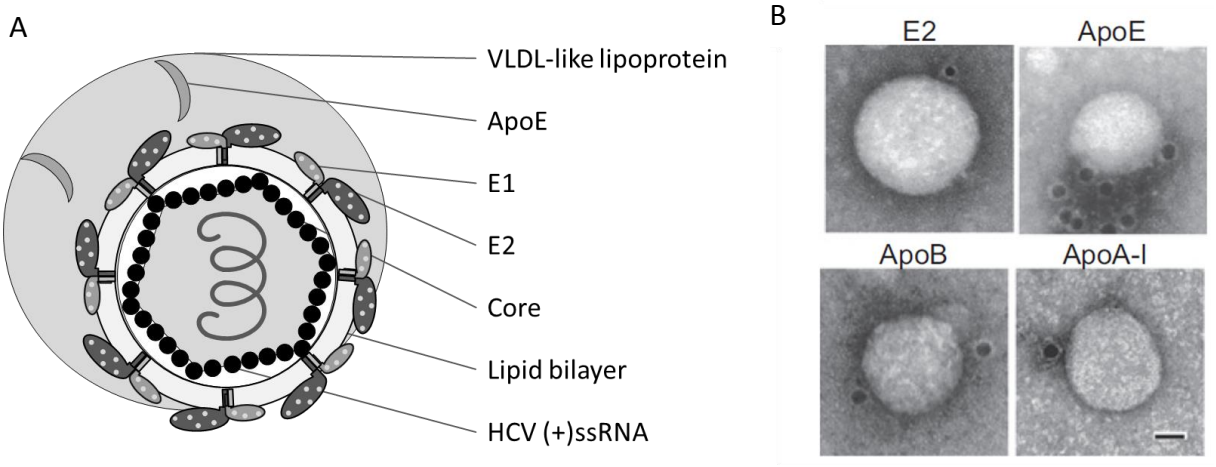


**Figure 2: HCV particle.** (A) Scheme of an HCV virion. The (+)ssRNA of HCV is encapsidated by Core. The heterodimer of E1 and E2 is incorporated into the ER-derived lipid bilayer. HCV is associated with lipoproteins. (B) Transmission electron microscopy pictures of HCV virions immunogold-labeled against the indicated proteins. Bar: 20 nm (Catanese et al. 2013).

The RNA genome of HCV is encased by the viral capsid composed of homolog interacting Core proteins and surrounded by a lipid bilayer 70 to 100 nm in diameter (Fig. 2) (Catanese et al. 2013, Gastaminza et al. 2010). The envelope glycoproteins E1 and E2 are incorporated into the membrane (derived from the endoplasmic reticulum, ER), serving as the receptor binding site. Additionally, virus particles are associated with lipoproteins, including low density lipoproteins (LDL) and very low density lipoproteins (VLDL) (Merz et al. 2011). Apolipoproteins (Apo) E and B and the LDL receptor all play an essential role in the binding and internalization of HCV particles (André et al. 2002). These lipo-viro-particles (LVP) showed a heterogeneity in RNA distribution in density gradients and revealed highest RNA peak at 1.08-1.11 g/mL in patients' serum due to this association (Kanto et al. 1994, Miyamoto et al. 1992).

### 2.2.2 HCV cell culture system

The first cell culture model to study HCV RNA replication was established in 1999 by the group of Lohmann, providing a replicon system in the hepatoma cell line Huh 7. In this system, a trimmed genome, including the non-structural proteins NS3 to NS5B of genotype 1b (Con1), was transfected into Huh 7 cells (Lohmann et al. 1999). Treatment of these cells with IFN led to viral clearance and more importantly, to a highly permissive cell clone termed Huh 7.5, which is still widely used in HCV research to date (Blight, McKeating, and Rice 2002). Although productive infection could be shown in chimpanzees for the subgenome H77 (Kolykhalov et al. 1997), no infectious viral particles could be produced in cell culture at this time. An improvement was the trans-complemented particle system

($HCV_{TCP}$). Structural proteins were transfected in *trans* together with the replicon system, leading to the assembly and release of virus particles and therewith, studies of entry and replication in one round infection (Steinmann et al. 2008).

In the meantime, virus entry was addressed by using a retroviral pseudotype system (HCVpp) (Bartosch, Dubuisson, and Cosset 2003), which consists of HIV gag-pol proteins and the HCV glycoproteins E1 and E2. Although these particles lack the characteristic association with lipoproteins, the attachment of HCV to several receptors was shown in further studies.

The breakthrough in the cell culture system was initiated by the isolation of a genotype 2a genome from a patient suffering a severe hepatitis, termed “Japanese fulminant hepatitis 1” (JFH1). Cloning and RNA-transfection in permissive Huh7 revealed high replication efficiency without further mutations (Kato et al. 2003) and the production of infectious HCV particles, HCVcc (Lindenbach et al. 2005, Wakita et al. 2005, Zhong et al. 2005). Additionally, genomic chimeras were constructed, in which the NS3 to NS5B proteins originate from JFH1 and the exchangeable Core to NS2 proteins from different genotypes. The most efficient chimera turned out to derive from J6, a genotype 2a isolate, designated JC1, which provides the proteins from Core to the first TM-domain of NS2 (Pietschmann et al. 2006). Further introductions of GFP or luciferase reporters allowed easy investigation of replication and infection (Koutsoudakis et al. 2006, Schaller et al. 2007). The combination of the highly permissive Huh7.5 cell line together with a potent infectious cycle allowed for the investigation of the full hepatitis C virus life cycle in cell culture, including entry, replication, assembly and release.

Several distinct models were used in the last decade to study different steps in the HCV life cycle. The CD81 receptor attachment was demonstrated by a truncated soluble version of E2 protein (Pileri et al. 1998). HCV glycoprotein-dependent cell fusion was assessed by raising fluorescence upon fusion (Kobayashi et al. 2006). Moreover, cell-to-cell spread and infection was investigated by a cell-based fluorescent reporter system with NS3/4A-mediated cleavage of a fluorescent substrate (Jones et al. 2010). Co-localization of the endocytosis machinery with HCV was visualized by lipophilic-dyes labelling the virus particles (DiD) (Coller 2009).

Regarding the observation of HCV RNA in extrahepatic tissues of HCV infected patients, like peripheral blood mononuclear cells (PBMCs) (Weissenborn et al. 2009), macrophages and microglia in brain tissue (Wilkinson, Radkowski, and Laskus 2009), other cell lines were described to replicate HCV. Moreover, the addition of CD81 and miR-122 increased permissiveness (Narbus et al. 2011). For example, human liver HepG2 cells (Date et al. 2004), mouse embryonic-fibroblasts (MEFs) (Chang et

al. 2006) and human brain microvascular endothelial cells (BMEC) (Fletcher et al. 2012) all support HCV replication and, in the case of BMECs, moderate productive infection.

However, it is important to note that the replication of HCV in Huh7.5 cells does not reflect the *in vivo* situation, since these cells do not polarize and are not surrounded by a hepatic environment with bile canaliculi. These disadvantages can be partially overcome with DMSO treatment or the use of HepG2 cells. Experiments with HepG2 also revealed a reduction of polarization upon HCV infection (Mee et al. 2010, Mee et al. 2009, Sainz and Chisari 2006). However, the need for primary cultures is obvious. Several approaches have been made to address this need. Primary human hepatocytes (PHH) showed a lower density and thus a higher infectivity of viral particles in comparison to HCVcc (Podevin et al. 2010). An *ex vivo* model established from human adult liver slices has demonstrated productive infection with patient virus inoculum (Lagaye et al. 2012). And most recently, induced pluripotent stem cells (iPSC) and human embryonic stem cell (hESC)-derived hepatocytes have been shown to support infection and replication, allowing virus-host interactions to be studied in greater detail (Roelandt et al. 2012, Schwartz et al. 2012).

### 2.2.3 Animal models

Over the last decade humans and chimpanzees were the only known naturally susceptible hosts for hepatitis C virus infection. However, the recent isolation of canine hepacivirus (CHV) and non-primate hepacivirus (NPHV) in dogs and horses provides evidence for a broader host spectrum (Burbelo et al. 2012, Kapoor et al. 2011).

The chimpanzee model was very important in the first years of HCV discovery and research. Infectivity of patient- as well as cell culture-derived HCV particles could be proven (Alter et al. 1978, Lindenbach et al. 2006). Also, the clinical course of the disease (Bukh 2004) and several promising drug combinations were tested in this model (Olsen et al. 2011).

Different mouse models have been developed to gain further knowledge about HCV pathogenicity and immune responses. Although these models lack the overall human background of immune cell interactions, they are a good alternative to the delicate chimpanzee models. The transgenic mouse model contributed to the understanding of pathogenesis, but ultimately, did not mimic the *in vivo* situation due to variable genome integration, extensive protein expression and protein action without liver inflammation (Kremsdorf and Brezillon 2007). To overcome the species barrier, the minimal required human entry receptors CD81 and OCLN were transiently delivered into mice. However, while the mice were now permissive for HCV entry and protein translation, HCV failed to replicate effectively (Dorner et al. 2011). Transgenic mice for CD81, SR-BI, CLDN1 and OCLN even failed in viral entry (Hikosaka et al. 2011). Another approach focused on the multiple passage of HCV

on mice-derived cells, but this led to mutational changes within the glycoproteins and a murin-tropic virus (mtHCV) that was not infectious (Bitzegeio et al. 2010).

A new xenotransplantation approach based on tissue-engineering for ectopic transplantation was done by Chen et al. They stabilized human hepatocytes in a polymeric scaffold and transplanted this so-called human ectopic artificial liver (HEAL) into an immunocompetent mouse. In this case, human liver function could be maintained for several weeks and processes such as drug metabolism could be investigated (Chen et al. 2011).

Chimeric mice were generated by chemically injuring the liver of the mice and injecting human hepatocytes. Due to injury, human cells could proliferate and establish a xenotransplant, in which HCV infection could be studied (Bissig et al. 2010, Mercer et al. 2001). However, early mortality, bleeding tendency or the need for a high dose of hepatocytes problematized these models. Nevertheless, drug responses for new DAA combinations were successfully tested in line with clinical studies (Chayama et al. 2012, Ohara et al. 2011).

Recently, a novel dually-engrafted mouse model was established by Washburn et al. They demonstrated the possibility to transplant human hepatocyte progenitors as well as human blood cord-derived CD34+ hematopoietic stem cells (HSC) into transgenic liver-injured mice, generating a humanized liver in the context of a human-derived immune response (Washburn et al. 2011). Nevertheless, whether or not all the introduced components properly develop remains to be seen, especially since the species-specific cytokines and adhesion molecules are not suitable and HLAs are lacking.

### 2.2.4 Genome organization and viral proteins

HCV comprises a 9.8 kb positive-sense, single-stranded RNA genome ((+)ssRNA) with an internal ribosomal entry site (IRES) at its 5' noncoding region (NCR) enabling Cap-independent translation. An open reading frame (ORF) coding for the 3000 aa long polyprotein and a 3' NCR follow (Fig. 3). The highly conserved regions within the 5' and 3' NCR (X-tail) are crucial for replication in cell culture and *in vivo* (Friebe and Bartenschlager 2002, Kolykhalov et al. 2000). The polyprotein is cleaved into the structural and nonstructural proteins. The ER-residing signal peptidase (SP) processes the capsid protein Core and the two envelope glycoproteins E1 and E2 (Fig. 3, black arrows), which are important for particle formation, as well as the nonstructural viroporin p7. Moreover, the auto-protease NS2 cleaves itself from NS3 (Fig. 3, grey surrounded arrow), whereas the following nonstructural proteins, including the NS3-4A protease and NTPase/RNA helicase complex, the NS4B and NS5A proteins and the RNA-dependent RNA polymerase (RdRp) NS5B, are cleaved by the viral protease NS3-4A after self-liberation in *trans* (Fig. 3, black surrounded arrows).

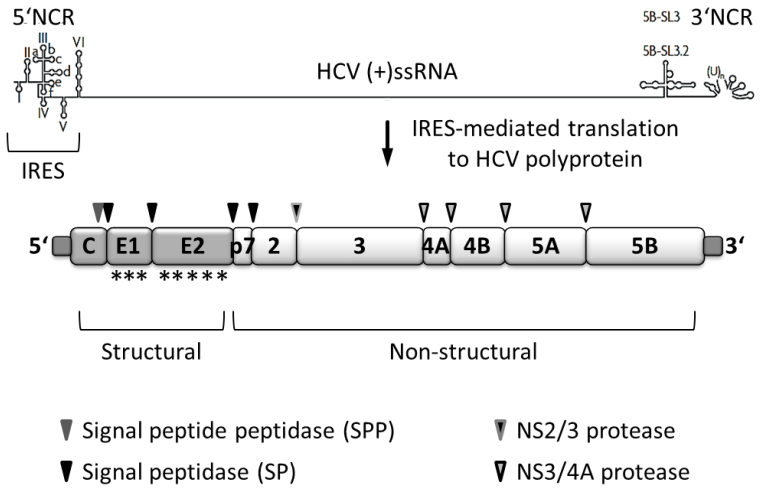


**Figure 3: HCV genome and polyprotein organization scheme.** The (+)ssRNA is flanked by a 5' and a 3'NCR and the CRE elements (SB-SL) important for IRES-mediated translation as well as negative and positive strand replication (modified after Moradpour, Penin, and Rice 2007). The polyprotein is cleaved co- and post-translationally by the host cell peptidases or the viral proteases as indicated (arrowhead). The glycoproteins are glycosylated during translation (asterisk).

The Core protein is directed to the ER via a signal sequence between Core and E1 and is further processed to its mature 174 aa form by the signal peptide peptidase (SPP) (Fig. 3, grey arrow) (McLauchlan et al. 2002). Core acts as a homodimer with two domains (Boulant et al. 2005). The first is the basic N-terminus with RNA binding and protein/capsid multimerization ability. Proteome-wide mapping has shown that it also interacts with several cellular proteins, thereby leading to disorders associated with HCV pathology (de Chassey et al. 2008). The second is the hydrophobic domain, which binds to lipid droplets (Hope and McLauchlan 2000) and can therefore serve as RNA packaging protein. The RNA is delivered by NS5A. Therewith, Core is a crucial protein for virus capsid assembly in association with lipid droplets and for the formation of lipo-viral-particles (Masaki et al. 2008).

The glycoproteins E1 and E2 are the surface proteins of the assembled viral particle. They function in receptor-binding, endocytosis and particle assembly. Within the ER, they act as a non-covalent heterodimer (Dubuisson et al. 1994, Duvet et al. 1998) and within virus particles, in a disulfide-bound covalent complex (Vieyres et al. 2010). Both proteins have a transmembrane domain (type I) which retains them in the ER after translation (Cocquerel et al. 1999, Cocquerel et al. 1998, Cocquerel et al. 2002). Important for proper folding is the mutual expression (Patel, Patel, and McLauchlan 2001) and the N-linked glycosylation of either 4-6 or 11 sites within their ectodomains (Goffard et al. 2005, Goffard and Dubuisson 2003, Zhang et al. 2004). (The mechanism is described in more detail in chapter 2.2.6.)

The viroporin p7 was shown to act as a cation channel (Griffin et al. 2003, Premkumar et al. 2004), which promotes the production of infectious virus by protecting the particle from premature low pH exposure (Steinmann et al. 2007). P7 was shown to act in endolysosmal as well as secretory compartments (Wozniak et al. 2010). Recent evidence also demonstrates a direct interaction of p7

with all structural proteins as well as the NS2 protein, thereby linking replication sites to virus assembly (Hagen et al. 2014, Tedbury et al. 2011).

The NS2 protein, together with the N-terminal part of NS3, comprises a cysteine protease, which mediates the cleavage of NS2/3 from the polyprotein (Santolini et al. 1995, Schregel et al. 2009), and thus enhances replication. Since NS2 interacts with structural as well as non-structural proteins (Popescu et al. 2011), it appears also to have an important role in virus replication and assembly (Ma et al. 2011, Stapleford and Lindenbach 2011). In particular, the NS2 interaction with p7 and NS3-4A links Core proteins on LDs to assembly sites (Counihan, Rawlinson, and Lindenbach 2011, Tedbury et al. 2011).

The N-terminal part of NS3 serves as a serine protease. Together with the cleavage-enhancing NS4A cofactor, the N-terminal domain processes the downstream polyprotein junctions in *trans* (Bartenschlager et al. 1995). The C-terminal part of NS3 contains a NTPase/RNA helicase, which unwinds double- and secondary structured single-stranded RNA probably to promote viral replication (Kim et al. 1995). Moreover, the helicase domain influences particle assembly: first, by interaction with NS2 (Counihan, Rawlinson, and Lindenbach 2011) to recruit Core on LDs to assembly sites and second, by interaction with Core and a possible role in RNA packaging (Jones et al. 2011, Raney et al. 2010). Both domains are anchored within membranes of the ER and the mitochondria (Wölk et al. 2000), thereby suppressing antiviral pathways within the host cell and promoting persistence and pathogenesis. The protease cleaves the innate immune response downstream adaptor of RIG-I, the MAVS (Cardif), as well as the TLR-3 adaptor TRIF and the T cell PTP (protein tyrosine phosphatases) (Brenndörfer et al. 2009, Li et al. 2005, Meylan et al. 2005).

An important protein for the functional RNA replication is the NS4B protein. Not yet completely understood, it contains several functions in virus replication and assembly (Jones et al. 2009). As a homo-oligomer, it interacts with other nonstructural proteins of HCV (Gouttenoire, Penin, and Moradpour 2010, Yu et al. 2006) as well as RNA (Einav et al. 2008). Besides the other NS3-5B proteins, which are also able to stimulate single-membrane vesicle formation (Romero-Brey et al. 2012), it induces the formation of the so-called membranous web and can serve as a scaffold by reorganizing ER derived membranes and trapping of lipid vesicles and proteins of the viral replication complex therein (Egger et al. 2002). Moreover, the environment for appropriate replication is accomplished by the accumulation of intracellular lipids and lipid droplets (LD) (Diamond et al. 2010, Su et al. 2002). LDs might serve as a connection between replication and the viral assembly mediated by Core and NS5A (Miyanari et al. 2007).

The NS5A phosphoprotein seems to have a function in RNA replication and viral assembly (Appel et al. 2008, Tellinghuisen, Foss, and Treadaway 2008). It binds to lipid droplets, which serve as a scaffold for viral replication, binds viral RNA and interacts with the Core protein (Huang et al. 2005, Masaki et al. 2008, Miyanari et al. 2007). The basal- and hyper-phosphorylation forms, modified by the casein kinase isoform α (CKIα) and the casein kinase II (CKII), could act as a switch between the interaction of host proteins facilitating replication or assembly (Evans, Rice, and Goff 2004). Besides Core, NS5A binds to the p7-NS2 complex and ApoE thereby promoting virus assembly (Benga et al. 2010, Popescu et al. 2011).

The RNA dependent RNA polymerase (RdRp) NS5B is the operating enzyme of the replication complex (Behrens, Tomei, and De Francesco 1996). It builds up new genome (+)ssRNA from the complementary (-)strand by *de novo* synthesis in association with a lipid membrane (Moradpour et al. 2004, Simister et al. 2009). The high mutation rate of HCV genomes is largely due to the lack of proof reading, with an error rate of 1:1000 ) (Powdrill et al. 2011).

### 2.2.5 HCV replication cycle

#### 2.2.5.1 HCV entry

HCV mainly infects hepatocytes in the liver. Therefore, it enters via the hepatic sinusoids associated with several lipoproteins. The first attachment is thought to take place at liver endothelial and dendritic cells via the lectins DC-SIGN (dendritic cell-specific intracellular adhesion molecule 3-grabbing nonintegrin) and L-SIGN (liver/lymph node-specific intracellular adhesion molecule 3-grabbing integrin). These lectins have a strong affinity for high-mannose-containing glycoproteins and thus serve as infection promoters for several viruses like HIV and HCV (Geijtenbeek et al. 2000, Lozach et al. 2004).

The first contact with the primary target cells is mediated by the cell surface heparan sulfate proteoglycans (HSPG) (Fig. 4). Like other viral surface proteins, the HCV glycoproteins E1, E2 and the associated ApoE bind to HSPG, mediating cell-contact (Barth et al. 2006). Together with these proteins, the scavenger receptor BI (SR-BI) recognizes the lipoproteins and further binds specifically the E2 protein (Dao Thi et al. 2012, Scarselli et al. 2002). Moreover, the low-density lipoproteins receptor (LDLR) is thought to not only have beneficial effects on binding, but also on replication (Albecka et al. 2012, Monazahian et al. 1999). In a following crucial step, E2 interacts specifically with its receptor, the tetraspanin CD81 (Pileri et al. 1998).

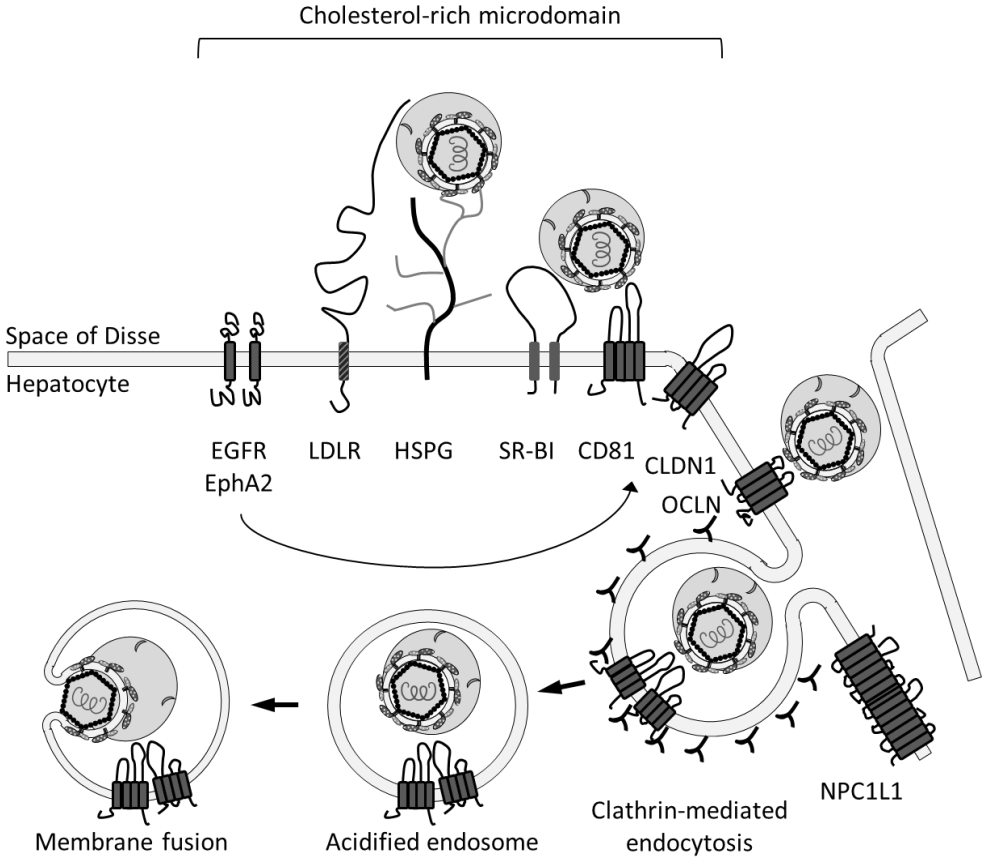


**Figure 4: Schematic entry process of HCV into human hepatocytes.** HCV mediates contact via glycosylations on the surface proteins E1 and E2 as well as the associated lipoprotein via the LDLR. Furthermore, E2 attaches specifically to CD81 and the lipoproteins interact with SR-BI. EGFR- and EphA2-signaling lead to the association of CD81 and CLDN1 and the combined attachment to the viral particle. Moreover, interaction with OCLN and NPC1L1 occur and clathrin- and dynamin-dependent endocytosis of HCV together with CD81 and CLDN1 takes place. After acidification, the viral- and endosomal membrane fuse and release the capsid into the cytoplasm.

A post-binding step also important for internalization is the attachment of the co-receptors. Therefore, the epidermal growth factor receptor (EGFR)-, ephrin receptor A2 (EphA2)- and protein kinase A (PKA) mediated signaling lead to the formation of a CD81-claudin 1 (CLDN1) complex (Evans et al. 2007, Farquhar et al. 2008, Lupberger et al. 2011). Likewise, another TJ-protein, the occludin (OCLN), is reorganized and serves as co-receptor (Benedicto et al. 2009). Together with CD81 and the lipoproteins, OCLN determines the species-tropism of HCV to humans (Ploss et al. 2009). The Niemann-Pick C1-like 1 (NPC1L1) protein is a cholesterol transporter and therefore also serves as an entry regulator (Sainz et al. 2012).

HCV internalization is mediated by clathrin- and dynamin –dependent endocytosis together with CD81 and CLDN1 (Blanchard et al. 2006, Farquhar et al. 2012). The subsequent acidification of the early endosomal compartment (Tscherne et al. 2006) and proposed reorganization of the glycoprotein fusion domains (Drummer, Boo, and Poumbourios 2007), lead to the uncoating of the viral capsid into the cytoplasm.

Besides cell-free virus propagation, cell-to-cell transmission of HCV was discovered to possibly promote a fast spreading infection within the liver. This mode of transmission uses most of the already described entry factors with the advantage of being almost resistant to neutralizing antibodies (Brimacombe et al. 2011, Timpe et al. 2008).

#### 2.2.5.2 HCV translation

After uncoating, the viral ss(+)RNA is directly transferred to translation via its internal ribosomal entry site (IRES) in the 5'NCR (Brown 1992, Tsukiyama 1992, Wang 1993). Besides the main structural features of the IRES (stem-lops II-IV), elements in the Core-coding region (Vassilaki 2008b) and the first stem loop within the 3'NCR are important for translation enhancement (Song 2006, Bradrick2006, Bung 2010). Additionally, a negative feedback mechanism is proposed by the interaction of 5' and 3' NCRs, resulting in a switch from translation to replication (Isken et al. 2007, Romero-López et al. 2012).

Several cellular host factors are necessary for HCV translation and replication. Initially the eukaryotic initiation factor eIF3 binds to stem-loop III and associates with the ribosomal subunit 40S (Buratti et al. 1998). Meanwhile, the eIF2 captures an initiator tRNA, important for translational onset and with the ability of eIF5 to recognize the start codon, the conformational change to the 80S ribosome occurs (Pestova et al. 1998). Another hepatic cell factor, the micro RNA-122 (miR-122), binds two sequence motives between the first and second 5'NCR loop (Jopling et al. 2005). Usually miRNAs inhibit translation of their complementary consensus sequences, thereby regulating gene activity (Fabian, Sonenberg, and Filipowicz 2010). But in HCV-infected cells, miR-122, together with the Argonaute 2 protein, enhances viral propagation in the liver by additional translational activation (Henke et al. 2008) and RNA stability (Shimakami et al. 2012).

#### 2.2.5.3 HCV replication

Most translated HCV proteins have numerous functions within viral replication, assembly and egress. Interestingly, all of them contain a membrane anchor, since the HCV life cycle takes place within a so-called membranous web (Fig. 5). Intracellular ER-derived membranes are mainly recruited by NS4B and other NS proteins (see 2.2.4) to form a microenvironment, sequestering viral proteins as well as specific host factors in close proximity to lipid droplets (LD) (den Boon and Ahlquist 2010, Miller and Krijnse-Locker 2008). Only nucleotides and small molecules can access the partitioned membrane surrounded replication vesicles, whereas proteins like nucleases and proteases are excluded (Fig. 5, replication) (Quinkert, Bartenschlager, and Lohmann 2005). Recent studies have shown that these vesicles may arise from ER protrusions that form double-membrane vesicles (DMV), still connected with the ER and serving as storage compartments (Romero-Brey et al. 2012).

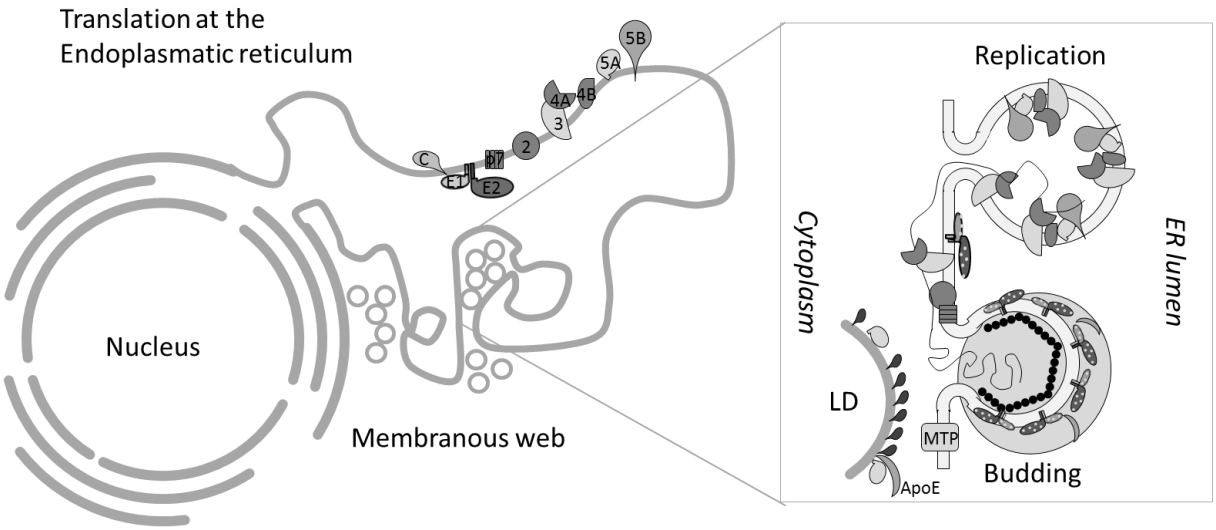


**Figure 5: Schematic ER-association of HCV, replication complexes and assembly.** After uncoating, the (+)ssRNA can be directly translated at the ribosomes into the ER. The polyprotein is cleaved into the single proteins, which remain associated with membranes. NS proteins trigger the formation of the membranous web, where replication takes place. From the replication caverns the RNA is probably sequestered to assembly sites, where the association with Core from the lipid droplets (LD) and the glycoproteins takes place (according to Counihan, Rawlinson, and Lindenbach 2011).

Replication is initiated by the 3' NCR of the positive RNA strand. It builds up a structural interaction between a *cis*-acting RNA element (CRE) in NS5B within the x-tail and another upstream region critical for starting negative-strand transcription (Friebe et al. 2005). Therefore, the RdRp binds to the polyU end with a stem loop nearby and initiates transcription with the help of other supporting factors, limiting negative strand synthesis (Lohmann et al. 1997). By contrast the 3' NCR of the negative strand allows *de novo* initiation by RdRp binding at a small single stranded RNA terminus preferentially ending with G, leading to plenty (+)ssRNA (Reigadas et al. 2001). Synthesis requires a matching dinucleotide primer for initiation (Ferrari et al. 2008).

Several viral and host factors promote efficient replication. NS3 stimulates transcription, presumably by unwinding secondary structures (Kim et al. 1995), and with an adverse effect, NS4B further binds and withdraws RNA (Einav et al. 2004, Piccininni et al. 2002). Furthermore, NS5A plays a concentration-dependent role and may mediate the RNA transport of RNA to assembly sites (Quezada and Kane 2009, Shirota et al. 2002). Again miR-122 increases RNA synthesis (Jopling et al. 2005). Furthermore, the vesicle transport protein hVAP-A (human VAMP-associated protein) is important for targeting HCV-NS5A and NS5B to cholesterol-rich membranes (lipid rafts), supporting replication complex formation (Gao et al. 2004).

*In vivo* chronic infected livers (30% of all hepatocytes) revealed up to 10 (+)ssRNA genomes per infected cell (Bigger et al. 2004), whereas in cell culture 100 copies of negative-stranded RNA and 1000 of positive were found (Quinkert, Bartenschlager, and Lohmann 2005). After entering the cell,

the incoming (+)ssRNA is degraded fast, whereas (-)ssRNA is found 4 to 6 hours after uptake. Both rise again to a concentration plateau at 24 to 48 hours for genotype 2a JFH1 (Keum et al. 2012). Looking at the protein levels within the cell, the abundance of 1,000,000 NS proteins reveals that only a small portion is involved in replication and that most (+)ssRNA is required for translation and protein expression, competing with virus assembly (Quinkert, Bartenschlager, and Lohmann 2005).

#### 2.2.5.4 Lipoparticle assembly

HCV particles associate with lipoproteins and are therefore called lipoviral particles, which is unique to the *Flaviviridae*. The density and lipid-composition of these lipoviral particle resemble that of VLDLs and LDLs containing Apolipoprotein (Apo) E (Merz et al. 2011), ApoB and ApoCI (Andre 2002, Meunier et al. 2008). Moreover, E1 interacts directly with ApoE and B (Mazumdar et al. 2011).

Within the ER, the microsomal triglyceride transfer protein (MTP) initiates VLDL formation by transferring lipids co-translationally onto ApoB proteins (Jamil et al. 1998). Further lipidation is not well understood, but may occur via fusion with LDs in the ER, as initiated by MTP and the addition of the exchangeable ApoE (Rustaeus et al. 1998, Wang, Gilham, and Lehner 2007). Alternatively, lipidation may take place in post-ER compartments, probably in the Golgi, through which the lipoproteins could be secreted in a COPII-dependent manner (Gusarova, Brodsky, and Fisher 2003, Gusarova et al. 2007). Thus, the dependency of HCV release on ApoE and by extension, on VLDLs has been the subject of controversy. At the same time, these publications shared a common reduction in virus production by inhibition of MTP (Jiang and Luo 2009, Nahmias et al. 2008). These observations point to an important role of ApoE-associated LDs in HCV secretion and infectivity within the lumen of the ER.

In short, the virus gains several advantages with its association with lipoproteins. The host-derived lipoparticles shield the virus from antibodies and the developing immune response (Andre 2002, Thomssen, Bonk, and Thiele 1993). As mentioned above, different cholesterol transporters, SR-BI, LDLR and NPC1L1, are critically involved in HCV entry processes and increase attachment capacities to host cells. However, HCV therewith is dependent on other proteins involved in lipid metabolism for efficient HCV production. For example, cholesterol impairment in HCV particles reduces viral infectivity drastically, but not binding (Aizaki et al. 2008).

To date it is not clear whether HCV particles assemble in conjunction with the synthesis of VLDL particles or if association takes place during transport to the cell membrane; similarly, it is not clear whether these particles fuse or act side by side (Lindenbach 2013). But it has been shown that this association leads to an exceptional low density profile in chimpanzee serum (1.03 to 1.10 g/mL), as well as in cell culture (1.15 g/mL) harboring the most infectious particle fraction (Cai et al. 2005,

Hijikata et al. 1993, Lindenbach et al. 2005). Like the density, also the diameter of isolated particles *in vivo* and *in vitro* shows experimental differences in a range between 30 to 80 nm and 60 to 75 nm (He et al. 1987, Merz et al. 2011).

#### 2.2.5.5 HCV assembly

After HCV replication, NS5A can target the Core protein to LDs, and sequester RNA molecules (see chapter 2.2.4). This process is dependent on the MAPK-regulated cytosolic phospholipase A2 (PLA2G4A) (Menzel et al. 2012) and the diacylglycerol acetyltransferase I (DGATI) (Herker 2010). Furthermore, the Core protein that has accumulated on LDs is translocated to the ER near assembly compartments, supported by p7-NS2 and NS3-4A (in chapter 2.2.4). The interaction between the glycoprotein heterodimer, residing within the ER, and the viral RNA is triggered and allows particle formation, presumably on LDs, and budding in ER compartments, like other *Flaviviridae* (Bartenschlager et al. 2011). Moreover, association with lipoproteins takes place. During transport, p7 protects the virion from premature acidification (Wozniak et al. 2010).

It is important to note that the pathway of HCV release is still poorly understood. Studies have shown that post-assembled Core-proteins may traffic along with ApoE within the secretory pathway (Counihan, Rawlinson, and Lindenbach 2011). Further studies have revealed important roles in secretion for early, late and recycling endosomes (Coller et al. 2012, Lai et al. 2010). Moreover, the importance of the late ESCRT machinery (endosomal sorting complex required for transport), probably for membrane fission or transport into late endosomal/multivesicular bodies, has been shown (Tamai et al. 2012). However, the specific cellular organelles and transport compartments that HCV hijiacks for release still remain to be elucidated.

### 2.2.6 Post-translational modifications

Glycans comprise multiple functions in protein conformation, stability, functionality, solubility and antigenicity. Moreover, they can modulate cell-cell and cell-matrix adhesion by interacting with members of the carbohydrate-binding lectin family. One of the most common post-translational modifications is the site-specific N-linked glycosylation. Thereby, a glycan is enzymatically attached to the asparagine (Asn-X-Ser/Thr) of a protein during or after translation (Lodish et al. 2000).

Most oligosaccharides have the same branched precursor with 2 N-acetylglucosamine (GlcNAc), 9 mannose (Man) and 3 glucose (Glc) molecules, $Glc_3Man_9(GlcNAc)_2$. These are activated in the rough ER by a diphosphate linkage to dolichol (P-Dol), a carrier lipid in the ER membrane, and transferred to the nascent protein by the oligosaccharide-protein transferase (OST). Furthermore, this precursor serves as a substrate for different glycosyltransferases. For the development of the complex oligosaccharides, the precursor in the Golgi is trimmed (by ER α-mannosidase I) to a “Core”

comprising only of 2 GlcNAc and 3 Man residues. Mature glycoproteins separate into three classes (Fig. 5). Within the high-mannose form, only multiple mannose molecules are attached, besides the two GlcNAc. The complex type contains multiple GlcNAc as well as different saccharides. In the hybrid form are branches with mannose and some with complex saccharides (Lodish et al. 2000).

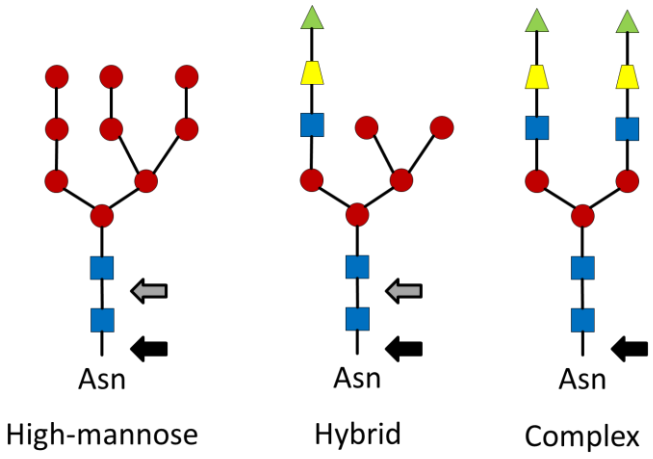


**Figure 6: Types of N-glycans.** The main structure is conserved in all oligosaccharide forms, $Man_3(GlcNAc)_2$ at the asparagine residue of the protein (GlcNAc: blue square; Man: red circle). The high-mannose type has only mannose attached. Within the complex form many different saccharides (colored forms) can be added. In the hybrid glycan, there is a mannose and a complex branch. PNGaseF digestes all forms from the protein (black arrow), whereas EndoH cleaves between the two GlcNAc leaving one at the protein (grey arrow) (modified after Stanley et al. 2009).

$Man_{7\text{-}9}(GlcNAc)_2$ exits the ER and is further processed by compartment specific enzymes in *cis*, *medial* and *trans* Golgi. Within the *medial*-Golgi, synthesis of hybrid- and complex-glycans is initiated by the N-acetylglucosyl transferase-I (GlcNAcT-I). After that, mannosidase II cleaves the α(1->3) and α(1->6) Man molecules. Now in the *trans*-Golgi, GlcNAc-II can attach other GlcNAc residues to form complex glycans. Another common modification of hybrid and complex glycans is the fucosylation of the Core GlcNAc residue. (Stanley et al. 2009).

Depending on the co-/post-translational protein folding, not all Asn-X-Ser/Thr sequences are oligosaccharide acceptors and not all glycosylations are modified within the Golgi - some can be shielded by conformational or other constrains. Additionally, the modification type also depends on the accessibility of the protein to the different glycosidases and by extension, is influenced by whether the protein travels through the Golgi at all (Lodish et al. 2000).

To gain knowledge about certain types of glycans enzyme-specific cleavage properties can be used. For discrimination between complex and high-mannose oligosaccharides, two enzymes can be applied. First of all, the amidase PNGase F, a peptide-N-glycosidase F, cleaves the whole branched glycan from the asparagine within the protein. Second, the Endoglycosidase H cleavage is specialized to certain glycan structures. It releases only high-mannose and hybrid N-glycans from the protein, thereby leaving the first GlcNAc at the asparagine side chain intact (Stanley et al. 2009).

## 2.3 Aims and objectives

In the last decades, research on hepatitis C virus has given many insights into important entry factors, translation, protein functions and the HCV replication cycle, but still little is known about the assembly and release of HCV particles. The complexity of this process, along with these late steps of the viral life cycle, is partially due to the coverage within the membranous web and the association with cellular membranes as well as monolayered lipid droplets. To date, the assembly site is theorized to be on or nearby lipid droplets, but the exact mechanism remains to be revealed. Moreover, the described association of HCV particles with low density lipoproteins gives rise to several questions about the interaction mechanism and the transport pathway within the cell.

Thus, the aim of this thesis is to further elucidate the late steps of HCV propagation. In particular, the presented work should improve the understanding of HCV release and shed light onto the intracellular pathway that HCV hijacks or modifies for its transport route. Therefore, a fluorescently-labeled HCV genome with a mCherry introduced into the surface protein E1 should be comprehensively characterized. The advantage of this tool is the visualization of structural proteins within the cell and the possibility to monitor assembly as well as assembled virus particles in live cell microscopy, without the need for further treatment or staining. Additionally, in combination with a tag for replication proteins, it is possible to discriminate between translation sites and virus assembly. Moreover, biochemical methods should be applied in combination with innovative microscopy techniques to reveal HCV passage and processing during release. Therewith, the ultimate goal of my thesis was to shed light onto the compartments HCV passes through during its release.

# 3 Material

## 3.1 Nucleotides

### 3.1.1 Oligonucleotides

| Name | Sequence | Target gene |
|---|---|---|
| HCV fw | 5’ gctagccgagtagcgttgggt 3‘ | 5'NCR (JFH+JC1) recognition |
| HCV rev | 5’ tgctcatggtgcacggtctac 3‘ | 5'NCR (JFH+JC1) recognition |
| HCV probe | 5’ FAM (Fluorescein)-tactgcctgatagggcgcttgcgagtg-TAMRA 3‘ | 5'NCR (JFH+JC1) recognition (between HCV fw and rev) |
| 5´pFK-AgeI | 5’ g*aaccggt*gagtacaccggaattgc 3‘ | JC1 5'NCR AgeI site recognition |
| 3´pFK-AgeI_E1 | 5’ ag*accggt*atccagcactgagatgc 3‘ | JC1-E1 AgeI site recognition |
| 5’pFK-JC1-E1_A4 | 5’ *gaagtgaagaa*cagcagtggcctctaccatgtg actaacgactgc 3‘ | H77 strain A4-sequenz in JC1 |
| 3’pFK-JC1-E1_A4 | 5’ gcagtcgttagtcacatggtagaggccactgct*gt tcttcacttc* 3‘ | H77 strain A4-sequenz in JC1 |
| 5'pFK_fw | 5’ tgtcgtacagcctccaggc 3‘ | Sequencing before 5’NCR AgeI site |
| 5'pFK-E1_fw | 5’ tcctggaggacggggttaatt 3‘ | Sequencing in E1 AgeI site |

Oligonucleotides were synthesized at metabion GmbH (Martinsried, Germany).

### 3.1.2 Other nucleotides

DNA ladder: 1kb Gene Ruler$^{TM}$ DNA Ladder Mix Fermentas GmbH (St. Leon-Rot, Germany)

PCR nucleotides: dNTPs Stratagen (La Jolla, USA)

## 3.2 Plasmids

### 3.2.1 HCV Plasmid

The utilized low copy number plasmids are all in the pFK vector including an ampicillin cassette and the HCV JC1 chimera (Lohmann et al. 2001). The HCV chimera C-846 J6 / 3´ JFH1 designated JC1 consist from two genotype 2a isolates with the 5' proteins from Core to the first TM-domain of NS2 originate from J6CF (Yanagi et al. 1999) and proteins after the first TM domain of NS2 to NS5B derive from JFH1 (Wakita et al. 2005).

| **Name** | **Description** | **Reference** |
|---|---|---|
| pFK_JC1 | Wild-type JC1 virus | (Pietschmann et al. 2006) |
| pFK_JC1-FlagE2 | Virus with a Flag tagged E2 protein | T. Pietschmann, TwinCore, Hannover, Germany |
| pFK_JC1-GFP-NS5A | Reporter virus with a GFP gene in the third domain of the NS5A protein between codon 382 and 383 | (Schaller et al. 2007) |
| pFK_JC1-GFP-NS5A/mCherry-E1 | Double labeled virus based on pFK_JC1-GFP-NS5A with a mCherry gene near the carboxy-terminus of E1 upstream of the transmembrane region | PhD thesis Carina Banning, 2011 |
| pFK_JC1-mCherry-E1 | Reporter virus with a mCherry gene near the carboxy-terminus of E1 upstream of the transmembrane region | PhD thesis Carina Banning, 2011 |
| pFK_JC1(A4) | Wild-type JC1 virus with the A4 sequence of the H77 strain in the E1 protein | chapter 4.1.11 |
| pFK_JC1(A4)-GFP-NS5A | Reporter virus with a GFP gene in NS5A and the A4 sequence of the H77 strain in the E1 protein | chapter 4.1.11 |
| pFK_JC1(A4)-GFP-NS5A/mCherry-E1 | Double labeled virus with the A4 sequence of the H77 strain in the E1 protein | chapter 4.1.11 |

| | | |
|---|---|---|
| pFK_JC1(A4)-mCherry-E1 | Reporter virus with a mCherry gene and the A4 sequence of the H77 strain in the E1 protein | chapter 4.1.11 |
| pFK_JC1(A4)-mCherry-E1_FlagE2 | Virus with a Flag tagged E2 protein and the A4 sequence of the H77 strain in the E1 protein | chapter 4.1.11 |

### 3.2.2 Expression plasmids

| **Name** | **Description** | **Origin/Reference** |
|---|---|---|
| pmCFP-C1 GalT | Marker for Golgi; modified pmCFP-C1 vector contains a fragment of β-1,4-galactosyltransferase fused to mCFP | P. Bastiaens, Max Planck Institute of Molecular Physiology, Dortmund (Rocks et al. 2010) |
| pOPIN(c)eGFP-EEA1 | Early endosome antigen 1, C-terminal tag for GFP | A. Musacchio, Max Planck Institute of Molecular Physiology, Dortmund, Germany |
| pOPIN(n)eGFP-Rab5A | Marker for early endosomes, N-terminal tag for GFP | |
| pOPIN(n)eCFP-Rab7A | Marker for late endosomes, N-terminal tag for GFP | |
| pOPIN(n)eCFP-Rab9A | Marker for late endosomes, N-terminal tag for GFP | |
| pOPIN(n)eGFP-Rab11A | Marker for recycling endosomes, N-terminal tag for GFP | |
| GFP-VSVG | Glycoprotein of the vesicular stomatitis Indiana virus (VSV), tagged with GFP | F. Perez, Institute Curie, Paris, France |
| pECFP-C1 CD74(li) | MHCII chaperon, which blocks the antigen binding pocket during intracellular transport, fused to CFP | M. Schindler, unpublished |

| | | |
|---|---|---|
| pSVBX24h mCherry-L5-S | Hepatitis B Virus small antigen, N-terminally fused to mCherry | V. Bruß, Helmholtz Zentrum, Munich, Germany |
| pSVBX24h-L5-S | Hepatitis B Virus small antigen | |
| GFP-ApoE | Apolipoprotein E tagged with GFP | G. Randall, The University of Chicago, Chicago, IL/USA (Coller et al. 2012) |

## 3.3 Bacteria Strains

OneShot®Top10 Life Technologies GmbH, Invitrogen; Darmstadt, Germany)

Chemically competent Escherichia coli (F-mcrA Δ (mrr-hsdRMS-mcrBC) ϕ80lacZΔM15 ΔlacX74 recA1 araD139 (araleu) 7697 galU galK rpsL (StrR) endA1 nupG

## 3.4 Eukaryotic Cell Line

Huh 7.5 (Blight, McKeating, and Rice 2002)
human hepatoma cell line, permissive for HCV replication

## 3.5 Media

### 3.5.1 Media for bacteria

| **Name** | **Ingredients** |
|---|---|
| Luria-Bertani (LB)-Medium | 10g/l Bacto-Trypton, 5g/l Bacto-Yeast extract,<br>8g/l NaCl, 1g/l Glucose, 100mg/l ampicillin or canamycin, pH = 7.2 |
| Luria-Bertani (LB)-Agar plates | 15g agar was dissolved in 1l LB-medium and autoclaved. After cooling to 55°C, 1 mg/mL ampicillin was added |
| SOC-Medium | 20g/l Bacto-Trypton, 5g/l Yeast extract,<br>2.5mM NaCl, 10mM MgCl2, 10mM MgSO4, 20mM Glucose (Life Technologies GmbH, Invitrogen; Darmstadt, Germany) |

### 3.5.2 Media for cell culture

| Name | Ingredients |
|---|---|
| DMEM | Dulbecco's modified Eagle Medium + GlutaMAX™-I supplemented with 10% [v/v] heat inactivated FCS, 1 mM sodium pyruvate, 120 µg/mL penicillin/ streptomycin and 1% [v/v] MEM non-essential amino acids (NEAA) (Life Technologies GmbH, Gibco; Darmstadt, Germany) |

### 3.5.3 Additives for cell culture media

| Name | Manufacturer |
|---|---|
| DMSO | Merck KGaA (Darmstadt) |
| Fetal calf serum (FCS), heat-inactivated | Life Technologies GmbH, Gibco (Darmstadt, Germany) |
| MEM non-essential amino acids (NEAA) | Life Technologies GmbH, Gibco (Darmstadt, Germany) |
| Penicillin/Streptomycin | PAA Laboratories GmbH (Cölbe, Germany) |

## 3.6 Enzymes

### 3.6.1 Restriction enzymes

Restriction endonucleases were purchased from New England Biolabs GmbH (Frankfurt, Germany) or Fermentas GmbH (St. Leon-Rot, Germany) and used with the buffer systems approved by the manufacturer.

### 3.6.2 Other enzymes

| Name | Manufacturer |
|---|---|
| 0.05% Trypsin-EDTA | Life Technologies GmbH, Gibco (Darmstadt, Germany) |
| Dream Taq™ DNA polymerase | Fermentas GmbH (St. Leon-Rot, Germany) |
| FastAP™ | Fermentas GmbH (St. Leon-Rot, Germany) |

## 3.7 Inhibitors

RNasin® Plus RNase Inhibitor Promega GmbH (Mannheim, Germany)

## 3.8 Antibodies

### 3.8.1 Primary Antibodies

| Antigen | Description | Dilution | Manufacturer/ Reference |
|---|---|---|---|
| HCV Core | monoclonal mouse antibody (clone C7-50), detects aa21-40 of HCV Core | IF/FACS 1:100<br>WB 1:1000 | Abcam (Cambridge, UK) |
| HCV E2 | broad range neutralizing monoclonal mouse antibody (clone AP33) | IF/FACS 1:100<br>WB 1:1000 | Genentech, Inc. (San Francisco, USA); (Owsianka et al., 2005) |
| HCV E1(A4) | monoclonal mouse antibody detects the A4 sequence of H77 strain E1 | IF/FACS 1:100<br>WB 1:1000 | (Dubuisson et al. 1994) |
| HCV NS5A | monoclonal mouse antibody (clone 2F6/G11) detects aa2054-2295 of HCV genome | IF 1:100<br>WB 1:1000 | IBT GmbH (Binzwangen, Germany) |
| HCV NS3 | monoclonal mouse antibody detects AA1322-1662 of HCV genome | IF: 1:100<br>WB: 1:1000 | T. Pietschmann, TwinCore, Hannover, Germany |
| Flag tag | monoclonal mouse antibody detects the Flag-sequence | FACS 1:100<br>WB: 1:1000 | Sigma-Aldrich, Chemie GmbH (Munich, Germany) |
| Anti-FLAG M2 Affinity gel<br><br>Flag peptide | monoclonal mouse antibody covalently attached to agarose, detects the Flag-sequence<br><br>FLAG peptide sequence DYKDDDDK,<br>for the elution of Flag-tagged proteins | IP:<br>30 µL/sample<br><br>250 µg/ml | Sigma-Aldrich, Chemie GmbH (Munich, Germany) |

| | | | |
|---|---|---|---|
| β-actin | loading control for Western Blot, monoclonal mouse antibody (clone AC-15) | WB 1:5000 | Sigma-Aldrich, Chemie GmbH (Munich, Germany) |
| α-GFP | polyclonal rabbit antibody detects GFP, and its variants EGFP, RFP, YFP, and CFP, etc | IF: 1:100 | BioVision, Inc. (Milpitas, California, USA) |
| α-mCherry | polyclonal rabbit antibody detects mCherry | IF: 1:100<br>WB: 1:1000 | BioVision, Inc. (Milpitas, California, USA) |
| α-HB1 (HBV-S) | monoclonal mouse antibody detects aa 120-125 of the small surface antigen of HBV | WB: 1:1000 | D. Glebe, Medizinische Virologie, Justus-Liebig-Universität Gießen, Gießen, Germany |

### 3.8.2 Secondary Antibodies

| **Name** | **Dilution** | **Manufacturer/Reference** |
|---|---|---|
| IRDye® 800 goat anti-mouse IgG (H+L) | 1:5000 | LI-COR Biosciences GmbH (Bad Homburg, Germany) |
| IRDye® 680 goat anti-rabbit IgG (H+L) | 1:5000 | LI-COR Biosciences GmbH (Bad Homburg, Germany) |
| Alexa Fluor® 488 goat anti-mouse IgG (H+L) | 1:200 | Life Technologies GmbH, Invitrogen (Darmstadt, Germany) |
| Alexa Fluor® 555 goat anti-mouse IgG (H+L) | 1:200 | Life Technologies GmbH, Invitrogen (Darmstadt, Germany) |
| Alexa Fluor® 633 goat anti-mouse IgG (H+L) | 1:200 | Life Technologies GmbH, Invitrogen (Darmstadt, Germany) |
| Goat anti-mouse HRP | 1:10000 | Dianova GmbH (Hamburg, Germany) |
| Goat anti-rabbit HRP | 1:10000 | Dianova GmbH (Hamburg, Germany) |

## 3.9 Reagents

### 3.9.1 Reagent systems (kits)

| Name | Manufacturer |
|---|---|
| Caspase-Glo® 3/7 Assay | Promega GmbH (Mannheim, Germany) |
| Developer G153 A/B | AGFA Gevaert N.V. (Mortsel, Belgium) |
| Luziferase Assay System | Promega GmbH (Mannheim, Germany) |
| Lysisbuffer (P2) | Qiagen (Hilden, Germany) |
| Neutralisationbuffer (P3) | Qiagen (Hilden, Germany) |
| NucleoSpin® RNA | Macherey Nagel GmbH & Co.KG (Düren, Germany) |
| OneStep RT-PCR Kit | Qiagen (Hilden, Germany) |
| Duolink® in vitro PLA® Olink AB | Sigma-Aldrich, Chemie GmbH (Munich, Germany) |
| Plasmid Midikit (25) | Qiagen (Hilden, Germany) |
| PureYield™ Plasmid Midiprep | Promega GmbH (Mannheim, Germany) |
| RapidFixer G354 | AGFA Gevaert N.V. (Mortsel, Belgium) |
| Resuspensionbuffer (P1) | Qiagen (Hilden, Germany) |
| SuperSignal® West Pico/Femto | Thermo Fisher Scientific (Waltham, USA) |
| T7 RiboMAX™ Express Large Scale RNA Production System | Promega GmbH (Mannheim, Germany) |
| TA Cloning® Kit | Life Technologies GmbH, Invitrogen (Darmstadt, Germany) |
| Takara DNA Ligationkit | Böhringer Ingelheim (Heidelberg, Germany) |
| UltraClean® 15 DNA Purification Kit | Dianova GmbH (Hamburg, Germany) |
| Wizard® DNA Clean-Up System | Promega GmbH (Mannheim, Germany) |

### 3.9.2 Buffers and Solutions

| Name | Ingredients |
|---|---|
| 10x DreamTaq Buffer | Fermentas GmbH (St. Leon-Rot, Germany) |
| 1x PBS | 1.37 M NaCl, 27 mM KCl, 12 mM $KH_2PO_4$, 65 mM $Na_2HPO_4x2H_2O$ (pH 7.4) |
| 20% sucrose solution | 20% [w/v] Sucrose in PBS, sterile filtration |
| 2x RNA loading buffer | Thermo Fisher Scientific (Waltham, USA) |
| 50x TAE | 500 mM Tris-HCl, 250 mM sodium acetate, 50 mM $Na_2EDTA$ |
| 6x DNA loading dye | Thermo Fisher Scientific (Waltham, USA) |
| CoIP lysis buffer | 0.05 M Tris, 0.15 M NaCl, 1 mM EDTA, pH 7.4, 1% Triton X-100 and fresh protease inhibitor |
| CoIP wash buffer | 0.05 M Tris, 0.15 M NaCl, pH 7.4 |
| Cytomix | 120 mM KCl, 0.15 mM $CaCl_2$, 10 mM $K_2HPO_4/KH_2PO_4$ (pH 7.6), 25 mM Hepes, 2 mM EGTA, 5 mM $MgCl_2$; pH adjusted to 7.6 with KOH; sterile filtration; before electroporation addition of 2 mM ATP (pH 7.6) and 5 mM Glutathione (pH 7.6) |
| DEPC Water | 0.5% [v/v] DEPC in $H_2O_{dest}$ incubated overnight and autoclaved |
| FACS Buffer | 1% [v/v] FCS in PBS |
| Mowiol | 0.2 M Tris-HCl, pH 8.5; 12% [w/v] Mowiol 4-88; 30% [w/v] glycerol |

#### 3.9.2.1 Western Blot and Proteins

| Name | Ingredients |
|---|---|
| Block Buffer | 10% powdered milk in PBS |
| 5x SDS loading buffer | 250 mM Tris-HCl (pH 6.8), 50% [v/v] glycerol, 15% [w/v] SDS, 0.01% [w/v] bromophenol blue, 25% [v/v] β-mercaptoethanol |
| PBS-T | 0.1% Tween20 in PBS |

| | |
|---|---|
| Ponceau S | 0.1% [w/v] Ponceau S; in 5% acetic acid |
| Protein Ladder | PageRuler™ Plus Prestained Protein ladder (Thermo Fisher Scientific, Waltham, USA) |
| RIPA Buffer | 150 mM NaCl, 50 mM Tris-HCl (pH 8), 1% [v/v] Nonidet P-40, 0.5% [w/v] sodium desoxycholate, 0.1% [w/v] SDS, 5 mM EDTA |
| SDS running buffer | 25 mM Tris, 192 mM glycine, 0.1% [w/v] SDS |
| Transfer buffer | 25 mM Tris, 192 mM glycine, 20% [v/v] MeOH, 0.05% [w/v] SDS |

### 3.9.3 Chemicals

| **Name** | **Manufacturer** |
|---|---|
| 2-Mercaptoethanol | Merck KGaA (Darmstadt, Germany) |
| 30% Acrylamide-bis solution (37.5:1) | Merck KGaA (Darmstadt, Germany) |
| Agar | Carl Roth® GmbH & Co.KG (Karlsruhe, Germany) |
| Agarose | Carl Roth® GmbH & Co.KG (Karlsruhe, Germany) |
| Ampicillin | Ratiopharm GmbH (Ulm, Germany) |
| APS (Ammoniumperoxdisulfate) | Sigma-Aldrich, Chemie GmbH (Munich, Germany) |
| Bacto-Trypton | BD Biosciences Pharmingen (San Diego, USA) |
| Bovine serum albumin (BSA) | Sigma-Aldrich, Chemie GmbH (Munich, Germany) |
| Brom phenole blue | SERVA (Heidelberg, Germany) |
| cOmplete, ULTRA, Mini EDTA-free, EASYpack | Roche GmbH (Mannheim, Germany) |
| DAPI (4',6-diamidin-2-phenylindole, dihyrochlorid) | Life Technologies GmbH, Invitrogen (Darmstadt, Germany) |
| DEPC (Diethylpyrocarbonat) | Carl Roth® GmbH & Co.KG (Karlsruhe, Germany) |
| DMSO (Dimethylsulfoxid) | Sigma Aldrich (St. Louis, USA) |

| | |
|---|---|
| Ethanol (EtOH) | Carl Roth® GmbH & Co.KG (Karlsruhe, Germany) |
| Ethidiumbromid | Carl Roth® GmbH & Co.KG (Karlsruhe, Germany) |
| Glycerol | Carl Roth® GmbH & Co.KG (Karlsruhe, Germany) |
| Glycine | Carl Roth® GmbH & Co.KG (Karlsruhe, Germany) |
| $H_2O$ nuclease free | Promega GmbH (Mannheim, Germany) |
| $H_2O_2$, 30% | Sigma-Aldrich, Chemie GmbH (Munich, Germany) |
| HCL (hydrochloric acid) | AppliChem GmbH (Darmstadt, Germany) |
| HCl (Hydrogen chloride) | AppliChem GmbH (Darmstadt, Germany) |
| Hepes | Carl Roth® GmbH & Co.KG (Karlsruhe, Germany) |
| IPTG | Carl Roth® GmbH & Co.KG (Karlsruhe, Germany) |
| Isopropanol | Carl Roth® GmbH & Co.KG (Karlsruhe, Germany) |
| $K_2HPO_4$ | Merck KGaA (Darmstadt, Germany) |
| Kanamycin | Ratiopharm GmbH (Ulm, Germany) |
| KCl (Potassium chloride) | Merck KGaA (Darmstadt, Germany) |
| $KH_2PO_4$ | Merck KGaA (Darmstadt, Germany) |
| KOH (Potassium hydroxide) | Carl Roth® GmbH & Co.KG (Karlsruhe, Germany) |
| LB-agar | Carl Roth® GmbH & Co.KG (Karlsruhe, Germany) |
| LB-medium | Carl Roth® GmbH & Co.KG (Karlsruhe, Germany) |
| L-Glutathione reduced | Carl Roth® GmbH & Co.KG (Karlsruhe, Germany) |
| Methanol | Sigma-Aldrich, Chemie GmbH (Munich, Germany) |
| $MgCl_2$ (Magnesium chloride) | Carl Roth® GmbH & Co.KG (Karlsruhe, Germany) |
| Mowiol 4-88 | Carl Roth® GmbH & Co.KG (Karlsruhe, Germany) |
| MTT Thiazolyl Blue Tetrazolium Bromide | Sigma-Aldrich, Chemie GmbH (Munich, Germany) |

| | |
|---|---|
| $Na_2HPO_4$ | Merck KGaA (Darmstadt, Germany) |
| NaCl (sodium chloride) | Carl Roth® GmbH & Co.KG (Karlsruhe, Germany) |
| NaOH (sodium hydroxide) | Carl Roth® GmbH & Co.KG (Karlsruhe, Germany) |
| Nonidet P-40 | Sigma-Aldrich, Chemie GmbH (Munich, Germany) |
| OptiPrep™ | Axis-Shield GmbH (Heidelberg, Germany) |
| PFA (Paraformaldehyde) | Carl Roth® GmbH & Co.KG (Karlsruhe, Germany) |
| Ponceau S | AppliChem GmbH (Darmstadt, Germany) |
| Protein G PLUS-Agarose | Santa Cruz Biotechnolog, Inc. (Heidelberg, Germany) |
| Roti®-C/I Chloroform/Isoamyl alcohol (24:1, v/v) | Carl Roth® GmbH & Co.KG (Karlsruhe, Germany) |
| saponin | Carl Roth® GmbH & Co.KG (Karlsruhe, Germany) |
| SDS Ultrapure (Sodium dodecyl sulfate) | Carl Roth® GmbH & Co.KG (Karlsruhe, Germany) |
| Skim milk powder | Carl Roth® GmbH & Co.KG (Karlsruhe, Germany) |
| Sodium acetat | Promega GmbH (Mannheim, Germany) |
| Sodium acetate | Promega GmbH (Mannheim, Germany) |
| Sodium desoxycholate | Sigma-Aldrich, Chemie GmbH (Munich, Germany) |
| Sucrose, Ultrapure Bioreagent | Avantor Performance Materials (Deventer, The Netherlands) |
| TEMED (N,N,N',N'-Tetramethylethylenediamine) | Sigma-Aldrich, Chemie GmbH (Munich, Germany) |
| Tris (Tris[hydroxymethyl]aminomethane) | Carl Roth® GmbH & Co.KG (Karlsruhe, Germany) |
| Triton X-100 | Carl Roth® GmbH & Co.KG (Karlsruhe, Germany) |
| Tween 20 | Carl Roth® GmbH & Co.KG (Karlsruhe, Germany) |
| UltraPure™ Phenol:Chloroform:Isoamyl | Life Technologies GmbH, Invitrogen (Darmstadt, |

| | |
|---|---|
| Alcohol (25:24:1, v⁄v) | Germany) |
| X-Gal (5-bromo-4-chloro-3-indolyl-β-D-galactopyranoside) | Carl Roth® GmbH & Co.KG (Karlsruhe, Germany) |

## 3.10 Laboratory Equipment

| **Name** | **Manufacturer** |
|---|---|
| Aspiration system, VACUSAFE | IBS/INTEGRA Biosciences GmbH (Fernwald, Germany) |
| Centrifuge, Heraeus™ Megafuge™ 40 | Thermo Fisher Scientific (Waltham, USA) |
| Centrifuge, Heraeus™ Pico™ 21 Microcentrifuge | Thermo Fisher Scientific (Waltham, USA) |
| Centrifuge, Rotina 420 R | Hettich GmbH & Co.KG (Tuttlingen, Germany) |
| $CO_2$ incubator, Heracell 150i | Thermo Fisher Scientific (Waltham, USA) |
| Flow cytometer, FACSCanto II / FACSAria IIu™ | B&D, Becton Dickinson, Immuncytometry Systems (San José, USA) |
| Flow HERAsafe | Thermo Fisher Scientific (Waltham, USA) |
| Gene Pulser Xcell System Electroporator | Bio-Rad Laboratories GmbH (Munich, Germany) |
| Horizontal electrophoresis system for DNA/RNA separation, OwlTM Gel System | Thermo Fisher Scientific (Waltham, USA) |
| Hotplate stirrer, Variomag MONOTHERM | Thermo Fisher Scientific (Waltham, USA) |
| Imaging system, Gel DocTM XR+ System | Bio-Rad Laboratories GmbH (Munich, Germany) |
| Incubation shaker, Multitron | Infors AG(Bottmingen/Basel, Switzerland) |
| LightCycler® 480 | Roche GmbH (Mannheim, Germany) |
| Manual Dispenser, Multipette® plus | Eppendorf GmbH (Hamburg, Germany) |

| | |
|---|---|
| Microplate reader, Infinite® M200 | Tecan Group Ltd. (Männedorf, Switzerland) |
| Mini Trans-Blot® Cell, Wet blotting system | Bio-Rad Laboratories GmbH (Munich, Germany) |
| Nanodrop 2000c™, UV-Vis Spectrophotometer | Thermo Fisher Scientific (Waltham, USA) |
| Nikon Ti Eclipse equipped with the Perkin Elmer UltraViewVox System (Yokogawa CSU-X1) | Nikon Instruments (New York, USA) PerkinElmer (Massachusetts, USA) |
| Odyssey Imaging System | LI-COR Biosciences GmbH (Bad Homburg, Germany) |
| Odyssey Infrared Imaging System | LI-COR Biosciences GmbH (Bad Homburg, Germany) |
| Optima L7-65 Ultracentrifuge | Beckman Coulter GmbH (Krefeld, Germany) |
| PCR Cycler, Mastercycler® | Eppendorf GmbH (Hamburg, Germany) |
| Pipette controller, PIPETBOY acu | IBS, INTEGRA Bioscience (Zizers, Switzerland) |
| Pipette controller, Pipetus® | Hirschmann Laborgeräte (Eberstadt, Germany) |
| Power Supply, PowerPacTM Basic | Bio-Rad Laboratories GmbH (Munich, Germany) |
| Power Supply, Standard Power Pack P25 | Biometra® Biomedizinische Analytik GmbH (Göttingen, Germany) |
| Rocking and rotating mixer, RM 5-V | Ingenieurbüro CAT (Staufen, Germany) |
| Single and Multi Channel Pipettes, Eppendorf | Eppendorf GmbH (Hamburg, Germany) |
| Special accuracy weighing machine | Sartorius AG, Göttingen |
| SW 28/ SW 55Ti Rotor Package, Swing Bucket | Beckman Coulter GmbH (Krefeld, Germany) |
| Thermomixer® comfort | Eppendorf GmbH (Hamburg, Germany) |
| UV Transilluminator | Bachofer (Reutlingen, Germany) |
| Vertical electrophoresis system for protein separation, Minigel-Twin | Biometra® Biomedizinische Analytik GmbH (Göttingen, Germany) |

| | |
|---|---|
| Vortex Mixer, Vortex Genie®2 T | neoLab Migge Laborbedarf (Heidelberg, Germany) |
| Waving platform shaker, Polymax 1040 | Heidolph Instruments (Schwabach, Germany) |

## 3.11 Consumables

| **Name** | **Manufacturer** |
|---|---|
| Amersham Hyperfilm™ ECL | GE Healthcare (Munich, Germany) |
| Cell culture flasks (25-175 cm²) | Sarstedt AG & Co (Nümbrecht, Germany) |
| Centrifugation Tubes, Polyallomer/Thinwall, Ultra-Clear™(SW28,55Ti) | Beckman Coulter GmbH (Krefeld, Germany) |
| Conical tubes, BD Falcon™ (15-50 mL) | B&D, Becton Dickinson (San José, USA) |
| Cover Slips | Gerhard Menzel GmbH/ Thermo (Braunschweig, Germany) |
| Cryo-Tubes | Sarstedt AG & Co (Nümbrecht, Germany) |
| FACSClean™ | B&D, Becton Dickinson (San José, USA) |
| FACSFlow™ | B&D, Becton Dickinson (San José, USA) |
| FACSRinse™ | B&D, Becton Dickinson (San José, USA) |
| Filter Pipette tips (10-1000µl) | Sarstedt AG & Co (Nümbrecht, Germany) |
| Forceps | A. Dumont & Fils (Montignez, Switzerland) |
| Gene Pulser/Micro Pulser Cuvette, 0.4 cm | Bio-Rad Laboratories GmbH (Munich, Germany) |
| Glass bottles | SCHOTT AG (Mainz, Germany) |
| Microscope slides | Gerhard Menzel GmbH/ Thermo (Braunschweig, Germany) |
| MILLEX GP 0.45 µm filter | Millipore/ Merck Chemicals GmbH (Schwalbach, Germany) |

| | |
|---|---|
| Multiwell culture plates, CELLSTAR® | Greiner Bio-One GmbH (Frickenhausen, Germany) |
| Neubauer counting chamber | W. Schreck (Hofheim, Germany) |
| Nitrocellulose Membran 0.4µm | GE Healthcare (Munich, Germany) |
| Parafilm M | Pechiney Plastic Packaging (Chicago, USA) |
| Reaction tubes (0.5-2 mL) | Sarstedt AG & Co (Nümbrecht, Germany) |
| Serological pipettes | Sarstedt AG & Co (Nümbrecht, Germany) |
| Whatman paper | GE Healthcare (Munich, Germany) |
| WillCo-dish® Glass Bottom Dishes | WillCo Wells B.V. (Amsterdam, The Netherlands) |

## 3.12 Software

| **Name** | **Company** |
|---|---|
| AxioVision Microscope Software | Carl Zeiss Microscopy (Jena, Germany) |
| FACS Diva Software | B&D, Becton Dickinson (San José, USA) |
| GraphPad Prism Software | GraphPad Software (La Jolla, USA) |
| i-control™ Software | Tecan (Männedorf, Switzerland) |
| Image Lab™ Software | Bio-Rad Laboratories (Hercules, UK) |
| Microsoft Excel 2013 | Microsoft Corporation (Redmond, WA/USA) |
| NanoDrop 2000/2000c | Thermo Fisher Scientific (Waltham, USA) |
| Quantity One®, Version 4.6.9 | Bio-Rad Laboratories GmbH (Munich, Germany) |
| Serial Cloner Software | Serial Basics (France) |
| Volocity 6.2 3D Image Analysis Software | PerkinElmer (Waltham, USA) |

# 4 Methods

## 4.1 Molecular biological methods

### 4.1.1 Polymerase chain reaction (PCR)

Polymerase chain reaction (PCR) enables the amplification of a specific DNA sequence. In a repeated thermo-cycle DNA double-strands are denaturized and oligonucleotide primers with a sequence complementary to the template DNA anneal, followed by the elongation of the nascent DNA strand via the heat-stable DNA-polymerase.

In this study the DreamTaq Polymerase was used, which elongates the DNA strands with Poly-A ends and is therefore applicable to TA-vector subcloning. The PCR reaction in 35 cycles was carried out in 50 µL volume with 100-500 ng DNA, 5 µL 10xTaqReactionbuffer, 0.5 µL 100 pmol 5'- and 3' Primer each, 3 µL 10 mmol dNTP-mix and 0.25 µL 5 U/µL polymerase. A schematic PCR cycle is shown in Table 1. As a control PCR fragments were separated via agarose gel.

**Table 1: PCR cycling profile**

| Step | Temperature | Duration | Cycle |
|---|---|---|---|
| Initial denaturation | 96°C | 5 min | 1x |
| Denaturation | 96°C | 45 s | |
| Primer annealing | 64°C | 60 s | 35x |
| Elongation | 72°C | 60 s | |
| Final elongation | 72°C | 15 min | 1x |
| | 4°C | ∞ | |

### 4.1.2 Agarose gel electrophoresis

Gel electrophoresis in 0.6-1% [w/v] TAE-agarose gels was conducted to separate DNA fragments in an electric field by size. Intercalation of ethidium bromide allows visualization of DNA strands under UV-light (λ = 366nm).

### 4.1.3 DNA purification from agarose gels and solutions

For extraction, DNA of interest was cut out of the agarose gel and purified via the UltraClean™ 15 DNA Purification kit according to the manufacturer's instructions. DNA was eluted from the silica milk by addition of 7 or 30 µL deionized $H_2O$ depending on the size of fragment.

### 4.1.4 DNA cleavage by restriction endonucleases

Restriction digests were performed to create overhanging, complementary DNA ends for further cloning of DNA fragments into a vector. Furthermore, digest was performed to verify a specific sequence-length within a vector. The digest was performed for 30 min at 37°C in 20 µL volume with 0.5 µL sequence-specific enzymes, 2 µl of 10x FastDigest Green buffer and 2-5 µL DNA. Vector digest was additionally incubated with 0.5 µL alkaline phosphatase to prevent recircularization.

### 4.1.5 DNA/RNA quantification by spectrophotometry

Concentrations of DNA and RNA were measured with the NanoDrop 2000 spectrophotometer via absorbance at 260 nm.

### 4.1.6 DNA Ligation

The enzymatic activity of ligases is used to join free 3' OH ends to 5' phosphate ends of sticky as well as blunt end dsDNA. Reaction was performed overnight at 14°C according to the manufacturer's instructions by adding plasmid DNA and insert to the ligase solution I of the Takara Kit (Böhringer Ingelheim, Germany) with a ratio of 1:4. Before the transformation of DNA into competent bacteria (4.1.8) Solution III was added with a dilution of 1:10.

### 4.1.7 TA subcloning

Subcloning into the pCR™2.1 vector (Invitrogen) facilitates the ligation of PCR products into a plasmid. Single thymidine repeats at the 3'-site of the linearized vector enable direct attachment of PCR products with poly- adenine 5'-ends without endonuclease digestion. Furthermore, the vector system allows blue/white selection after bacterial transformation based on a β-galactosidase gen. In case of PCR-fragment insertion the gen is disrupted and the X-gal substrate cannot be processed to a blue product. Therefore, the growing bacterial colonies appear to be white.

Reaction was performed overnight at 14°C in 10 µL volume according to the manufacturer's protocol by adding 0.5-4 µL PCR product to 1 µL TA-vector together with 1 µL 10x Reaction Buffer and 1 µl T4 DNA Ligase (5U). After transformation (4.1.8), bacteria were seeded on agar plates with 40 µL IPTG (0.1 M) and 40 µL X-Gal in DMSO (20 mg/mL).

### 4.1.8 Heat shock transformation of competent *E. coli*

Transformation of OneShot®TOP10 chemically competent *E. coli* was done to amplify plasmid DNA. 18 µL bacteria were thawed on ice and incubated for 15 min with 2 µL DNA for attachment at the cell surface. The heat shock at 42°C for 45 sec allows DNA uptake by pore formation. After 2 min recovery on ice, bacteria grew for 30 min at 37°C shacking in SOC-medium. Afterwards they were plated and incubated on LB-agar plates with the corresponding antibiotic for selection of desired DNA plasmid at 37°C overnight. For blue/white selection, X-gal and IPTG were additionally added to the plates.

### 4.1.9 Isolation of plasmid DNA from bacterial suspensions

One colony of an agar plate was incubated in a suspension culture overnight at 37°C shacking to amplify plasmid DNA. Depending on the resistance cassette of the plasmid 100 µg/mL ampicillin and 50 µg/mL kanamycin were added respectively to 5 mL LB-medium for mini- or 100 mL for midi-cultures. Both were centrifuged at 4000 rpm 30 min at 4°C prior to DNA extraction via alkaline bacteria lysis (Birnboim and Doly 1979) followed by purification.

#### 4.1.9.1 Midi preparation

For large quantities of DNA, extraction was done via Plasmid Midikit (25, Qiagen) or PureYield™ Plasmid Midiprep Kit with silica-membrane columns according to the manufacture's recommendations respectively. DNA was eluted in 500 µL DNase free $H_2O$. Quality was confirmed by NanoDrop (4.1.5) and agarose gel (4.1.2).

#### 4.1.9.2 Mini preparation

For small quantities of DNA extraction was done with Buffers from Qiagen. Bacterial pellet was solved in 300 µL cold resuspension buffer (P1) and lysed after mixing with 300 µL lysis buffer (P2). Neutralization was achieved by addition of 300 µL buffer P3. After centrifugation at 14000 rpm for 30 min at 4°C supernatant was vigorously mixed with 500 µl isopropanol and incubated for 5 min at RT. Following another centrifugation for 45 min, precipitated DNA was washed with 70% EtOH and centrifuged for 5 min. The pellet was dissolved in 50 µL $H_2O$ after 1 hour of drying top to bottom. Appropriate insertion of the DNA fragment was confirmed by restriction digest (4.1.4) and agarose gel 4.1.2).

### 4.1.10 DNA sequencing

Sequencing was done by Eurofins MWG Operon (Ebersberg, Germany) to verify the integrity of DNA sequences. DNA was diluted to 100 ng/µL in 15 µl deionized $H_2O$. The corresponding primers (section 3.1.1) were diluted to 10 pmol in 15 µl $H_2O$.

### 4.1.11 Molecular cloning - Reconstitution of the A4-sequence

Since no antibody is available for the E1 protein of HCV JC1 (J6, genotype 2a), there is the possibility of site directed mutagenesis with the help of SOE-PCR (splicing by overlap extension) to introduce the substitutions I197S, T199G, G200L and M202H. For this method a pair of 5' and 3' end primer flanking the E1-protein within the JC1-genome is needed. In this study primer for the AgeI-endonuclease sequence within the 5'NCR and one in the C-terminal part of E1 were used (5´pFK-AgeI, 3´pFK-AgeI_E1, 3.1.1). Furthermore, a primer pair with the A4-sequence of H77 covering the resembling site in JC1-E1 is essential (5'pFK-JC1-E1_A4, 3'pFK-JC1-E1_A4, 3.1.1). The first PCRs generated two constructs ranging from the respective end to the mutated sequence. Since both PCR products contain the mutated sequence, they can overlap within the next PCR resulting in one amplification reaching from one AgeI site to the other, including the mutated sequence in the middle of the product. Thereafter, the DNA was separated on an agarose gel (4.1.2), extracted (4.1.3) and ligated into a TA vector (4.1.7). The DNA was sequenced to prove the correct mutations (4.1.10). This construct was digested with AgeI enzymes (NEB) (4.1.4) and the correctly mutated DNA was ligated into the original JC1 vector (4.1.6; 3.2.1). This reconstituted sequence can by recognized by an anti-E1 Mab A4 (Dubuisson et al. 1994).

### 4.1.12 *In vitro* transcription and RNA isolation

For the production of HCV virus within the permissive cell line Huh7.5 (+)ssRNA has to be transcribed *in vitro* (modified after (Kato et al. 2006)) and transfected into the cells. During transcription the T7 RNA polymerase binds the T7 promoter producing viral-genomic RNA till it is stopped via the terminator and the ribozyme cuts out unnecessary vector sites e.g. the ampicillin cassette (Koutsoudakis et al. 2006). The (+)ssRNA of HCV therefore starts with the 5'-non-coding region and ends with its 3'-NCR.

After 3 hours digest of 10 µg pFK vector using 2 µL of the restriction enzyme MluI (NEB) and another 0.5 µL after 1.5 h in 100 µL volume at 37°C, the vector is linearized after its T7 terminator-sequence, right after the ribozyme. The plasmids were cleared with the Wizard® DNA Clean-Up System or the NucleoSpin® Gel and PCR Clean-up Kit (Macherey-Nagel) according to the manufacturer's protocol. The DNA was eluted with 30 µL nuclease-free water and stored at -80°C to prevent recircularization.

The *in vitro* transcription was performed with 1 µg linearized DNA in 8 µL nuclease-free water, 10 µL 2x Express Buffer and 2 µL Express T7 Enzyme Mix, with the addition of 1 µL RNasin® Plus RNase Inhibitor at 37°C for 30 min following the instructions of T7 RiboMAX™ Express Large Scale RNA Production System (Promega). Isolation of RNA was assessed by phenol/chloroform extraction. After addition of 78 µL RNase free $H_2O$, 1 volume (100 µL) UltraPure™ Phenol:Chloroform:Isoamyl Alcohol

(25:24:1, v/v) was added and vigorously mixed for 1 min. Following a centrifugation at 14000 rpm for 2 min the RNA-containing aqueous phase on top was separated and mixed with 1 volume Chloroform:Isoamyl (24:1, v/v). Another centrifugation step was done and the upper phase again was separated and incubated on ice for 5 min with a mixture of 1 volume isopropanol with 0.1 volume 3 M sodium acetat. After 10 min centrifugation at 4°C the precipitated RNA was washed with 70% EtOH and afterwards dried at RT for 2 min before resuspension in 20 µL RNase free $H_2O$.

Complete vector linearization and RNA production was verified by agarose gel with DEPC water (4.1.2). Both nucleotide concentrations were assessed by NanoDrop (4.1.5) and preparations were stored at -80°C.

### 4.1.13 RNA isolation from cells and supernatant

To quantify viral RNA out of electroporated or infected cells as well as their supernatant by quantitative reverse-transcription polymerase chain reaction (qRT-PCR) (4.1.14) it has to be isolated. Therefore the NucleoSpin RNA Kit (Macherey Nagel) was used according to the supplier's protocol. Either cells or 100 µL supernatant were lysed with 350 µL RA1 buffer (including 3.5 µL 2-mercaptoethanol) by vortexing. Afterwards lysates were cleared over the provided column and furthermore bound on the second one, followed by washing steps with an ethanol containing buffer and removal of contaminating DNA by digestion. Elution was performed with 30 µL $H_2O$ and samples were stored at -80°C.

### 4.1.14 RNA quantification by qRT-PCR

For amplification and quantification of viral RNAs within cells or their supernatant by quantitative reverse-transcription polymerase chain reaction (qRT-PCR) the OneStep RT-PCR Kit (Qiagen) was used. In this approach viral RNA isolated by the NucleoSpin RNA Kit (Macherey Nagel) (4.1.13) is reverse transcribed and amplified in the same reaction mix. As the reaction progresses the amplified DNA is detected in real time. For this purpose a sequence specific DNA probe coupled to a fluorescent marker was used. The probe hybridizes to the complementary DNA strand during PCR while the 5' endonuclease activity of the polymerase cleaves the oligonucleotide, leading to a separation of fluorescent-marker and quencher molecule and therefore to a signal showing specific amplification. The fractional PCR cycle number at which the detection level exponentially overgrows the threshold for the first time, is known as the cycle threshold (Ct). It is used for calculating the expanse of product.

4 µL of isolated RNA samples as well as a predefined standard dilution series of *in vitro* transcribed HCV-RNA are mixed with 0.4 µM (final) of HCV-5' NCR specific primers (HCV fw, HCV rev, 3.1.1), 0.2 µM (final) DNA probe (HCV probe, 3.1.1) as well as 0.1 µL enzyme mix and 2 µL 5x reaction buffer.

After reverse transcription in the LightCycler® 480 (Roche) samples are heated to 95°C for 15 minutes to activate the DNA polymerase and simultaneously inactivate the reverse transcriptase. Therewith, the following PCR is initiated for 45 cycles like depicted in Table 2. The absolute quantification was done with the help of a standard curve and the calculation of the absolute number of viral RNA copies within the samples.

**Table 2: qRT-PCR profile**

| Step | Temperature | Duration | Cycle |
|---|---|---|---|
| Reverse transcription | 50°C | 20 min | 1x |
| Activation of Taq Pol | 95°C | 5 min | 1x |
| Cycling | 95°C<br>60°C | 15 s<br>45 s | 45x |
| Cooling | 40°C | 5 min | 1x |

## 4.2 Cell biological methods

### 4.2.1 Cultivation and passage of eukaryotic cells

The human hepatoma cell line Huh7.5 was cultivated in appropriate medium (3.5.2) at 37°C in a 5% $CO_2$ atmosphere in a humidified cell culture incubator. The monolayer was cultivated in 125 cm2 flasks up to 80% confluence. Cells were passaged 3 times a week in a 1:3 dilution by 5 min incubation with Trypsin/EDTA. The proteolytic activity was stopped by medium addition. For seeding, cells were counted in a Neubauer counting chamber and diluted corresponding to the experiment planned.

### 4.2.2 Cryopreservation and thawing of cells

For preservation cells were detached and counted. After centrifugation at 900 rpm for 5 min cells were resuspended in an appropriate volume of 10% [v/v] DMSO, 40% [v/v] FCS and 50% DMEM to achieve a cell density of 2x 10^6/mL for each cryo-tube. Tubes were immediately frozen at -80°C and one day later in liquid nitrogen.

For thawing, cells were warmed pretty quick and transferred to 30 mL pre-warmed culture medium. Moreover cells were spun down to wash out DMSO, resuspended in fresh medium and cultivated in a 25 cm² flask.

### 4.2.3 Transfection of Huh 7.5 cells

For introduction of DNA or RNA into eukaryotic cells transient pores must build up in the cellular membrane. This can be achieved for example through electroporation, chemical-based transfection or lipid-based transfection.

#### 4.2.3.1 Electroporation

Huh7.5 cells were transfected with *in vitro* transcribed (+)ssRNA or cotransfected with DNA by electroporation (modified after (Kato et al. 2006)).

Cells were detached, washed two times with PBS and centrifuged at 900 rpm for 5 min. Per electroporation 6.5x 10^6 cells were resuspended in 400 µL cytomix with freshly added 2 mM ATP and 5 mM glutathione (end concentration). 5 µg RNA (thawed on ice) were added to the mixture in electroporation cuvettes and pulse was given by Gene Pulser Xcell System Electroporator (Bio Rad) with 975 µF and 270 V which should not take longer than 25 ms. Cells were immediately transferred into warm cell culture medium and seeded according to the experimental set up. Medium change was performed 4-8 hours post transfection to remove dead cells.

### 4.2.4 FACS (fluorescence activated cell sorting)

Flow cytometry is a useful tool to study cell characteristics within single cells in a high-throughput system. In a fluidic stream single cells pass a light and several laser beams, thereby giving information by the scattered light about their size (forward scatter, FCS), their complexity (sideward scatter, SSC) and different fluorescent properties.

Electroporation and transfection efficiencies of Huh7.5 cells with fluorescently-tagged reporter viruses were analyzed via BD FACS CantoII or Aria-IIIa with the blue laser for 488 nm excitation of GFP. In addition Aria-IIIa has a 561 nm laser included to excite the fluorophore mCherry.

Cells were washed with PBS and detached by incubation with trypsin/EDTA.Cell pellet was resuspended in medium to inactivate trypsin and washed twice with PBS after centrifugation at 900 rpm for 5 min. Cells were resuspended and fixed in 2% PFA in PBS for 20 min at 4°C prior to FACS analysis with the Diva software. There is also the possibility for fluorescently labeling of different proteins within the cell by immunostaining (4.4.3).

## 4.3 Biochemical methods

### 4.3.1 Cell lysis and preparation of total protein extracts

For the preparation of total protein extracts for SDS-PAGE, coIP or deglycosylation cells were washed with PBS and detached by trypsin/EDTA. Cells were resuspended in medium for inactivation of

trypsin and washed twice with PBS after centrifugation at 1200 rpm for 5 min. Afterwards the pelleted cells were resuspended in RIPA-buffer, CoIP-lysis buffer (3.9.2) or 0.5% NP-40 in $H_2O$ respectively. After 10 min incubation at 4°C cell debris were pelleted at 13000 rpm, 4°C for 10 min. Depending on the experiment solubilized proteins within the supernatant were further processed for SDS-PAGE (see section 4.3.4), coimmunoprecipitation (coIP) (section 4.3.2), deglycosylation (section 4.3.3) or stored frozen at -80°C.

### 4.3.2 Coimmunoprecipitation

To elucidate weather two proteins interact directly with each other coimmunoprecipitation (coIP) was done. The principle of this method is the specific antibody-based recognition of one interaction partner followed by precipitation of the antibody-protein complex via binding of the antibodies $F_c$ terminus to protein G agarose beads. In case of a direct interaction, the protein of interest is coprecipitated and can be visualized by Western Blot (4.3.5).

Therefore, 19.5 x10^6 with viral RNA electroporated Huh7.5 cells were detached and washed with cold PBS 56 h pEP. Cells were sheared through a syringe in 800 µL CoIP lysis buffer (3.9.2) and rotated on a wheel for 20 min at 4°C before centrifugation of cell debris at 17000 g for 10 min. In the meanwhile, an agarose-matrix with coupled anti-Flag tag antibodies (3.8.1) was washed twice with CoIP wash buffer (3.9.2) and once with 0.1 M glycin (pH 3.5) to remove unbound antibodies. After three additional washing steps with CoIP wash buffer, the cleared protein containing supernatant as well as 1x *complete* protease inhibitor (Roche) were added to 30 µL matrix and incubated on a wheel over night at 4°C. Thereafter, the matrix was washed three times for removal of unspecific bound protein. Proteins were released from the matrix by 20 µL 5x SDS loading buffer (3.9.2.1) and 5 min boiling at 95°C.

### 4.3.3 Endoglycosidase digest

Glycosylation is a posttranslational modification of proteins. After or during translation into the endoplasmatic reticulum a dolichol-phosphat is added at the amino acid asparagine. Linked to Dol-P the oligosaccharide precursor ($Glc_3Man_9(GlcNAc)_2$) can be further processed by trimming the glucose residues. Oligosaccharides which maintain this so called mannose-rich form are designated as EndoH-sensitive. Otherwise, proteins can be transported to the Golgi compartment, where the mannose residues are cleaved and further processed by adding e.g. galactose and N-acetylglucosamin (GlcNAc), leading to a complex form (EndoH-resitant).

To elucidate the character of this glycosylations a digest with amidases can be performed. The enzyme Endoglycosidase H (EndoH) hydroxylates only mannose residues, whereas Peptide-N-

Glycosidase F (PNGaseF) cleaves GlcNAc and asparagine residues in many N-glycan chains with mannose- as well as hybrid and complex glycosylation sites.

19.5x10^6 cells were electroporated and cultured in a 125 cm² flask for 56 h. Afterwards, cells were detached and washed twice with PBS before lysis by adding 720 µL 0.5% NP-40 in $H_2O$ takes place for 10 min at 4°C. Cell debris was spun down at 17000 g for 5 min. In parallel, virus containing supernatant out of 10 flasks was concentrated via ultracentrifugation (4.6.1.1) or additional gradient centrifugation (4.6.2) and resuspended in either 100 or 50 µL PBS. 10x Glycoprotein denaturation buffer (NEB) was added to the supernatant after cell lysis or virus containing culture supernatant and boiled at 95°C for 10 min. Following a short centrifugation, samples were subdivided into 3 equal fractions. The first was the untreated control, the second was digested with EndoH and the third with PNGaseF. For a 16 µL aliquot 2.1 µL 10x G7 buffer (PNGaseF) or G5 buffer (EndoH) were added, as well as 2.1 µL 10% NP-40 and 0.3 µL $H_2O$. To start the hydroxylation 0.1 µL PNGaseF or 0.5 µL EndoH were added to the reaction mixture and incubated at 37°C for 15 min or 5 min respectively. The reaction was stopped by addition of 5.25 µL 5x SDS loading buffer (3.9.3.1) and boiling at 95°C for 10 min. The samples were further separated by SDS-PAGE (4.3.4) and stained in Western Blot (4.3.5; 4.4.1).

### 4.3.4 SDS-polyacrylamide-gel electrophoresis (SDS-PAGE)

A discontinuous SDS-polyacrylamide-gel electrophoresis (SDS-PAGE) was used for the separation of proteins under denaturizing conditions according to their molecular mass by an electric field. The anionic detergent sodium dodecyl sulfate binds to the amino acid residues of proteins thereby creating a strong negative surface, independently of their own charge, which is proportional to their mass. Disulfide bonds are separated by the addition of 2-mercaptoethanol and secondary as well as tertiary structures are disrupted while boiling the samples at 95°C for 5 min. The upper stacking gel concentrates the proteins into a single thin band, whereas the lower separation gel separates the proteins by size. Small proteins migrate relatively fast towards the positive electrode while bigger proteins are more delayed in doing so.

For SDS-PAGE the native protein conformation was disrupted and negatively charged by adding 5x SDS loading buffer (3.9.2.1). After boiling at 95°C for 5 min samples were loaded onto 12 or 15% gels together in tandem with the Prestained Protein Ladder Page Ruler. A schematic recipe for a gel is shown in Table 3. Electrophoresis within the separation gel was conducted at 80 V and further processed at 160 V using 1xSDS running buffer (3.9.2.1).

**Table 3: SDS-PAGE gel mixture**

| | separation gel 12% | stacking gel 5% |
|---|---|---|
| $dH_2O$ | 4.95 mL | 3.4 mL |
| 1.5 M Tris/HCl pH8.8 | 3.75 mL | -- |
| 1 M Tris/HCl pH 6.8 | -- | 650 µL |
| 30% Acrylamide-bis | 6 mL | 850 µL |
| 10% filtered SDS | 150 µL | 50 µL |
| 10% [w/v] APS | 150 µL | 50 µL |
| TEMED | 6 µL | 5 µL |

### 4.3.5 Western Blot

Before detection by antibodies after SDS-PAGE the separated, negatively charged proteins are transferred along an electric field vertical to the gel onto a Protean BA83 (0.2µm) nitrocellulose membrane in a PROTEAN® wet blotting system (BIO-RAD) for 60 min at 330 mA in transfer buffer (3.9.2.1). To check whether the transfer was successful the membrane was stained with Ponceau S (4.3.6). After a washing step with PBS, unspecific bonds to the membrane were saturated by 10% [w/v] milk powder in PBS for 1 h, followed by antibody staining (4.4.1).

### 4.3.6 Ponceau-S staining

For verification of correct blotting (4.3.5) nitrocellulose membranes were stained for 2 min with 0.1% Ponceau-S (3.9.2.1) which allows visualization of 5 µg protein. Thereafter, the membrane was washed with distilled water followed by blocking buffer (3.9.2.1).

## 4.4 Immunological methods

### 4.4.1 Immunodetection on nitrocellulose membranes

The staining of proteins on nitrocellulose membranes after SDS-PAGE (4.3.4) and Western Blot (4.3.5) was done with primary antibodies specifically targeting protein-epitopes and secondary antibodies linked to a reporter enzyme like horseradish peroxidase (HRP) or to a fluorophore (IRDye).

After blocking the membrane in 10% [w/v] milk powder in PBS for 1 h, primary antibodies (3.8.1) were diluted 1:1000 in 5% milk powder in PBS and incubated overnight slightly shaking at 4°C. Following three washing steps with 0.1% Tween 20 in PBS for 10 min to remove unspecific bound antibodies, the membrane was incubated with secondary antibody (1:10000 for HRP or 1:5000 IRDye; 3.8.2) in 5% milk powder in PBS for 3 h at RT. Thereafter, washing was repeated and detection was initiated with either chemiluminescence or Odyssey infrared imaging system (LI-COR).

Allowing a chemiluminescent-based detection SuperSignal® West Pico or Femto substrate was equally distributed on the blot surface according to manufacturer's protocol and incubated for 4 min at RT. Excess solution was removed and the protein bands were developed in a dark chamber using Amersham Hyperfilm™ (GE healthcare).

### 4.4.2 Immunofluorescence staining for microscopy

Immunofluorescent microscopy is based on specific staining of cellular or viral proteins within a cell. It's called direct immunofluorescence if the antigen specific antibody is coupled directly with a fluorophore. Whereas indirect immunofluorescence describes the recognition of the antigen-antibody-complex by a secondary antibody coupled to a fluorescein. The latter normally enhances the signal through simultaneous binding of several secondary antibodies to one primary. The fluorophores are excited by monochromatic light and emit according to the Stokes shift long wave light. With this technique the intracellular localization of proteins was examined.

Before staining cells were electroporated with viral RNA and/or cellular fusion proteins. $0.25x10^5$ cells were grown in a 24 well plate on 12 mm cover slips and prepared after indicated time points. Cells were washed twice with PBS to remove cell culture medium and fixed for 20 min at 4°C with 2% [w/v] PFA in PBS. Some samples were directly mounted in Mowiol 4-88 (Roth). Following two additional washing steps, cells were permeabilized for 10 min at RT in 1% [w/v] saponin in PBS. Thereafter one wash step was followed by saturation of unspecific interactions with 10% [v/v] goat serum in PBS for 30 min at RT. Primary antibodies (2.8.1) were diluted 1:100 in 30 µL 1% [v/v] goat serum in PBS and incubated on the cover slips within a humid environment for 2 h at RT. Afterwards samples were dipped in PBS three times to remove unbound antibodies and incubated with 1:200 diluted secondary antibody (2.8.2) in 1% goat serum/PBS for 1 h in the dark. Subsequently, three washing steps in PBS and two in $dH_2O$ to remove salts followed as well as mounting of the cover slips on a glass slide with 5 µL Mowiol 4-88 (Roth). Slides were dried at RT overnight in the dark, stored at 4°C and analyzed by spinning disc confocal fluorescence microscopy (Nikon Ti Eclipse UltraViewVox System).

### 4.4.3 Immunofluorescence staining for flow cytometry

For the detection and quantification of intracellular proteins within a cell population, proteins can be immunostained comparable to microscopy (4.4.2). Prior to FACS measurement, cells were washed with PBS and detached by incubation with trypsin/EDTA. After resuspension in medium to inactivate trypsin, cells were washed twice with PBS in FACS-tubes and spun down at 1200 rpm for 5 min. Subsequently, cells were fixed for 20 min in 2% [w/v] PFA in PBS, washed twice and permeabilized for 10 min at RT in 1% [w/v] saponin in PBS. After two additional washing steps unspecific interactions were blocked with 10% [v/v] goat serum in PBS for 30 min at RT. After centrifugation supernatant was removed and pelleted cells were resuspended in 80 µL primary antibody (3.8.1) diluted 1:100 in 1% [v/v] goat serum in PBS at 4°C. One hour later cells were washed three times and incubated for another half hour in 80 µL secondary antibody (3.8.2) diluted 1:500 in 1% [v/v] goat serum in PBS at 4°C in the dark. Following three additional washing steps cells could be analyzed via BD FACS Canto-II or Aria-IIIa with the Diva Software.

### 4.4.4 Proximity Ligation Assay (PLA)

The Proximity Ligation Assay (PLA) allows the detection of proteins, protein interactions and modifications with high specificity and sensitivity. Even transient or weak interactions can be measured by microscopy.

For PLA, electroporated Huh7.5 cells on cover slips were fixed with 2 % PFA at different time points pEP. Cells were permeabilized for 15 min with 1% saponin and blocked for 45 min with 5% BSA. Proteins were detected with primary antibodies (3.8.1) from rabbit directed against E1-mCherry and either one from mouse against E2, Core, NS3 or NS5A 1:100 in 1% BSA for 2 h at RT.

Afterwards, samples were treated according to the protocol of the manufacturer (Duolink, Sigma Aldrich). In short, the cells were washed and incubated with two species-specific secondary antibody-probes coupled with a short DNA-sequence. Upon close proximity of the two targeted proteins due to an interaction, the DNA sequences were ligated and rolling-circle amplification with fluorescently-labeled nucleotides can occur. Thereby, spots of a green fluorescent substrate are build, which allows detection of the interaction in fluorescent microscopy (Nikon Ti Eclipse UltraViewVox System). For statistics, Volocity software implemented automated spot counting was used with a maximum spot size of 0.8 µm.

## 4.5 Microscopy

In this study microscopy was done with the Nikon Ti Eclipse equipped with the Perkin Elmer UltraViewVox System (Yokogawa CSU-X1).

### 4.5.1 Live Cell Imaging

Reporterviruses which express internal fluorescent fusion proteins can be studied via live cell microscopy by excitation of the fluorophore and tracking of the emitted light over time. In this system, movement of proteins can be assessed in real time. $0.45x10^6$ cells were seeded in a 35 mm dish with optical bottom (WillCo) and cultivated for the indicated times. Microscopy was done in a humidified chamber with 5% $CO_2$ at 37°C using a 60x objective and the *perfect focus* system of the Nikon Ti Eclipse UltraViewVox System. Video sequences were processed by the Volocity software.

### 4.5.2 Fluorescence Recovery after Photobleaching (FRAP)

This microscopy technique is used to track diffusion or transport of fluorescently labeled samples. An area of interest within the cell is bleached by a high laser beam in the specific spectral range. Afterwards the recovery of fluorescence in this area is recorded, giving a hint on diffusion or transportation of the labeled probes.

1.2x10^6 Huh7.5 cells were electroporated with JC1-E1-mCherry, seeded in a Willco-dish (WillCo Wells) and cultured for 56 h. Subsequently the dish was placed on the microscope. Within the cell, FRAP areas were selected for the areas of interest and a place with background fluorescence. A time lapse movie was taken, starting before bleaching and ending approximately 5 min later, depending on the experiment. Photobleaching was done in a single pulse for 60000 ms. Intensity profiles of the different chosen areas were computed in the Volocity Software (PerkinElmer) and calculated in Excel (Microsoft). Therefore, brightest intensity before bleaching was taken as 100% and lowest intensity after bleaching as 0%.

## 4.6 Virological methods

### 4.6.1 Harvesting and concentration of virus containing supernatant

Supernatant of cells with electroporated viral RNA was collected after 72 h out of 125 cm² flasks. To pellet cell debris, medium was centrifuged for 10 min at 3000 rpm and transferred to a new tube. Subsequently, supernatant was used for infection (4.6.3) or concentration (4.6.1.1; 4.6.2).

#### 4.6.1.1 Ultracentrifugation

32 mL of cleared supernatant was transferred to an ultracentrifugation tube for the SW 28 rotor (Beckman Coulter). Each supernatant was carefully underlaid with 5 mL sterile filtered 20% [w/v] sucrose in PBS and for accurate weight balanced with PBS. Centrifugation took place in the Optima L7-65 Ultracentrifuge (Beckman Coulter) for 90 min at 28000 rpm and 4°C. Afterwards the supernatant was tipped away and the tube rimes were dried on a tissue. The virus pellet was dissolved in an adequate volume of PBS or medium (50 or 100 µL) and resuspended overnight at 4°C. Subsequent infection (4.6.3), gradient centrifugation (4.6.2), deglycosylation (4.3.3) or SDS-PAGE (4.3.4) was performed or virus was stored frozen at (-80°C).

#### 4.6.1.2 Concentration of small volumes

For concentration of small volumes (up to 1 mL) virus containing supernatant, it was transferred to a 1.5 mL reaction tube and underlaid with 200 µL sterile filtered 20% [w/v] sucrose in PBS. Samples were centrifuged at 21000 g for 90 min at 4°C before removing the supernatant with a pipette and resuspending the virus pellet with either medium or PBS depending on the following experiments like infection (4.6.3) or SDS-PAGE (4.3.4).

### 4.6.2 Gradient equilibrium centrifugation

In this study gradient centrifugation was done to separate virus particles out of the supernatant depending on their density and to separate them from single proteins and unspecific membrane-associated ones. This can give a hint on correct particle assembly and release.

Gradient fraction were prepared by mixing decreasing amounts of serum free medium with increasing amounts of iodixanol density medium (OptiPrep), to achieve fractions from 14, 18, 22% to 26, 30, 34 and 38% iodixanol. Starting with the lightest every fraction is transferred to an ultracentrifugation tube for the Ti55 rotor (Beckman Coulter). Every other fraction is carefully laid under the other. The prepared gradient is subsequently overlaid with the concentrated virus, which was resuspended overnight in 1x *complete* protease inhibitor in PBS. After centrifugation at 34000 rpm and 4°C for 20 h in the Optima L7-65 Ultracentrifuge (Beckman Coulter) each fraction was recovered by transferring the initial volume in separate reaction tubes. Therefore a pipette was dipped slightly under the rim of the fluidic surface and indicated volume was sucked away. After recovering the fractions, each was diluted 1:2 with PBS and centrifuged again at 21000 g and 4°C for 90 min to concentrate virus particles or proteins in a pellet. Thereafter supernatant was pipetted away and pellet was resuspended either in 5xSDS loading buffer (3.9.2.1) for SDS-PAGE (4.3.4) or further processed for deglycosylation (4.3.3).

### 4.6.3 Infection of eukaryotic cells with HCV

Huh7.5 cells were seeded one day prior to infection in a 96 well plate (5000 cells/well), 24 well plate (150000 cells/well) or 12 well plate (350000 cells/well). Medium was replaced by virus containing supernatant and after 6 hours of incubation again replaced by fresh medium. 72 h after infection cells were analyzed via FACS (4.2.4) or microscopy (4.5).

## 4.7 Statistical methods

The Pearson's correlation coefficient (r) is used to determine the degree of linear dependence between two fluorescent intensities. The value 1 is a complete positive correlation, whereas 0 is none. The coefficient was further squared to accent differences in the results. It was improved in the $19^{th}$ century by Karl Pearson. For colocalization every cell was cropped and Pearson's $r^2$ value calculated according to Costes colocalization.

For calculation of Pearson's coefficient as well as spot counting of PLA the mean and standard deviation were used. Therefore, all different counts of one sample are added and divided by the number of total counts. For the standard deviation the difference of every data point from the mean is calculated, then squared and the results are added and again divided by the number of total counts. Finally the square root of this number depicts the standard deviation. For the counting of E1-mCherry and NS5A-GFP spots as well as for counting of PLA interaction sites the one-way ANOVA with Bonferroni post-test was used to assess significance levels.

# 5 Results

The overall goal of this thesis was to improve the understanding of the intracellular transport route HCV exploits for release. Therefore, a mCherry-labeled HCV construct was comprehensively characterized. This fluorescent HCV was examined with innovative microscopy techniques and by biochemical methods to shed light on the intracellular passage of HCV and the assembly of its structural proteins prior to release.

## 5.1 Characterization of mCherry-labeled HCV E1

To visualize the surface protein E1, the gene for the monomeric red-fluorescent protein mCherry was introduced at amino acid (aa) position 336 upstream of the C-terminal transmembrane-domain within E1 of the replication competent chimeric HCV JC1 genome. Additionally, E1-mCherry was cloned into the JC1-NS5A-GFP genome, in which GFP is introduced into the third domain of NS5A (Schaller et al. 2007) (Banning, 2011). This results in the simultaneous production of GFP-labeled NS5A and mCherry-labeled E1 proteins and allows to discriminate sites of RNA replication and translation from structural protein expression and trafficking. The previous investigations by Banning in 2011 yielded promising results pointing towards a functional assembly and release of the fluorescent HCV. However, a complete and careful characterization of these constructs allowing to conclude that insertion of the fluorescent tag does not interfere with particle production, assembly and release was still lacking. Hence, it was first essential to comprehensively investigate a variety of virological parameters of the fluorescently labeled HCV genomes and compare them to native unlabeled HCV.

### 5.1.1 Reconstitution of an E1 internal recognition sequence

JC1 is a chimeric genome, in which the ORF from Core to the first TM-domain of NS2 originates from the J6 isolate, while the ORF for the non-structural proteins that range from NS2(TM2) to NS5B is derived from JFH1 (Pietschmann et al. 2006). Neither is there an antibody available which is directed against the JC1-E1 protein, nor does any other antibody with cross-reactivity exist. Therefore, a well-defined amino acid sequence within E1 was reconstituted from the strain H77 (genotype 1a) (see method 4.1.11). Therein, 4 aa were mutated by SOE-PCR and cloned into the E1 gene (Fig. 7). With this approach, the JC1-E1 protein could be immunostained using the published mouse anti-E1(A4) antibody (Dubuisson et al. 1994).

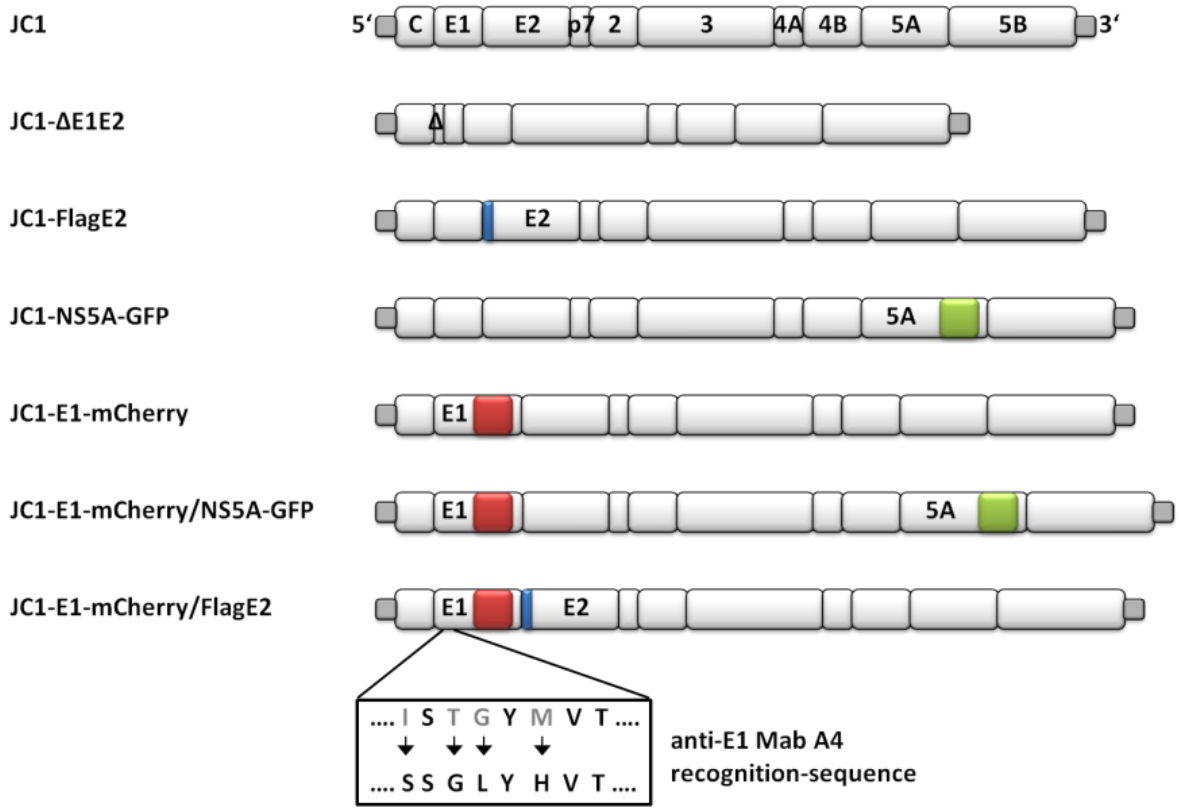


**Figure 7: Schematic presentation of HCV genomes.** The graph gives an overview of the HCV JC1 genome variants used in this thesis. The single ORFs are indicated in the wild-type JC1 genome. All HCV variants were constructed with and without the reconstituted A4-sequence. Furthermore, a JC1 genome with a Flag tag sequence within E2 was kindly provided by T. Pietschmann (Institute of Experimental Virology, Twincore, Hannover).

### 5.1.2 Stable expression of E1-mCherry

Insertions of genes for the expression of fluorescent fusion proteins can lead to protein instability and degradation due to misfolding or improper post-translational modifications. Thus, adequate protein expression of E1-mCherry was needed to be confirmed. Additionally, it was analyzed if E1 and E1-mCherry are detectable by introduction of the A4 sequence and staining with the anti-E1(A4) antibody. Huh7.5 cells were electroporated with *in vitro* transcribed RNA of the different genomes and cultured for 48 h (see methods 4.1.12; 4.2.3). Afterwards, cells were lysed (4.3.1), proteins were separated by SDS-PAGE (4.3.4) and HCV structural proteins were analyzed by Western Blot (4.3.5; 4.4.1).

As shown in Figure 8, electroporation of all constructs led to the detection of a band at the proper size of 21 kDa for the Core protein. Also bands for E2 were detectable at their expected size of 70 kDa, except in JC1-ΔE1E2, where E1 and E2 were deleted. In comparison with the JC1 wild-type and the previously characterized JC1-NS5A-GFP virus (Schaller et al. 2007), Core and E1 were expressed at similar levels by the fluorescent HCV variants (Fig. 8). Since HCV proteins are translated

as a polyprotein precursor and cleavage occurs post-translationally, we concluded that the remaining proteins are also adequately expressed. Moreover, in comparison between JC1 and JC1(A4) in lane 2 and 7, E1 is readily detectable at its predicted size of 31 kDa by anti-E1 Mab A4, leading to the conclusion that the epitope can be specifically recognized within the denaturated protein. Importantly, looking at the mCherry labeled E1 proteins, e.g. lane 5 and 9, E1-mCherry runs at its calculated size of 60 kDa (31 kDa E1 and 28.8 kDa mCherry) and can be stained with anti-mCherry as well as with the anti-E1(A4) antibody. However, after EP of JC1(A4)-E1-mCherry constructs, there was an additional protein band detectable in lane 9 and 10, which runs at 35 kDa. To check, whether this unspecific band is a degradation product due to the mCherry label, further analysis via Western Blot was done.

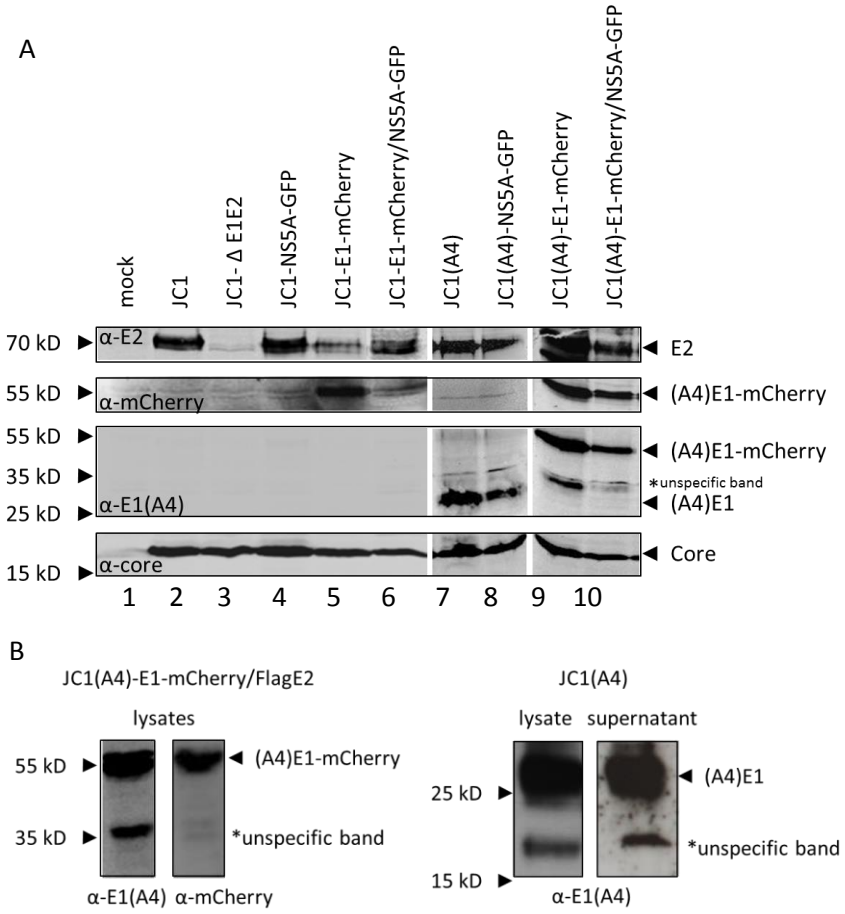


**Figure 8: Protein expression of HCV genomes with and without a fluorescence tag.** 48 h post-electroporation (pEP) proteins of electroporated Huh7.5 cells were detected by immunoblot in a 1:1000 dilution with specific antibodies against E2 (AP33) and Core (C7-50). E1 was detected with the A4 Mab or with anti-mCherry. Detection was assessed by an anti-mouse IRDye 800 or anti-rabbit IRDye 680 ab (1:1000). The lane number is written below. (B) Proteins in lysate and concentrated supernatant were stained with either anti-E1(A4) or anti-mCherry (1:1000). Detection was assessed by an anti-mouse or rabbit HRP ab (1:10000). The protein size is depicted on the left.

Huh7.5 cells electroporated with RNA of JC1(A4)-E1-mCherry/FlagE2 and JC1(A4) (4.2.3) were lysed (4.3.1). The supernatant of JC1(A4) cells was concentrated via ultracentrifugation over 20% sucrose (4.6.1). Proteins were separated by SDS-PAGE and detected by Western Blot (4.3.4; 4.3.5; 4.4.1). This revealed that in contrast to the anti-E1(A4) staining of E1-mCherry, the detection with anti-mCherry antibody did not result in an unspecific band at 35 kDa (Fig. 8B). Likewise, staining of the unlabeled E1 protein in lysates or out of the supernatant with an anti-E1(A4) antibody showed an unspecific

band, too. Whereas E1 runs at 31 kDa, the smaller band can be found around 17 kDa. Therewith, the unknown protein appears independently of the mCherry-fusion and was only found after anti-E1(A4) staining. Thus, the labeled proteins were correctly expressed and processed from the polyprotein and did not show any signs of degradation.

To determine whether the reconstituted A4 sequence was detectable within the native proteins, Huh7.5 cells were electroporated with *in vitro* transcribed RNA of JC1-E1-mCherry/FlagE2 and JC1(A4)-E1-mCherry (4.1.12; 4.2.3). 48 h pEP intracellular structural proteins E1 and E2 were stained with A4 and E2 antibodies and analyzed by FACS (4.4.3; 4.2.6). As shown in Figure 9, each horizontal lane depicts one construct, mock in the upper, JC1-E1-mCherry/FlagE2 in the middle and JC1(A4)-E1-mCherry in the lower lane. The first column shows the fluorescence of the labeled E1-mCherry in all constructs. E1-mCherry is expressed from both constructs in 36% and 42% of the cells, respectively (Fig. 9, first column). In comparison, staining against E2 and E1 proteins (second column) revealed similar percentages. Accordingly, when E1 or E2 staining was plotted versus mCherry (lane 3), all cells expressing mCherry were also positive for E1 or E2 and percentages were similar to the respective single staining. In conclusion, anti-E1 Mab A4 can be used for staining of native and denaturated JC1(A4)-E1 proteins.

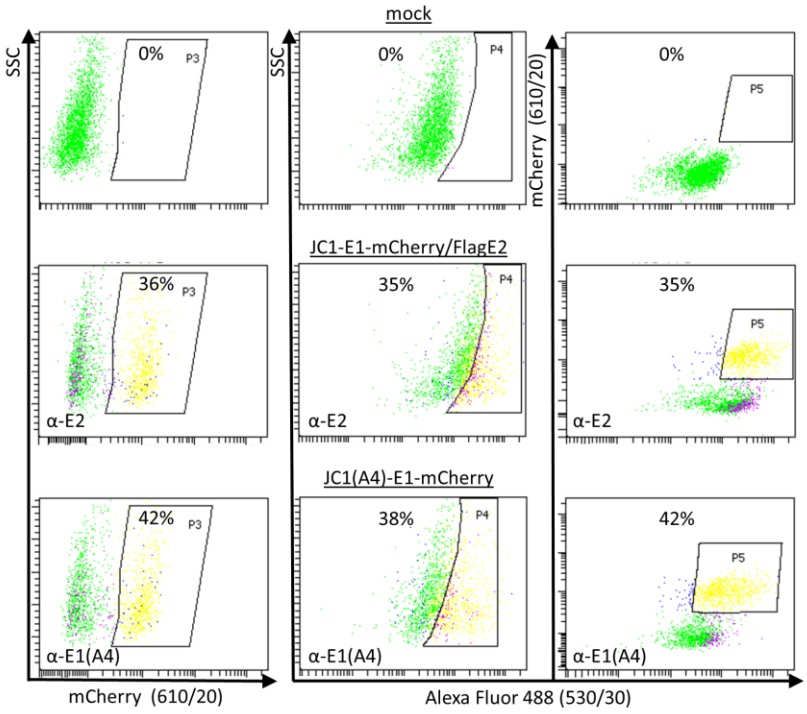


**Figure 9: FACS measurement after intracellular staining with A4 and E2 (AP33) antibodies.** 48 h pEP HCV proteins in Huh7.5 cells were stained with a 1:100 dilution of anti-E1 Mab A4 and anti-E2 (AP 33). The secondary ab was Alexa Fluor 488 (1:200) for analysis by FACS. Percentage of positive cells are blotted on the X-axis, while the internal mCherry fluorescence is shown on the Y-axis.

### 5.1.3 Subcellular distribution of E1-mCherry and untagged proteins

Even if fluorescence emission of the chromophore labeled protein is detectable, their intracellular localization could be altered. To determine whether the constructs with a fluorescent protein still

localized appropriately throughout the cell, immunofluorescence staining against all structural proteins as well as NS5A was performed. Therefore, Huh7.5 cells were electroportaed with *in vitro* transcribed RNA of the indicated genomes and cultured on cover slips for 48 h (4.1.12; 4.2.3). Afterwards, cells were fixed and proteins were stained with the indicated antibodies (4.4.2) for analysis by fluorescence microscopy (4.5).

For all genomes, Core, E2, E1 and NS5A located in their expected subcellular sites (Fig. 10, first columns). The Core protein showed its specific distribution in membranous-like structures with embedded ring-like structures (Barba et al. 1997, Rouillé et al. 2006), depicting lipid droplets on which Core accumulates (see magnifications in Fig. 10C). NS5A was distributed in membranous compartments, as well, representing the replication environment of HCV (Masaki et al. 2008, Miyanari et al. 2007). Furthermore, the staining of JC1-NS5A-GFP with anti-NS5A showed the same localization, since the antibody targets the fluorescent protein (Fig. 10B).

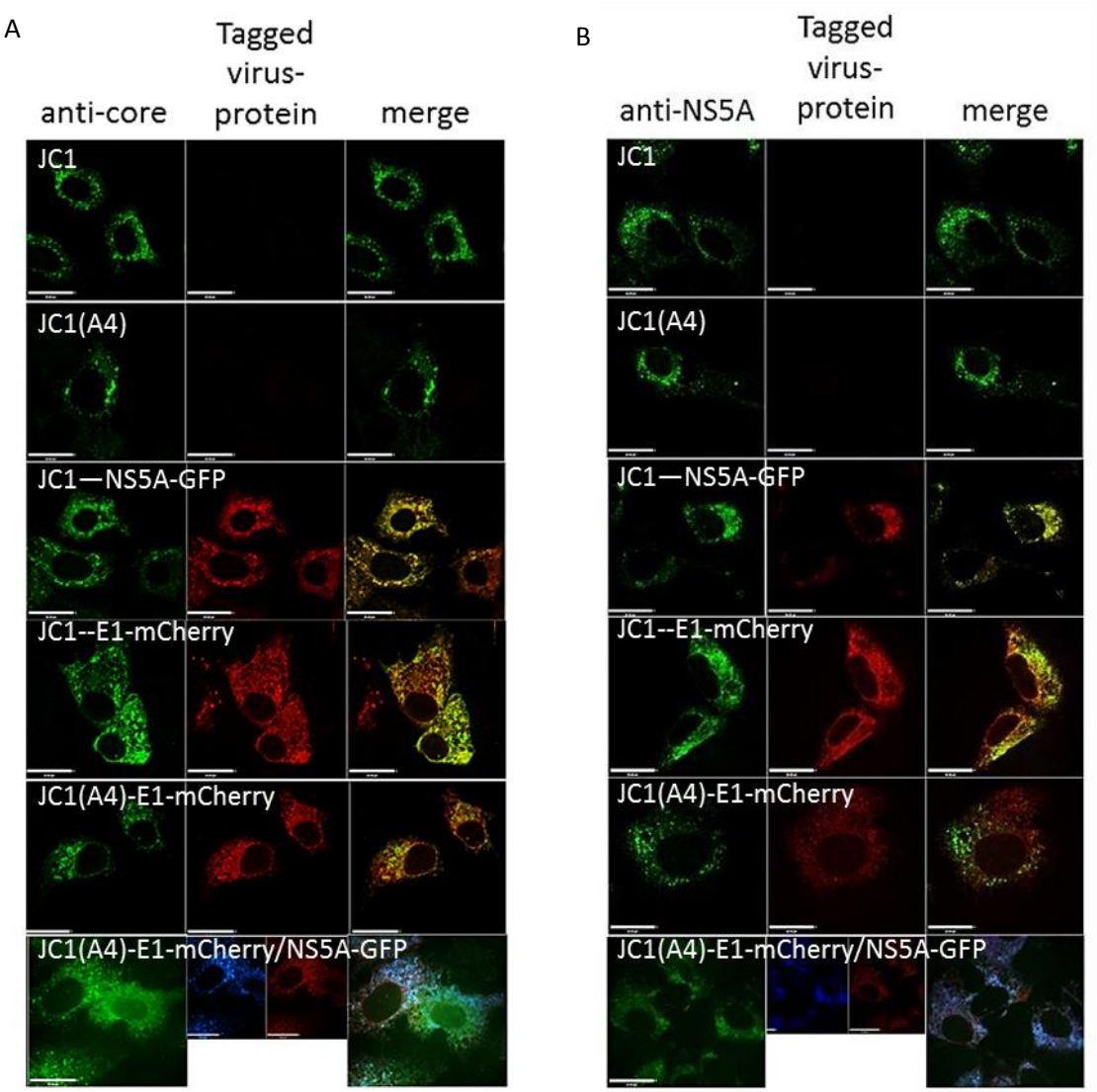

C

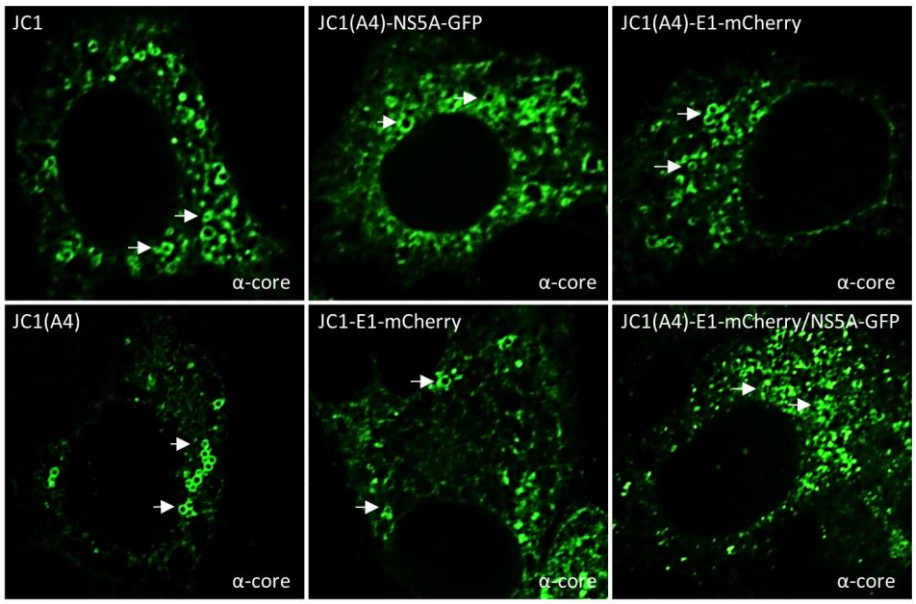


**Figure 10: Intracellular distribution of fluorescently-labeled and unlabeled HCV proteins.** Electroporated Huh7.5 cells were grown on coverslips and proteins were stained with the indicated antibodies (1:100) 48 h pEP. 1:200 diluted secondary ab was directed against mouse with Alexa Fluor 488 for mCherry-constructs, Alexa Fluor 561 for GFP-constructs and Alexa Fluor 405 for double-labeled constructs. Representative confocal images are shown with the stained protein in the left column and the internally labeled in the middle. (A) Depicted is anti-Core and (B) anti-NS5A. Bar: 20 µm. (C) Magnifications of the Core-staining.

E2 was concentrated at perinuclear regions, consistent with its ER association (Duvet et al. 1998, Rouillé et al. 2006). While staining of the JC1-E1 protein was not possible until now, the reconstitution of the A4-epitope overcame this challenge. The JFH1-E1-protein (genotype 2a) was previously described to localize like E2 (Rouillé et al. 2006). Thus, the unmodified as well as the fluorescently-labeled E1 proteins revealed an ER-like staining at a perinuclear region, emphasizing its association with E2. In line with these data, the overlay of antibody staining and virus-internal fluorescence showed a strong colocalization of E2 and E1-mCherry (see magnification in Fig. 11C). Moreover, the merge of anti-E1(A4) staining and E1-mCherry illustrates that the antibody-staining is not that efficient, leading to an uneven protein pattern in comparison to wildly distributed E1-mCherry (Fig. 10C, panel JC1(A4)-E1-mCherry).

Taken together, localization of the unlabeled as well as the labeled proteins corresponds to the typical HCV subcellular distribution. In addition, colocalization of E2 and E1-mCherry was confirmed.

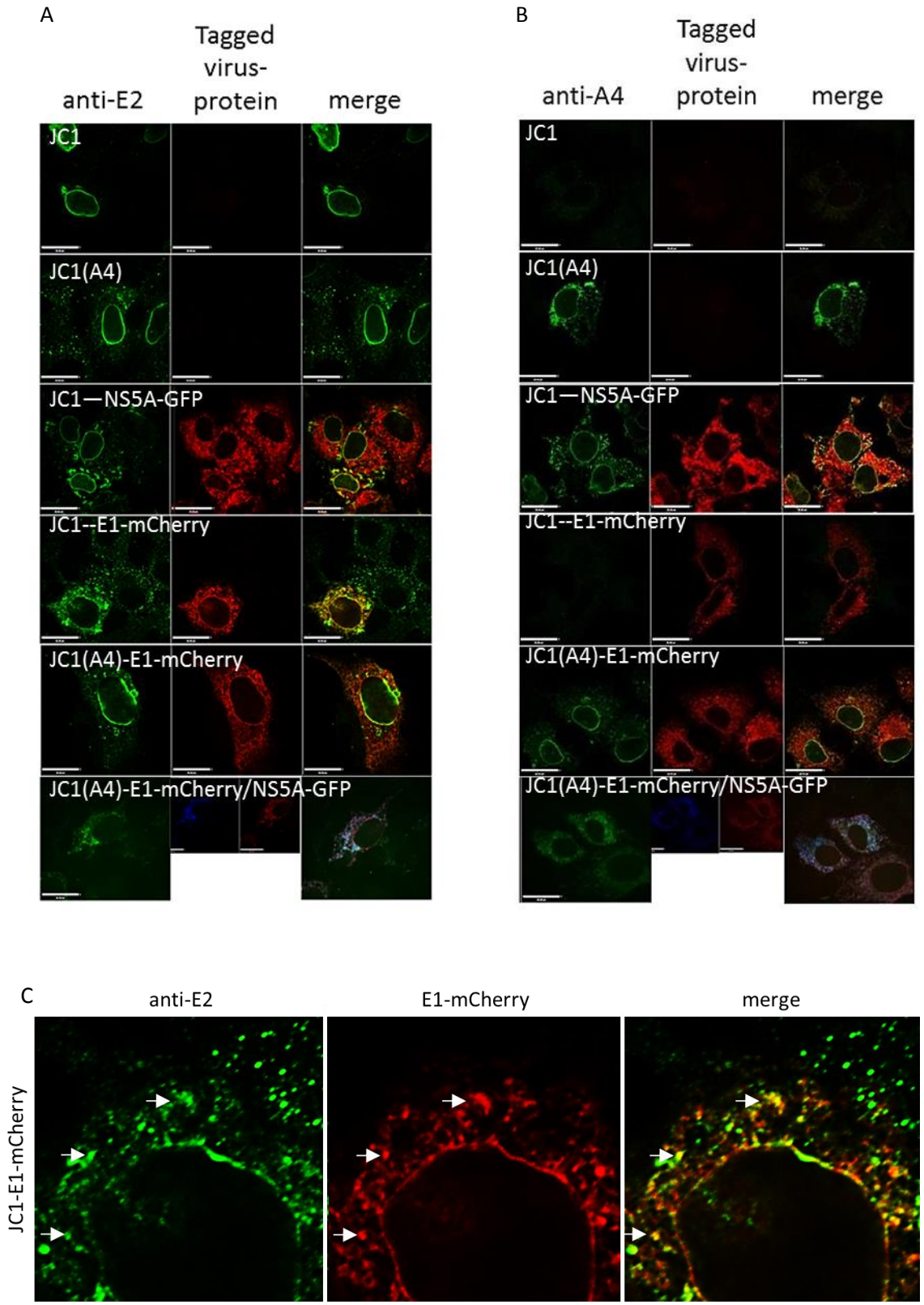


**Figure 11: Intracellular distribution of fluorescently-labeled and unlabeled HCV proteins.** Electroporated Huh7.5 cells were grown on coverslips and proteins were stained with the indicated antibodies (1:100) 48 h pEP. 1:200 secondary ab were directed against mouse with Alexa Fluor 488 for mCherry-constructs, Alexa Fluor 561 for GFP-constructs and Alexa Fluor 405 for double-labeled constructs. Representative confocal images are shown with the stained protein in the left column and the internally labeled in the middle. (A) Depicted for anti-E2 and (B) anti-E1(A4). Bar: 20 µm. (C) Magnifications of the E2 staining.

### 5.1.4 Heterodimer formation of E1-mCherry and E2

To elucidate whether the described interaction between E1 and E2 (Dubuisson et al. 1994, Duvet et al. 1998) still occurs in the presence of the fluorescent protein tag, a coimmunoprecipitation was performed. The JC1(A4)-FlagE2 genome allowing to precipitate E2 by an anti-Flag ab was compared to the JC1(A4)-E1-mCherry/FlagE2, expressing the mCherry labeled E1. JC1(A4) without a Flag-tag was used as a negative control for unspecific protein binding to the utilized protein G agarose. 1.3x10^7 Huh7.5 cells were electroporated with the *in vitro* transcribed RNA of the different genomes (4.1.12; 4.2.3) and coimmunoprecipitation was performed (4.3.2). Co-IP samples were then separated via SDS-PAGE (4.3.4) and immunostaining was done after transferring the proteins onto a nitrocellulose membrane (4.3.5; 4.4.1).

Equal protein expression of E1 and Core was confirmed within the cell lysates (Fig. 12, left panel). The precipitated proteins revealed no unspecific protein binding, shown by JC1(A4) (Fig. 12, right panel). Together with the Flag-tagged E2 protein, the unmodified E1 as well as the mCherry-labeled proteins were precipitated and run at their specific size of 31 kDa and 60 kDa, respectively (Fig. 12, right panel). These results demonstrated that the interaction between E1 and E2 is not disrupted by the mCherry-protein and proper heterodimer formation could be confirmed. Moreover, the Core protein was coprecipitated in both constructs, showing that also the interaction of E2 and Core still occurs under E1-mCherry expression.

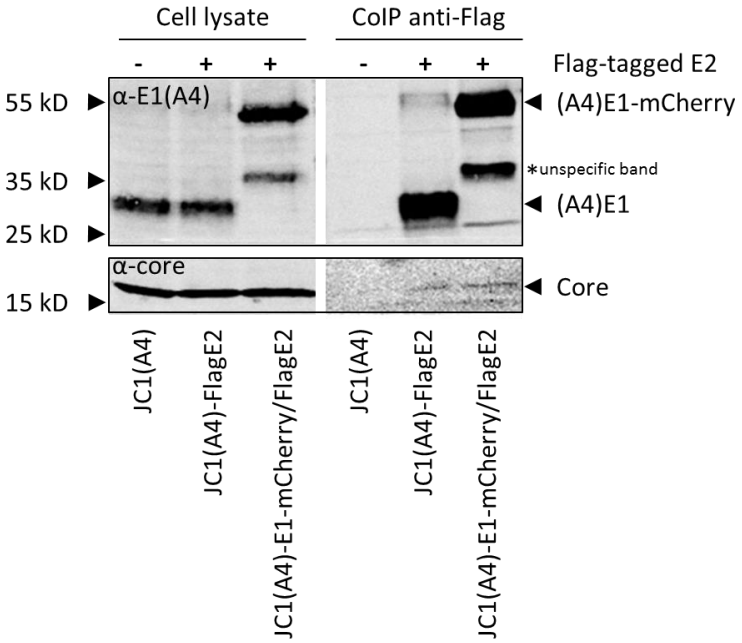


**Figure 12: Coimmunoprecipitation of E1-mCherry together with a Flag-tagged E2 protein.** Cell lysates of Huh7.5 cells 53 h pEP and CoIP eluates were immunostained after Western Blot in a 1:1000 dilution with specific antibodies against Core (C7-50) and E1 (A4). Detection was assessed by an anti-mouse IRDye 800 ab (1:1000). The protein size is depicted on the left.

### 5.1.5 E1-mCherry virus replicates with wild-type-like kinetics

The HCV life cycle is neatly regulated within a cell and is characterized by a complex interplay of different viral and cellular proteins. To check whether the expression of fluorescent proteins could

disrupt viral protein expression or replication over time, electroporated Huh7.5 cells (4.1.12; 4.2.3) were analyzed at several time points. The number of HCV positive cells was determined by intracellular Core-staining via FACS analysis (4.4.3; 4.2.6), protein production of the structural proteins was analyzed by Western Blot and RNA was isolated from the cells and the supernatant to quantify total viral RNA amounts by absolute qPCR (4.1.13; 4.1.14).

Figure 13A shows that the electroporation efficiencies differed between the used constructs from 24 h pEP onward. Nevertheless, all constructs showed increasing amounts of HCV positive cells, peaking at 40 h pEP, demonstrating similar kinetics. This led to the conclusion that the expression of fluorescent proteins does not influence viral production within these settings. In further experiments, results were normalized to FACS-positive cells. As confirmed by Western Blot, protein expression (Fig. 13C) as well as mean fluorescence intensity (Fig. 13B) within the whole cell population also increased over time. These results are in line with previous experiments, showing that protein expression is not altered upon insertion of fluorescence genes into the HCV genome.

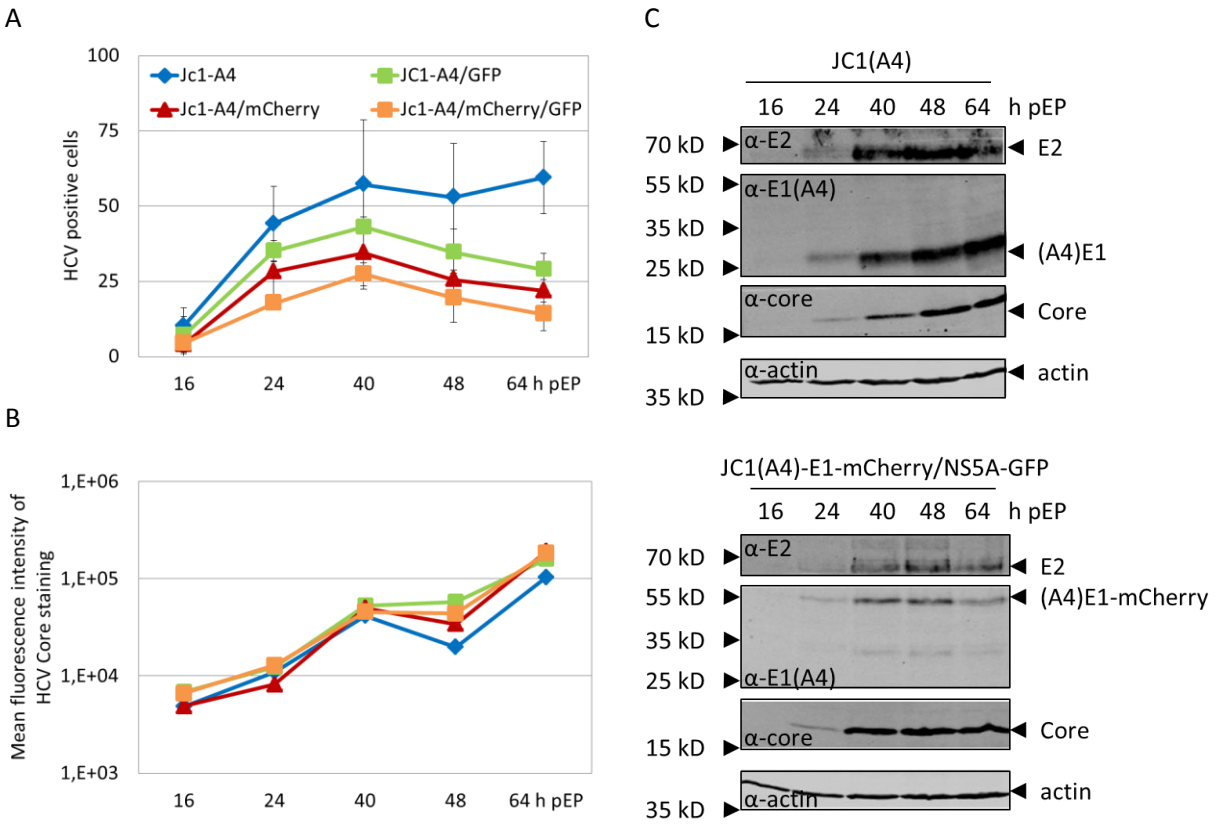


**Figure 13: Replication kinetics of HCV constructs with fluorescently-labeled versus unlabeled proteins.** 0.5x10^6 electroporated Huh7.5 cells were harvested at indicated time points pEP. (A) HCV Core proteins were stained and analyzed by FACS. The percentage of Core-positive cells is plotted. Error bars represent standard deviations of two independent experiments. (B) A respective graph of fluorescence intensity of the stained Core proteins is shown. (C) Cell lysates were separated by SDS-PAGE and proteins were stained in Western Blot with anti-E2, -E1, -core and -actin antibodies (1:1000), respectively. As secondary ab an anti-mouse IRDye 800 (1:1000) was used.

Intracellular RNA levels, when normalized to FACS positive cells, were slightly elevated up to 40 h pEP. At later time points, a transcriptional plateau developed, indicating enhanced replication pEP with saturation after two days (Fig. 14A). Comparing replication kinetics of the labeled and unlabeled constructs showed that RNA replication is stable at every time point, proving that fluorescence-labeling has no influence on replication. When the release of RNA into the supernatant of electroporated cells is analyzed over time, JC1(A4) showed 10-fold higher amounts of released RNA in comparison to the labeled viruses. However, a constant amplification of extracellular RNA was measured (Fig. 14B), confirming that the cells release RNA evenly throughout the entire experimental period.

In summary, all replicating HCV constructs exhibit the same biophysical properties, demonstrating similar kinetics in protein production and RNA transcription efficiency. Taken together, the fluorescence-label does not have an influence on protein expression and replication over time in HCV positive cells and is therefore well-tolerated.

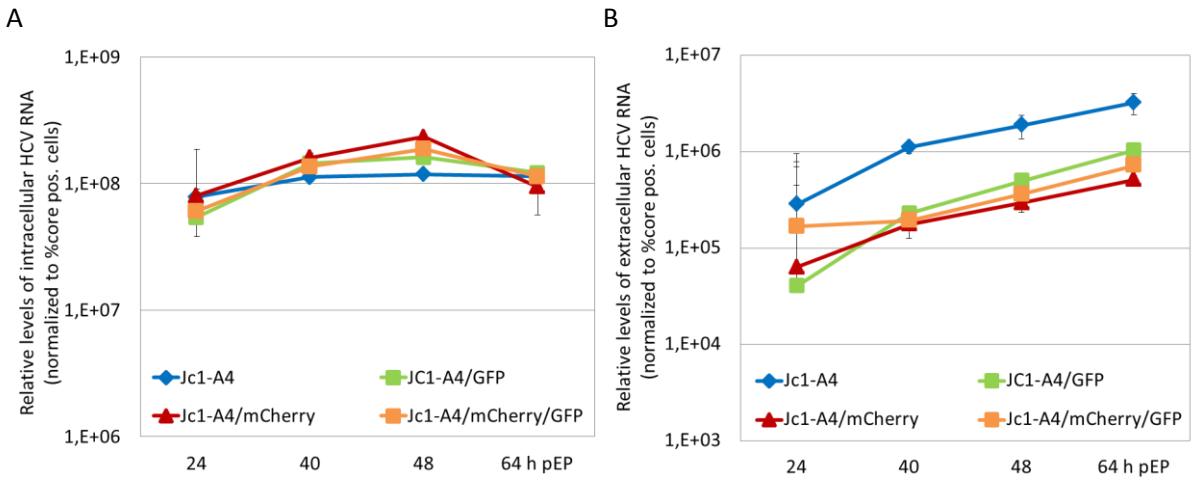


**Figure 14: Replication kinetics of HCV constructs with fluorescently-labeled versus unlabeled proteins.** 0.5x10^6 electroporated Huh7.5 cells were harvested at indicated time points after electroporation. (A) Cellular RNA and (B) RNA from the supernatant was isolated and transcribed in cDNA. The total cDNA amount was quantified by absolute PCR and further normalized to HCV positive cells in FACS. Error bars represent standard deviations of two independent experiments.

### 5.1.6 Release of viral proteins into the supernatant

The fluorescently-labeled HCV genomes should serve as a tool for the investigation of the assembly, transport and release of viral particles. Therefore, the egress of viral proteins into the supernatant was analyzed by Western Blot. It was also to be ensured that the detected viral RNA within the supernatant (5.1.5) was not unspecifically released, but in parallel with the structural viral proteins. Huh7.5 cells were electroporated with *in vitro* transcribed RNA and cultured for 48 h (4.1.12; 4.2.3).

Supernatants were harvested and concentrated via ultracentrifugation (4.6.1) and analyzed by Western Blot (4.3.4; 4.3.5; 4.4.1).

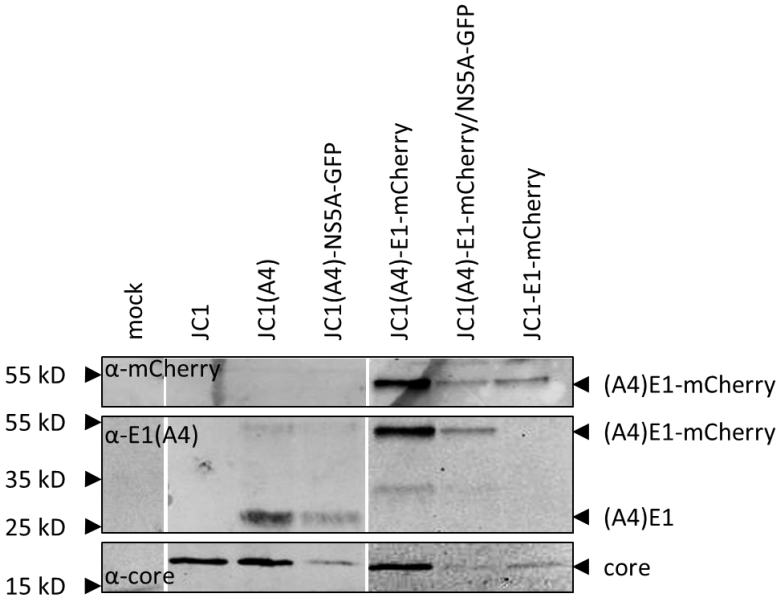


**Figure 15: Released viral proteins in the supernatant.** Supernatant of 2.6x10^7 electroporated Huh7.5 cells was harvested 48 h pEP and concentrated via sucrose gradient centrifugation over a 20% sucrose cushion. The samples were separated by 12% SDS-PAGE and analyzed by immunoblot with abs for E1(A4), mCherry and Core.

Viral structural proteins Core, (A4)E1 as well as (A4)E1-mCherry could be detected within the supernatants of HCV genome electroporated Huh7.5 cells (Fig. 15). Nevertheless, the total protein amount differs among the used constructs. Together with previous data showing proper heterodimer formation of E1 and E2 within the cell and the accumulating RNA in supernatant over time, these results indicated that viral particles were readily assembled and released into the supernatant.

### 5.1.7 E1-mCherry is incorporated into released hepatitis C virus particles

Viral structural proteins are released into the supernatant of HCV expressing Huh7.5 cells. However, it was not entirely clear, if the E1-mCherry is properly incorporated into assembled and released HCV particles. Therefore density gradient centrifugation was performed. Huh7.5 cells were electroporated with RNA of the JC1(A4) or the JC1(A4)-E1-mCherry genome, respectively, and cultured for 72 h (4.1.12; 4.2.3). Supernatants were harvested and concentrated via ultracentrifugation (4.6.1). Concentrates were loaded onto iodixanol (OptiPrep) gradients and equilibrium centrifugation was performed (4.6.2). Fractions were separated and analyzed with regards to correct protein insertion in association with lipoproteins by Western Blot (4.3.4; 4.3.5; 4.4.1) and RNA incorporation by absolute qRT-PCR (4.1.13; 4.1.14). Thus, the particle density profile after cellular release was determined.

First experiments revealed that E2, labeled and unlabeled E1 as well as Core proteins, all together are enriched within the same density fractions (4-6) between 1.08 to 1.16 g/ml with a peak around 1.11 g/ml (Fig. 16A). In addition, the lipoprotein ApoE, described to be highly associated with HCV

particles within patient serum and cell culture supernatant (Merz et al. 2011) was also detectable at 36 kDa in these particular fractions. A more finely graduated experiment showed the same density range peaking around 1.14 to 1.15 g/ml (Fig. 16B). Moreover, total RNA amounts within the fractions were determined and proofed a peak in the particular densities (Fig. 16B, graph, fraction 5-6). RNA was also found in intermediate density fractions (1.05 g/ml), reflecting the results from Jammart et al., who showed that these low density fractions are not infectious (Jammart et al. 2013). Therewith, JC1(A4) and JC1(A4)-E1-mCherry demonstrated the same high density profile, which was in line with published results in cell culture with 1.10 to 1.15 g/ml for infectious virus particles (Jammart et al. 2013, Lindenbach et al. 2005). These data confirm that all HCV structural proteins as well as viral RNA are present in the same density fraction as ApoE. Additionally, this demonstrates that the fluorescently-labeled surface protein E1 is not altered in its interactions with E2 and Core and therefore, is correctly incorporated into complete viral particles. Thus, we could show that the mCherry-label is well tolerated and does not disrupt viral particle assembly and release processes during the viral life cycle.

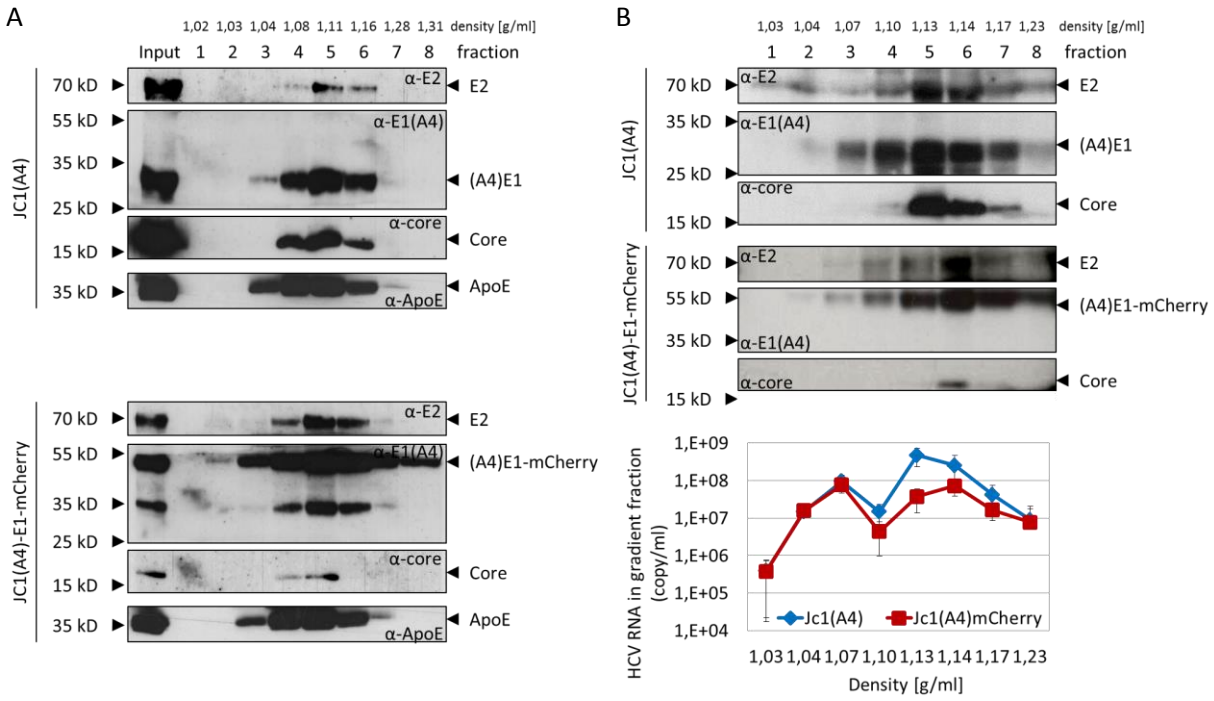


**Figure 16: Incorporation of E1-mCherry into viral particles demonstrated by density gradient centrifugation.** 6.6x10^7 (A) and 9.5x10^7 (B) Huh7.5 cells were electroporated with HCV genomes. Supernatants were harvested 72 h pEP. After concentration via sucrose gradient centrifugation over a 20% sucrose cushion, concentrates were loaded onto self-prepared density gradients ranging (A) in 6% steps from 8 to 38% or (B) in 4% steps from 14 to 38% iodixanol (OpiPrep). Following equilibrium centrifugation for 21 h, fractions were collected and again concentrated before the analysis of proteins by immunoblot staining with abs for E2, E1(A4), Core and ApoE (1:1000) or (B) before the RNA isolation for qRT-PCR. Error bars represent standard deviations of two independent experiments.

### 5.1.8 Infectivity of E1-mCherry containing viral particles is highly attenuated

Next, the infectivity of the released fluorescent viral particles was analyzed and compared to unlabeled HCV.

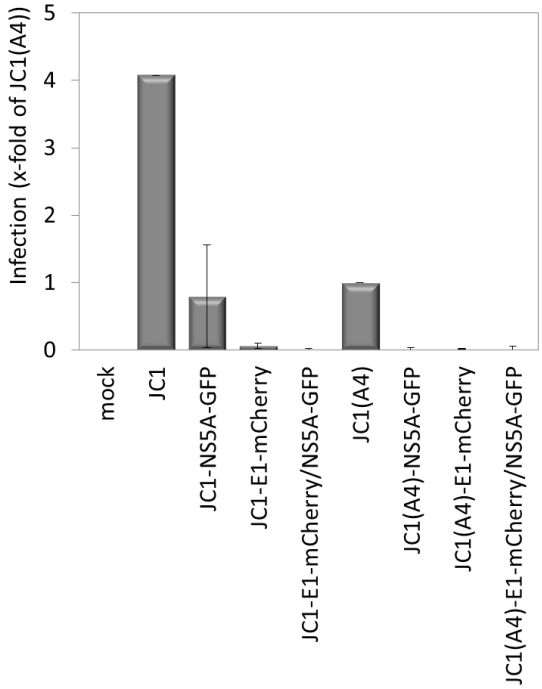


**Figure 17: Infectivity of E1-mCherry containing viral particles is highly attenuated.** Supernatant of 1.3x10^7 electroporated cells was harvested 72 h pEP and concentrated via ultracentrifugation prior to infection of Huh7.5 cells over three days. Afterwards, cells were harvested and stained against Core proteins for FACS measurement. Results were normalized to JC1(A4). Error bars represent standard deviations of three independent experiments.

Huh7.5 cells were electroporated with *in vitro* transcribed RNA of the different genomes and cultured for 72 h (4.1.12; 4.2.3). Supernatants were harvested and concentrated via ultracentrifugation. Huh7.5 cells were inoculated for 3 days with the concentrated virus particles (4.6.3). Afterwards, intracellular Core proteins were stained and analyzed by FACS (4.4.3; 4.2.6).

Of note, introducing the A4 sequence into JC1 E1 resulted in a 4-fold decreased infectivity of the JC1(A4) virus in comparison to wild-type JC1 (Fig. 17). JC1-NS5A-GFP showed high variations, depicted by the high standard deviation and showed also a 4-fold diminished infectivity. Mirroring this result, it was previously described that the GFP-tag leads to a 10-fold reduction in TCID50 (Schaller et al. 2007). Furthermore, JC1(A4)-NS5A-GFP was highly attenuated, but few infected cells were detectable by fluorescence microscopy. The mCherry-labeled constructs showed very few to no infected cells. Altogether, reconstitution of the A4-sequence and the NS5A-GFP tag led to strongly reduced infectivity, whereas the E1-mCherry tag disrupted infectivity. However, since this thesis focuses on the assembly and release of HCV particles, this observation was not a critical fundamental issue.

To summarize, a successful and comprehensive characterization of fluorescently-labeled E1-mCherry HCV genomes was carried out. Furthermore, we demonstrated that a fluorescent-protein in close proximity to the transmembrane region of E1 does not interfere with stable viral protein expression

and adequate intracellular protein distribution. Moreover, we observed wild-type-like replication kinetics in protein and RNA levels over time, suggesting that the mCherry-fusion did not have an adverse effect on RNA replication or protein production. E1-mCherry heterodimer-formation with E2 is not disrupted and results in correctly assembled viral particles in association with ApoE within the appropriate high-density fractions after gradient centrifugation. Nevertheless, infectivity of the fluorescently-labeled virions is highly attenuated. In conclusion, the E1-mCherry tag is well tolerated and a valuable tool for further studies in assembly and release.

## 5.2 Analysis of time-dependent behavior of structural proteins

The JC1-E1-mCherry genomes (5.1) were then exploited to study the spatio-temporal distribution and the dynamics of structural proteins with red fluorescence (mCherry) and to discriminate these from replication/translation sites labeled with green fluorescence (GFP) in confocal live cell microscopy.

### 5.2.1 E1-mCherry accumulations increase over time

Initially, Huh7.5 cells were electroporated with *in vitro* transcribed RNA from JC1-E1-mCherry/NS5A-GFP (4.1.12; 4.2.3), monitored by spinning disc live cell fluorescence microscopy and pictures were taken daily over a period of 4 days. As previously described, NS5A-GFP accumulated in dot like structures (Masaki et al. 2008, Miyanari et al. 2007), representing translation complexes. Furthermore, E1-mCherry showed an ER-like distribution but also appeared in dot-like accumulations. To define an accumulation, an arbitrary threshold of 0.8 µm in diameter was chosen. E1-protein accumulations seemed more defined at 2 to 4 days pEP in comparison to pictures taken at 24 h pEP (Fig. 18A). Moreover, the amount of non-structural NS5A-protein accumulation showed a decrease over time. The NS5A-GFP and E1-mCherry accumulations were automatically counted for several cells and the means were calculated and plotted in the graph in Figure 18B. Within the 96 h time period, the amount of E1-mCherry accumulations increased 2.4-fold (Fig. 18A,B; 24h mean(M)=15, SD=8; 48h M=32, SD=16; 72h M=39, SD=16; 93h M=36, SD=18), whereas NS5A-GFP complexes diminished 1.5-fold (Fig. 18A,B; 24h M=43, SD=16; 48h M=41, SD=16; 72h M=33, SD=16; 93h M=28, SD=15). The calculated ratio between structural and non-structural protein levels showed 3.25-fold elevation of structural protein accumulations (Fig. 18C; 24h M=0.38, SD=0.23; 48h M=0.83, SD=0.38; 72h M=1.28, SD=0.47; 93h M=1.89, SD=2.38). This suggests that replication commences quickly and efficiently after electroporation, while decreasing at later time points. By contrast, structural protein accumulates over time in the HCV life cycle, possibly representing assembly sites or assembled viral particles that could be located within transport compartments.

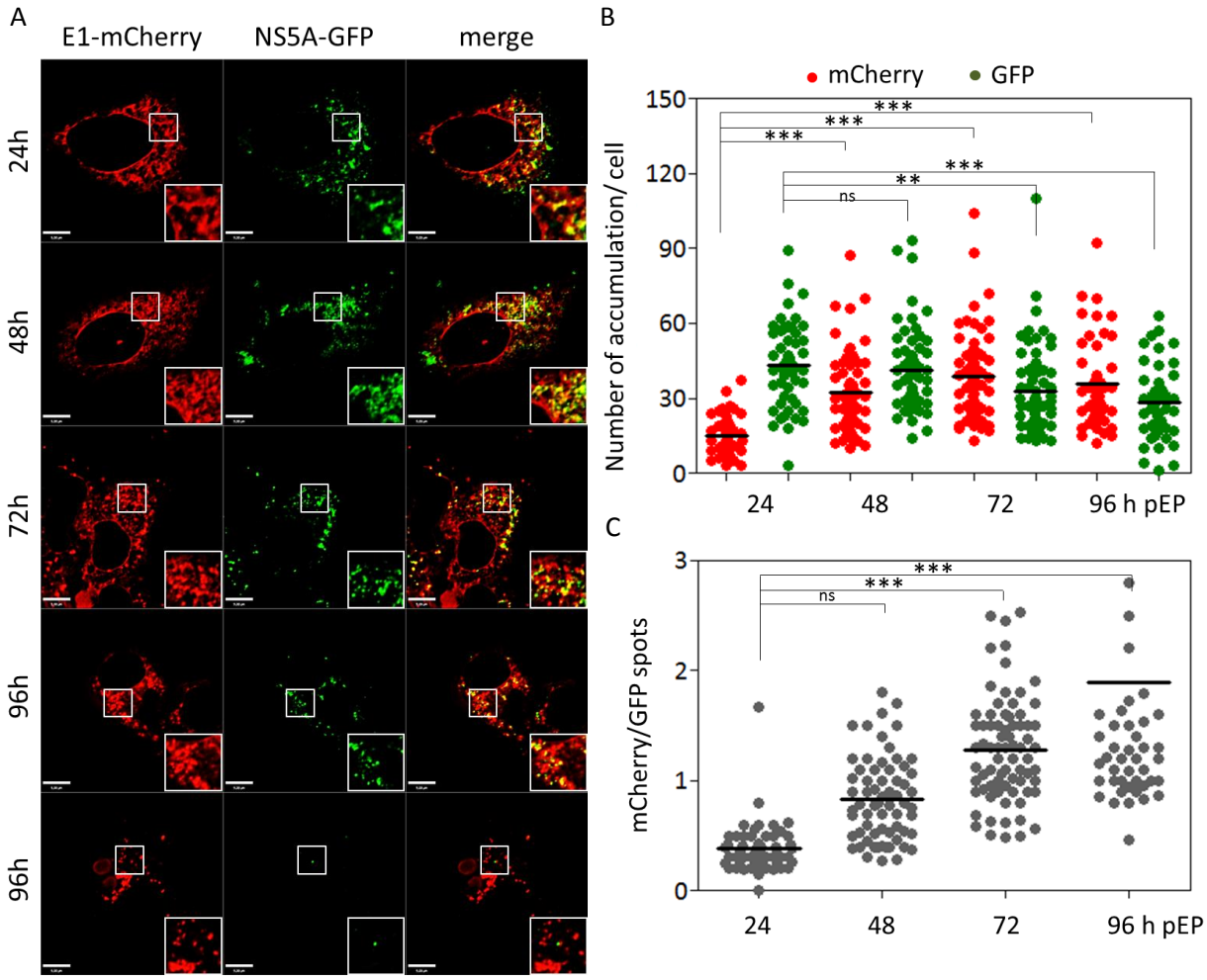


**Figure 18: E1-mCherry accumulations increase over time.** The genome JC1-E1-mCherry/NS5A-GFP was electroporated into Huh7.5 cells. (A) Cells were monitored by live cell microscopy and pictures were taken at the indicated time points after EP. White boxes indicate magnification sites, shown on the lower right. Bars: 9 µm. (B) Accumulations of E1-mCherry and NS5A-GFP with a maximal size of 0.8 µm were counted respectively in 22 to 38 cells per experiment with the spot finding tool of the Volocity software. (C) Ratios of E1-mCherry spots divided by NS5A-GFP spots are depicted. Error bars represent standard deviations of two independent experiments. Asterisks indicate significant differences compared to the 24 h measurement. *P ≤ 0.05, **P ≤ 0.01, ***P ≤ 0.001.

### 5.2.2 Structural protein interactions increase in a time-dependent manner

For the assembly of viral particles the three HCV structural proteins Core, E1 and E2 need to interact. To assess whether these interactions increase over time, as suggested by the increase in E1 accumulations (5.2.1), a proximity ligation assay was performed (see 4.4.4). Therefore, Huh7.5 cells electroporated with JC1-E1-mCherry RNA (4.1.12; 4.2.3) were grown on cover slips and fixed every day over a four day period. For PLA, proteins were detected with a rabbit antibody directed against E1-mCherry and a mouse antibody of the other proteins, respectively. Specific secondary antibodies, coupled with a short DNA-sequence, allow ligation and rolling circle amplification upon close proximity of the proteins during interaction. Thereby, a green fluorescent substrate is build, which allows detection of the interaction in fluorescence microscopy.

Since JC1-E1-mCherry emits red fluorescence, electroporated thus HCV expressing cells could be readily identified. By PLA, the interaction of E1-mCherry with E2, Core, NS3 and NS5 was assessed (Fig. 19, showing the E1-mCherry/E2 interaction, Fig. 21, shows representative E1-mCherry/Core interactions). Counting of PLA spots revealed that the interaction of the structural proteins E1-mCherry and E2 increased significantly from 48 h to 89 h pEP up to 2.16-fold (Fig. 19A,B; 24h M=24, SD=9; 48h M=34, SD=16; 72h M=47, SD=21; 93h M=49, SD=20). E1-mCherry and Core showed also a tendency for growing interaction (Fig.19B; 24h M=25, SD=16; 48h M=39, SD=15; 72h M=43 SD=15; 93h M=51, SD=29).

A

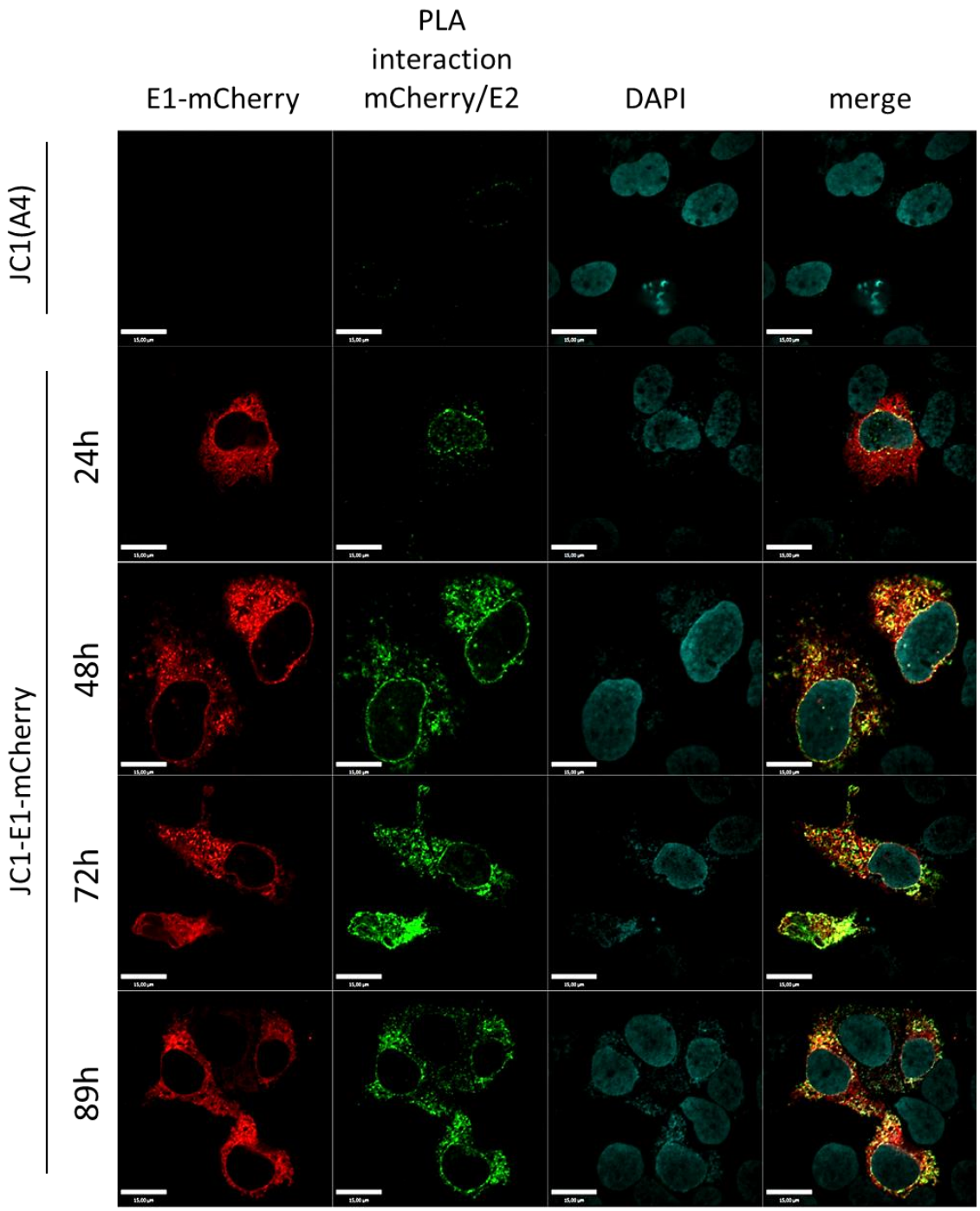

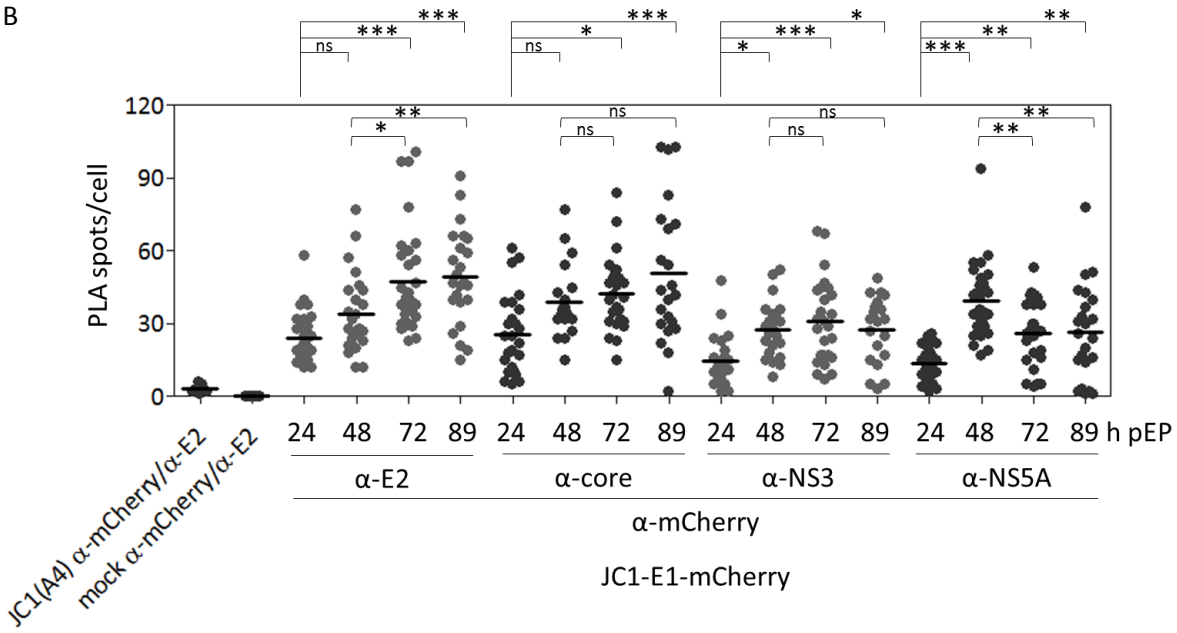


**Figure 19: Increasing interaction of structural proteins at late time points.** JC1-E1-mCherry was electroporated into Huh7.5 cells. At indicated time points pEP cells were fixed and PLA was performed with an anti-mCherry and either anti-E2, anti-core, anti-NS3 or anti-NS5A (1:100) as primary antibodies (4.4.4). (A) Representative pictures of the interaction of E1-mCherry (red) with E2 (PLA green) and DAPI (blue) labelling over the indicated time points are shown. Bars: 15 µm. (B) A minimum of 20 cells were analyzed for each time point using the Volocity software tool: spot counting, with a maximum size of 0.8 µm. Graphs give the mean number of PLA spots counted over different cells with the corresponding standard deviation. Asterisks give significant differences in the indicated groups. *P ≤ 0.05, **P ≤ 0.01, ***P ≤ 0.001.

In contrast, the interaction of E1-mCherry with the non-structural protein NS3 rapidly reached a plateau already 48 h pEP (Fig. 19B; 24h M=15, SD=11; 48h M=27, SD=12; 72h M=31 SD=17; 93h M=28, SD=14). Moreover, E1-mCherry and NS5A interactions decline from 48 h on (Fig. 19B; 24h M=14, SD=7; 48h M=39, SD=15; 72h M=26 SD=13; 93h M=27, SD=20). The results for the non-structural proteins suggest ongoing translation and replication processes with transient interaction of structural and NS proteins. The data for the structural proteins correspond to the enhanced structural protein accumulations at late time points of the HCV life cycle (5.2.1) and strengthen the idea of particle formation and ongoing intracellular assembly.

### 5.2.3 Structural and non-structural protein accumulations separate over time

It was hypothesized that E1-mCherry accumulations represent assembly or viral particle transport compartments. However, assembled viral particles do not contain NS5A-GFP or active translational areas. Hence it was examined whether E1-mCherry accumulations separate from the NS5A-GFP replication/translation sites within the cell. Huh7.5 cells were electroporated with *in vitro* transcribed RNA from the JC1(A4)-E1-mCherry/NS5A-GFP genome (4.1.12; 4.2.3). Two-hour-long videos were

recorded daily for 4 days by live cell fluorescence microscopy (4.5.1). As depicted in Figure 20A, 24 h pEP NS5A-GFP was largely distributed within the cell. In contrast, only traces of the surface protein E1-mCherry were detectable at this early time point (Fig. 20A, Video S1a). 48 h pEP structural proteins colocalized and moved together with replication/translation complexes (Fig. 20A,B 48 h, Video S1b), indicating translational sites in cooperative compartments. At 72 h pEP colocalizing and non-colocalizing spots were detectable (Fig. 20A,B 72 h, Video S1c). However, later time points showed higher separation levels of structural complexes and individual movement of the E1-mCherry accumulations (Fig. 20A,B 96 h, Video S1d). These results corroborate the aforementioned suggestion of viral particle accumulation and transport at later time points.

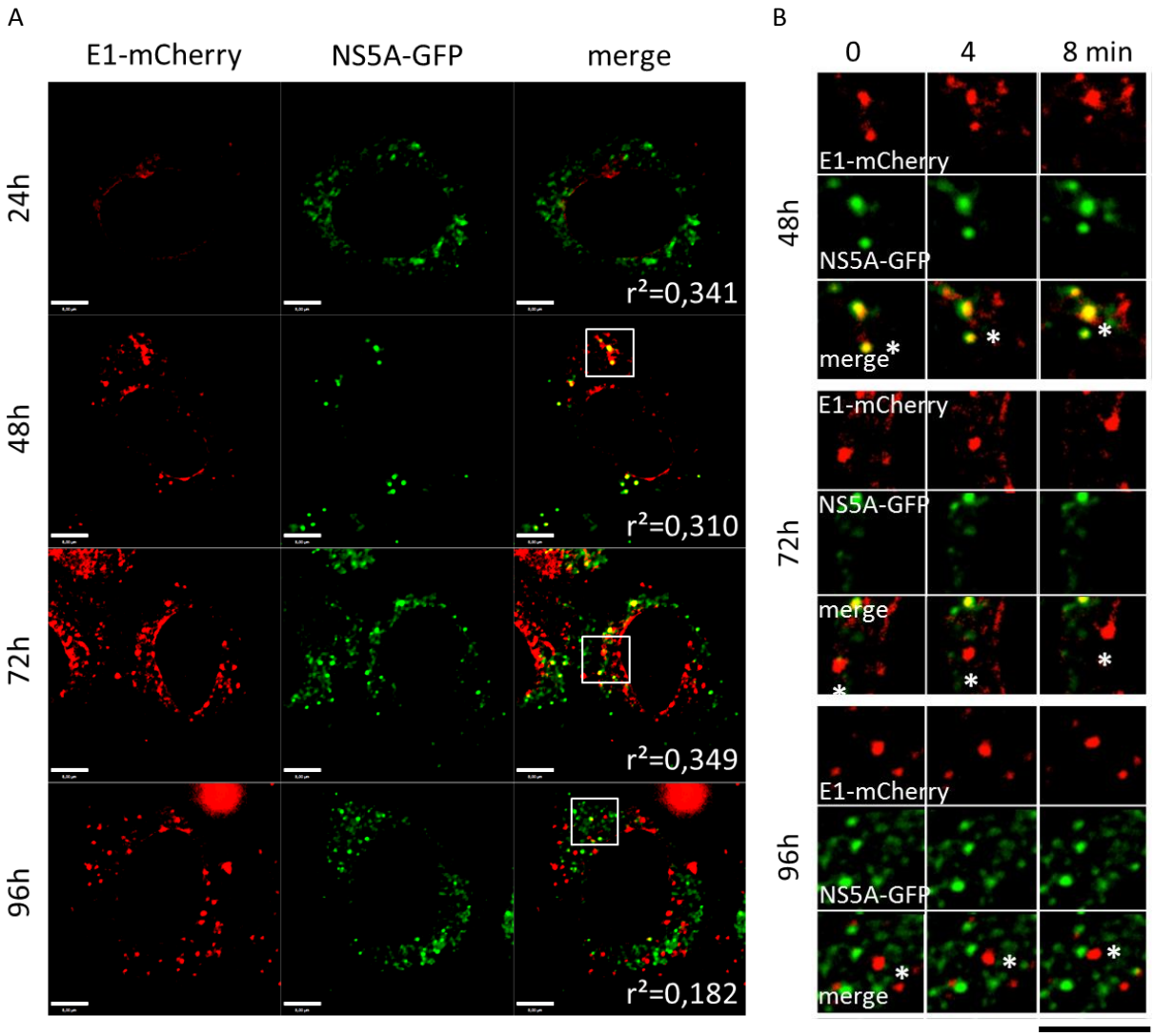


**Figure 20: Structural and non-structural protein accumulations separate over time.** JC1(A4)-E1-mCherry/NS5A-GFP was electroporated into Huh7.5 cells. Cells were seeded on wilco dishes specifically for live cell microscopy. (A) Cells were documented in live cell microscopy at indicated time points after EP. The white square depicts the area of magnification from part B. Bars: 8 µm. (B) Time lapse movies were recorded for 1 hour 17 min on each day. Three exemplary pictures of the movie sequences are shown, with the white asterisk following the movement of E1-mCherry. Videos S1a-d on supplementary CD, Bars: 8 µm.

### 5.2.4 E1-mCherry accumulations colocalize with E1/E2- and E1/Core-interaction sites

Going forward, we investigated whether E1-mCherry dot-like accumulations colocalize with the other structural proteins E2 and Core (5.2.1-3), an event that would be indicative of possible assembly and transport compartments at late time points. For that purpose, samples obtained by staining for the PLA interaction-reaction (5.2.1) were analyzed for colocalization of E1-mCherry accumulations and PLA-interaction spots. Therefore, pictures were magnified and colocalizations, appearing yellow in the merge, were highlighted with arrows (Fig. 21). Furthermore, fluorescence intensity profiles were generated for the lined areas in the merge pictures (Fig. 21, graphs). This clearly demonstrates a spatial association of E1-mCherry with E2 or Core at 48 and 72 h pEP (Fig. 21, arrows), which was supported by data shown in the fluorescence graphs. Here, E1-mCherry (red line) peak together with the PLA interaction signal of E2 or Core (green line) at several positions within the cell. Nevertheless, not all E1-mCherry accumulations overlap with the interaction sites. Thus, JC1-mCherry fluorescence indicates sites of protein translation; however the cumulated data also strongly suggests that punctate E1-mCherry accumulations represent areas of virus assembly or assembled viral particles.

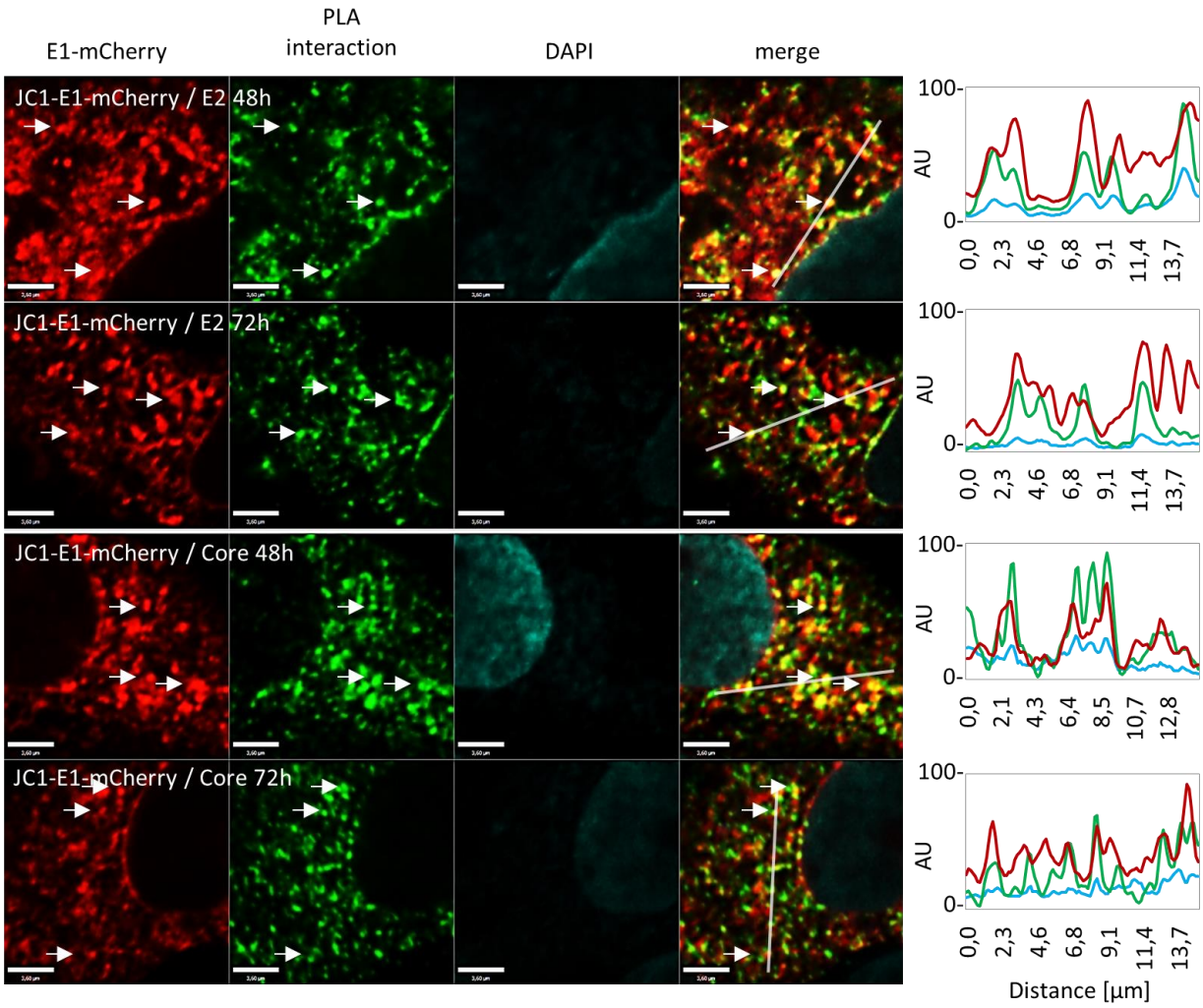

**Figure 21: E1-mCherry accumulations are sites of viral structural protein interaction at late time points.** Electroporated Huh7.5 cells with JC1-E1-mCherry were fixed and PLA was performed with an anti-mCherry (rb) and either anti-E2 (2 upper panels) or anti-core (lower panels) (1:100) as primary antibodies (4.4.4) 48 and 72 h pEP. Analysis was done by spinning disc microscopy for colocalization of PLA interaction spots and E1-mCherry accumulations. Representative colocalizations are highlighted by white arrows. Bar: 3.6 µm. On the right, each fluorescence profile of the lined area within the merge is depicted. The intensity is depicted in arbitrary fluorescence units (AU). E1-mCherry is red, the interaction in green and DAPI blue.

### 5.2.5 Peripheral E1-mCherry accumulations do not recover after photobleaching

The previous data suggested that E1-mCherry accumulations might at least in part represent compartments containing assembled viral particles. Thus, perinuclear ER associated E1-mCherry accumulations versus distant E1-mCherry accumulations might reveal differences in cellular transport connections. This question was assessed by FRAP analysis. For that purpose, JC1-E1-mCherry electroporated Huh7.5 cells (4.1.12, 4.2.3) were recorded in live-cell microscopy (4.5.1), while selected cellular areas were photobleached. Fluorescence recovery after photobleaching (FRAP) was assessed by measuring the fluorescent-intensity before and after bleaching, thereby gaining insights into protein diffusion or the transportation of the labeled probes (4.5.3).

The first picture in Figure 22A depicts a cell overview with a perinuclear E1-mCherry accumulation (upper circle) and one at a distant location (lower circle). Two magnified pictures are shown before bleaching, demonstrating movement of the distant aggregation (0 and 3 sec). At second 9 the mCherry fluorescence was bleached. The following video sequence proofs that the E1-mCherry accumulation proximal to the nucleus reappeared very rapidly after bleaching (Fig. 22A, upper white circle, 30-180 sec, Video S2), whereas the accumulation at a distal location did not reappear at all (lower circle). The same can be seen in the intensity profile (Fig. 22B), where the mean intensities of the bleached areas were plotted. The perinuclear region regained 3-fold more fluorescence within the first 15 seconds post-photobleaching. The fluorescence of the distal location remained at background levels after bleaching. Thus, peripheral E1-mCherry accumulations are no longer interconnected with translation-sites, where protein trafficking occurs quickly. Instead, these distant compartments revealed a transport compartment character.

A

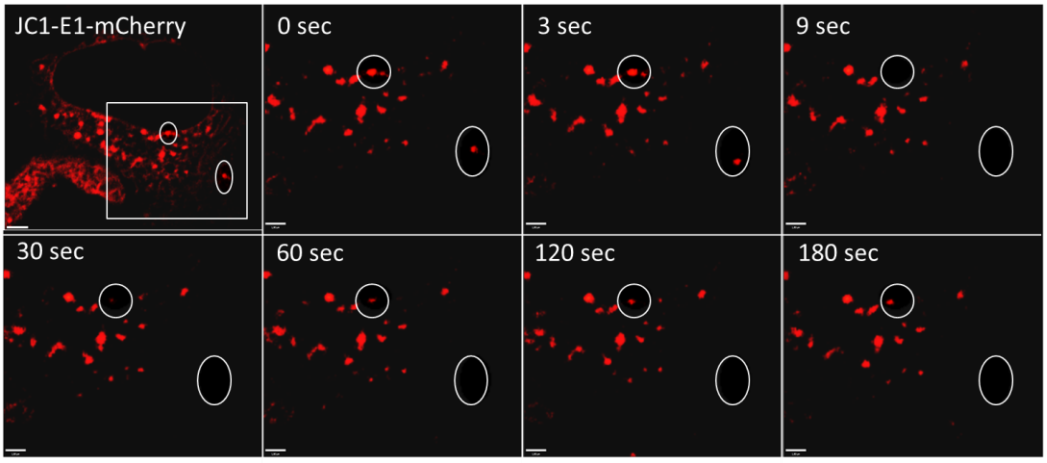

B

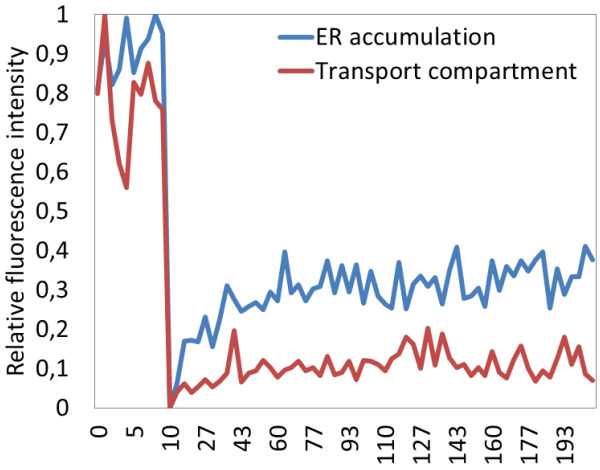


**Figure 22: E1-mCherry accumulations show transport compartment character.** Huh7.5 cells electroporated with JC1-E1-mCherry were analyzed by live cell microscopy 56 h pEP. (A) FRAP was conducted on the indicated areas. The video sequence over 180 sec of live-cell imaging is shown. Bars: 3.4 µm. The white square depicts the area of magnification. Bar: 1.8 µm. Video S2 on supplementary CD, Bars: 3.4 µm. (B) Fluorescence intensity of the depicted areas was assessed over time and normalized to the intensity before and after FRAP.

In summary, a time-dependent increase in structural E1-mCherry accumulations was observed, which coincided with an increase in the interaction between structural proteins over four days. While NS5A-accumulations decreased, the interaction between E1-mCherry and either NS5A or NS3 did not show any time-dependent character. Looking at later time-points, the accumulations of structural and non-structural proteins dissipated. As further support for the theory of viral particle formation at these time-points, the interaction-sites of structural proteins (E1/E2 and E1/Core) were observed colocalizing with several E1-mCherry accumulations. Moreover, photobleaching of distal E1-mCherry accumulations in comparison to perinuclear sites revealed transport-compartments disconnected from translational sites.

## 5.3 Investigation of different cellular pathways involved in HCV release

JC1-E1-mCherry was proven to be a useful tool for visualizing HCV structural E1 protein distribution and movement and it permits tracking of assembly sites where structural proteins assemble to virus particles within the cell. Therefore, it was used to characterize the transport pathway HCV hijacks for release.

Previous work (Banning, 2011) has hypothesized that HCV bypasses the Golgi on its way to the cell membrane. Both colocalization studies and inhibitor treatments suggested involvement of endosomes. In addition, the Core protein was also found to traffic within early endosomes (Lai et al. 2010), whereas others reported Core traveling along the secretory pathway and being retained in the Golgi after recycling endosomal-silencing (Coller et al. 2012).

Thus, it was more closely examined if the Golgi is involved in HCV transport and which cellular compartments are important for transition. To take advantage of the JC1-E1-mCherry construct, live cell microscopy was conducted to study the distribution and movement of E1-mCherry in combination with different cellular fusion proteins that mark cellular compartments.

### 5.3.1 HCV seems to bypass the Golgi during release

Initial investigations by Banning did not support the colocalization of E1-mCherry and the Golgi. To verify this by live cell microscopy, the DNA plasmid of a cellular protein, a fragment of the β-1,4-galactosyltransferase (GalT) fused to mCFP (Llopis et al. 1998, Rocks et al. 2010) and other cellular marker proteins were coelectroporated into Huh7.5 cells along with RNA from JC1-E1-mCherry, respectively (4.1.12; 4.2.3). GalT is a Golgi-residing enzyme, which metabolizes galactose to glycoprotein-bound acetylglucosamine and was thus used as a marker for the *trans*-Golgi. The small surface protein of hepatitis B virus (HBV-S) fused to mCherry (kindly provided by V. Bruß, Helmholtz Zentrum, Munich) and a YFP-fusion protein of Gaussia-luciferase (Rocks et al. 2010) served as controls for Golgi passage. HBV-S, in passing through the secretory pathway, travels from the ER to the Golgi and finally, to the plasma membrane and is highly glycosylated along the way. The Gaussia Luciferase is a naturally secreted bioluminescent protein from the marine copepod, *Gaussia princeps*. Optimized cDNA in a vector with a YFP-gene can also serve as a sensor for the secretory pathway (Badr et al. 2007, Tannous et al. 2005). Moreover, the lipoprotein ApoE-GFP (kindly provided by G. Randall, University of Chicago, Chicago) was used as a control for colocalization, since it is described to be associated with HCV particles (Merz et al. 2011). CD74(li) is a chaperone for the protein expression of the major histocompatibility complex (MHC) class II in antigen presenting cells. More importantly, it harbors a signal for endosomal targeting in its cytoplasmic tail (Cresswell 1994). In this study, CD74(li)-CFP served as a marker mainly for the ER and for late endosomes. However, it is important to note that it is also transported through the Golgi.

With spinning disk in combination with live cell imaging, different coelectroporated constructs were examined. In addition, several cells were analyzed to determine the Pearson's Correlation Coefficient (r). First, after coelectroporation with the Golgi-marker GalT, HBV-S was found to traffic through the secretory pathway, confirming previous studies (Patzer, Nakamura, and Yaffe 1984). As shown in Figure 23A, both proteins move alongside in the cell, validating the experimental setup (Fig. 23A, Video S3). Further coEPs of the Golgi-marker GalT (in green) with either HBV-S-mCherry, Gaussia-YFP or HCV JC1-E1-mCherry (each in red) were performed. As expected, HBV-S again colocalized with GalT and the Gaussia signal also overlapped with the one from GalT, leading to an $r^2$ of 0.42 and 0.42, respectively (Fig. 23B,C panel 1 and 2). These pictures were indicative of the Golgi passage of each protein. In contrast, no colocalization of HCV E1-mCherry and GalT-CFP was observed with an $r^2$ of 0.15 (Fig. 23B,C panel 3). As further controls for E1-mCherry localization, ApoE and CD74 were examined. ApoE demonstrated a partial colocalization with E1-mCherry accumulations ($r^2$=0.3), representing viral particle association. Since CD74(li) is mainly distributed within the ER, the results showed broad colocalization with E1-mCherry ($r^2$=0,6). Taken together, these results suggest that

there is no E1-mCherry movement within the *trans*-Golgi, indicating that HCV takes another pathway for release.

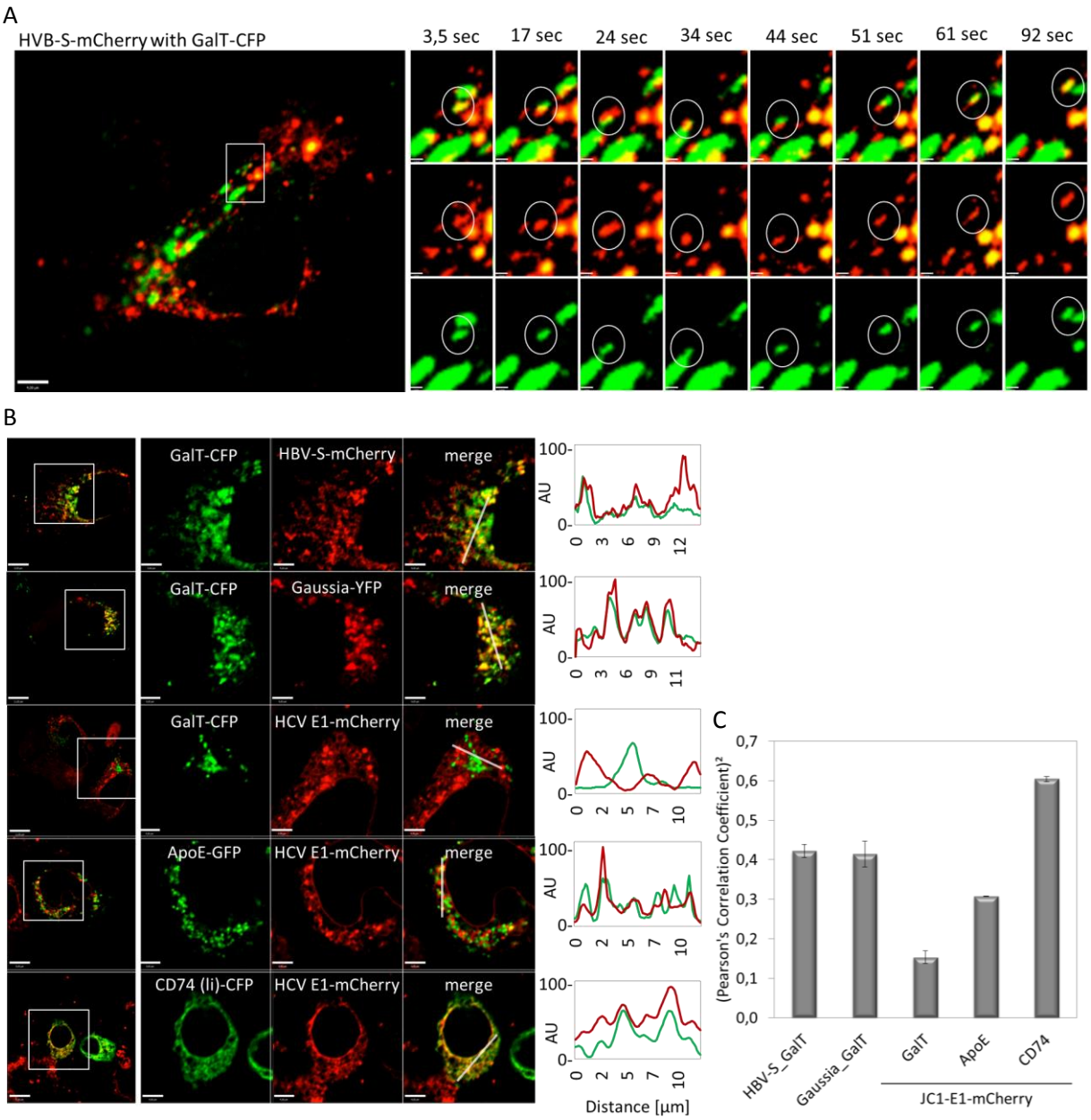


**Figure 23: No evidence for E1-mCherry movement within the Golgi.** Representative pictures of Huh7.5 cells 56 h pEP coelectroporated with (A) HBV-S-mCherry (in red) and GalT-CFP (in green) separated in a video sequence over 100 sec. The white circle depicts the co-movement. Bar: 4 µm. Video S3 on supplementary CD, Bar: 2 µm. (B) Co-EP of GalT-CFP with either HBV-S-mCherry, Gaussia-YFP or JC1-E1-mCherry in the 3 upper panels. The 2 lower show coEP of JC1-E1-mCherry with ApoE-GFP or CD74(Ii)-CFP. Bar: 11µm. The white square depicts the area of magnification. Bar: 4 µm. Fluorescence profiles of lined areas are depicted. The intensity is in arbitrary fluorescence units (AU). mCherry-tagged proteins are depicted in red, other proteins in green. (C) 3 to 11 cells were cropped and Pearson's Correlation Coefficient in square was calculated and plotted in the graph.

### 5.3.2 HCV E1 and E2 glycoproteins show a mannose-rich glycosylation pattern in cells and supernatant

To further challenge the hypothesis that HCV bypasses the Golgi, a biochemical assay was employed. The glycosidases EndoH and PNGaseF cleave modifications from glycosylated proteins. Whereas PNGaseF cleaves whole glycan residues from the protein binding-site of oligomannose, hybrid and complex glycans, EndoH removes specifically the high-mannose and hybrid structures. Thus, proteins with mannose attachments are exclusively and completely deglycosylated by EndoH and are referred to as “EndoH-sensitive”, indicating that they are not processed within the Golgi. To investigate whether HCV glycoproteins traverse through the Golgi RNA of JC1(A4) was electroporated into Huh7.5 cells and cultured for three days (4.1.12; 4.2.3). Cells were subsequently detached, divided into 3 different samples and were treated with either EndoH, PNGaseF or remained untreated (see method 4.3.3). As a control, the HBV-S protein was utilized, since it appears as unmodified and complex-glycosylated within the supernatant of transfected cells (Patzer, Nakamura, and Yaffe 1984). Complex saccharides are only added to a glycoprotein, during its transport through the *medial*- and *trans*-Golgi, where specified enzymes are located. Contrary, EndoH-sensitive glycoproteins were not processed and presumably not transported through the Golgi. The digested samples were analyzed by Western Blot (4.3.4, 4.3.5, 4.4.1). Antibodies directed against the structural proteins HBV-S, E1 and E2 were used to detect the shift in protein-sizes due to digestion.

First, the untreated HBV-S showed two distinct bands around 24 and 27 kDa, depicting the unprocessed and the complex-form. After EndoH treatment, both bands remained, showing EndoH resistance. In concordance with that, incubation with PNGaseF digested the complex-glycosylated form. As a result, the upper HBV-S band shifted lower, resulting in a thick 24 kDa band (Fig. 24A). Looking at the first panel in Figure 24B, E2 proteins were separated in the upper part, E1 in the lower. It is obvious that both EndoH and PNGaseF treatments resulted in the complete cleavage of saccharides from the structural E1 and E2 proteins of HCV, proving their EndoH sensitivity. The E2 protein size shifted from 70 kDa to 35 kDa, while E1 was no longer detectable at 31 kDa but around 18 kDa. Unfortunately, E1 could no longer be detected after PNGaseF treatment. As already reported, the slight migration difference of about 3 kDa between EndoH and PNGaseF treated samples is due to a residual N-acetlyglucosamine at every previous glycosylation site (Dubuisson et al. 1994). Shown on the right blot in Figure 24B, E1 and E2 showed a concentration-dependent sensitivity to EndoH, and as a control, to PNGaseF treatment. A slight EndoH- and PNGaseF- resistant double band was also previously reported (Op De Beeck et al. 2004, Rouillé et al. 2006). These results proved high-mannose glycosylation of E1 and E2, strongly confirming that HCV structural proteins are not processed by *medial*- or *trans*-Golgi enzymes.

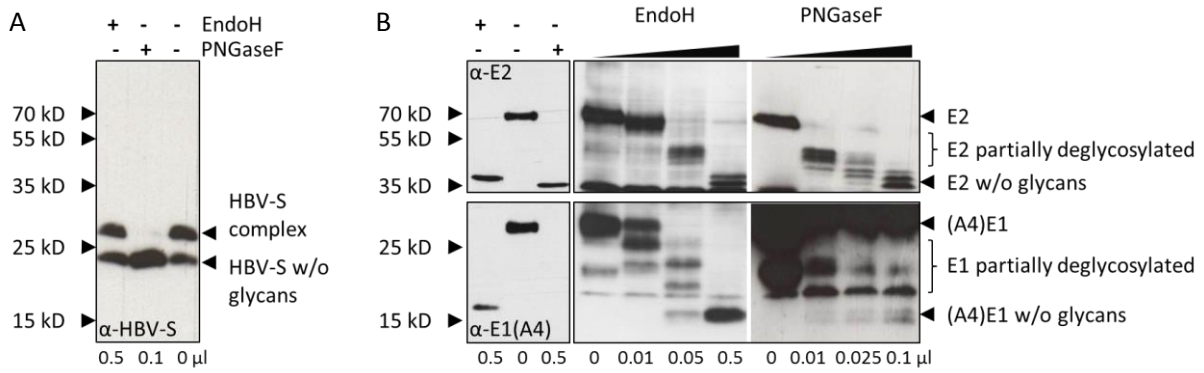


**Figure 24: Intracellular HCV structural proteins show an oligomannose glycan structure.** (A) 0.4x10^6 Huh7.5 cells were transfected with HBV-S via X-tremeGene according to the manufacturers' protocol. Supernatant was harvested 72 h pTF and digested with EndoH or PNGase, respectively, or left untreated at 37°C. Immunoblot was done with anti-HBV-S (1:2000). (B) 1.3x10^7 Huh7.5 cells were electroporated with JC1(A4) and cultured for 72 h. Cells were lysed in 0.5% NP40 and digested with the indicated enzymes and volumes (lower line) at 37°C. Proteins were stained with anti-E2 (upper part) and anti-E1 (lower panel) (1:1000). Secondary antibodies were HRP-coupled anti-mouse IgGs (1:10000).

The possibility has to be considered that only assembled viral particles would be transported within the Golgi and thus, only a small proportion of glycoproteins would be processed. Therefore, the glycoproteins within assembled viral particles were also analyzed for complex and high-mannose oligosaccharides. Supernatants were taken from Huh7.5 cells electroporated with JC1(A4) RNA,(4.1.12, 4.2.3) and concentrated via sucrose gradient centrifugation (4.6.1). Concentrates were separated by density equilibrium centrifugation over an iodixanol (OptiPrep) gradient (4.6.2). The different fractions were divided into untreated, EndoH and PNGaseF digested samples (4.3.3) and were analyzed by immunoblot (4.3.4, 4.3.5, 4.4.1).

Figure 25 only shows fractions 3 to 6, since 5 and 6 were reported to be infectious (with a density of 1.12 and 1.16 g/ml) and 3 and 4 represent less infectious particles (1.06, 1.08 g/ml) (Jammart et al. 2013). This is additionally demonstrated by the staining of the Core protein in these fractions (lower panel), whose amount decreased in fraction 4 and 3. In line with previous results, both structural proteins shifted completely upon EndoH digest, revealing oligomannose attachments. Interestingly, looking at fraction 4, which was reported to contain fewer infectious viral particles, a slight EndoH resistant band of E2 is visible (red asterisk). The same observation was made in fraction 3 of an independent experiment. So far, the results demonstrated that not only cell associated E1 and E2, but also E1 and E2 glycoproteins in infectious assembled HCV particles are EndoH sensitive and were thus not processed in the Golgi compartments. Moreover, a weak EndoH-resistant fraction was observed in less infectious particles.

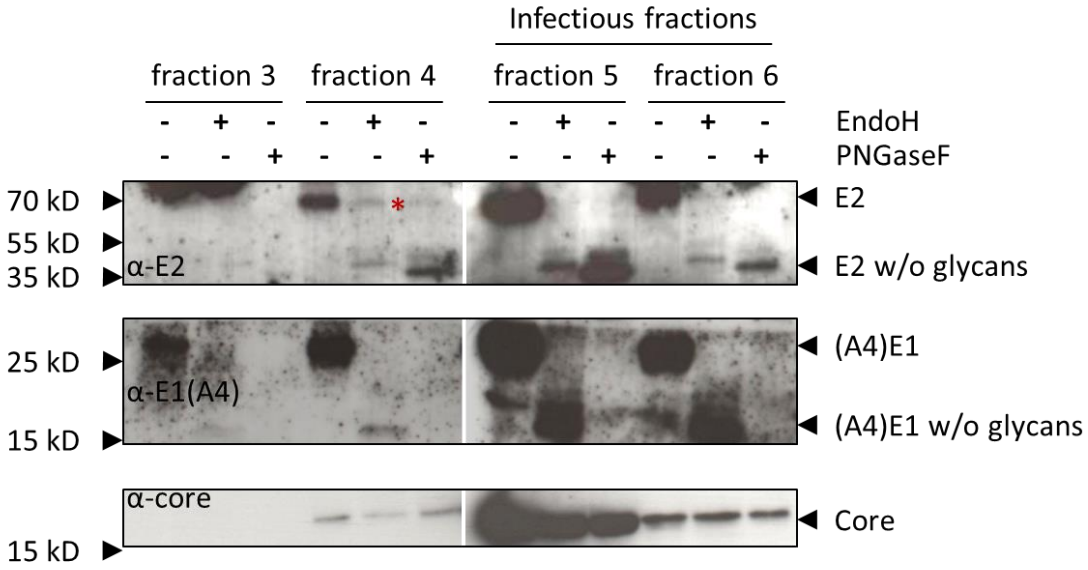


**Figure 25: HCV virion associated structural proteins reveal an oligomannose glycan structure.** 1.56x10^8 Huh7.5 cells were electroporated with JC1(A4) and cultured for 72 h. Supernatant was collected and concentrated via ultracentrifugation. The concentrate was loaded onto an iodixanol (OptiPrep) gradient (8-38% in 6% steps) and separated by equilibrium centrifugation. The fractions again were reduced and divided into untreated, EndoH (0.5 µl) and PNGaseF (0.5 µl) treated groups. Representative Western Blot of the digested proteins was stained with antibodies against E2, E1(A4) and Core. Untreated, EndoH and PNGaseF digested samples are shown next to each other for every fraction. Densities were the following: fr.3=1.06; fr.4=1.08; fr.5=1.12; fr.6=1.16 g/ml

### 5.3.3 E1-mCherry localizes to endosomal compartments

The eukaryotic cell provides several transport pathways, which can be used by viruses to trigger their cellular release. For HCV, the importance of the secretory pathway, endosomes, ESCRT and several related mechanisms have already been discussed (Coller et al. 2009, Counihan, Rawlinson, and Lindenbach 2011, Lai et al. 2010, Tamai et al. 2012). Previous studies from our lab by Banning with inhibitors for different cellular pathways indicate that blockage of the Golgi is not sufficient to inhibit HCV release, whereas endosomes are important. To further corroborate these finding, several cellular fusion proteins (described below) were coelectroporated with JC1-E1-mCherry in order to shed light on the hijacked transition route. VSV-G fused to GFP was used as a control for Golgi trafficking (kindly provided by F. Perez, Institute Curie, Paris). VSV-G is the surface protein of the vesicular stomatitis Indiana virus (VSV) within the Rhabdoviridae family. It was shown to be transported from the ER to the Golgi, in which it is processed in an EndoH-resistant fashion (Bergmann, Tokuyasu, and Singer 1981, Zilberstein et al. 1980). For the examination of different trafficking pathways, several Rab-proteins were also used (kindly provided by A. Musacchio, Max Planck Institute of Molecular Physiology, Dortmund). Rab proteins belong to the family of Ras-like GTPases. They are involved in the regulation of intracellular traffic pathways and are specific for certain compartments (Grosshans, Ortiz, and Novick 2006). To give an overview of the proteins utilized, their compartments and specific functions are shown in Table 1.

**Table 4: Cellular trafficking-specific proteins and their functions.**

| protein | compartment | function |
|---|---|---|
| EEA1 | early endosome | Effector protein of Rab5, acts as a bridge between vesicle and target (Rubino et al. 2000), interaction with t-SNARE for fusion events (McBride et al. 1999) |
| Rab5 | early endosome | Motility and heterotypic and homotypic fusion of plasma membrane-derived endocytotic vesicles and endodsomes (Sönnichsen et al. 2000) |
| Rab7 | perinuclear late endosome | Vesicle transport from endosomes to the *trans*-Golgi (Barbero, Bittova, and Pfeffer 2002) |
| Rab9 | late endosome | Vesicle transport from endosomes to the *trans*-Golgi, present on endosomes that display bidirectional microtubule-dependent motility (Barbero, Bittova, and Pfeffer 2002) |
| Rab11 | recycling endosome | Recycling through perinuclear recycling endosomes to distinct sites of the plasma membrane; polarized transport (Sönnichsen et al. 2000) |

Huh7.5 cells were coelectroporated with JC1-E1-mCherry RNA together with DNA-plasmids of the different cellular proteins (4.1.12, 4.2.3). Cells were analyzed by live cell microscopy for colocalization and cotrafficking. Consistent with previous results, no colocalization or comovement of E1-mCherry and VSV-G was observed, arguing against E1 trafficking through the Golgi (Fig. 26, Video S3). By contrast, partial colocalization of E1-mCherry with the late endosomal markers Rab7A and Rab9A was detected (Fig. 26). No codistribution or -movement was shown with the recycling endosomal protein Rab11A and only marginal comovement was observed with the early endosomal markers EEA1 (early endosome antigen 1) and Rab5A. These results further support the notion that the endosomal compartment is used by HCV for its transport to the cell membrane.

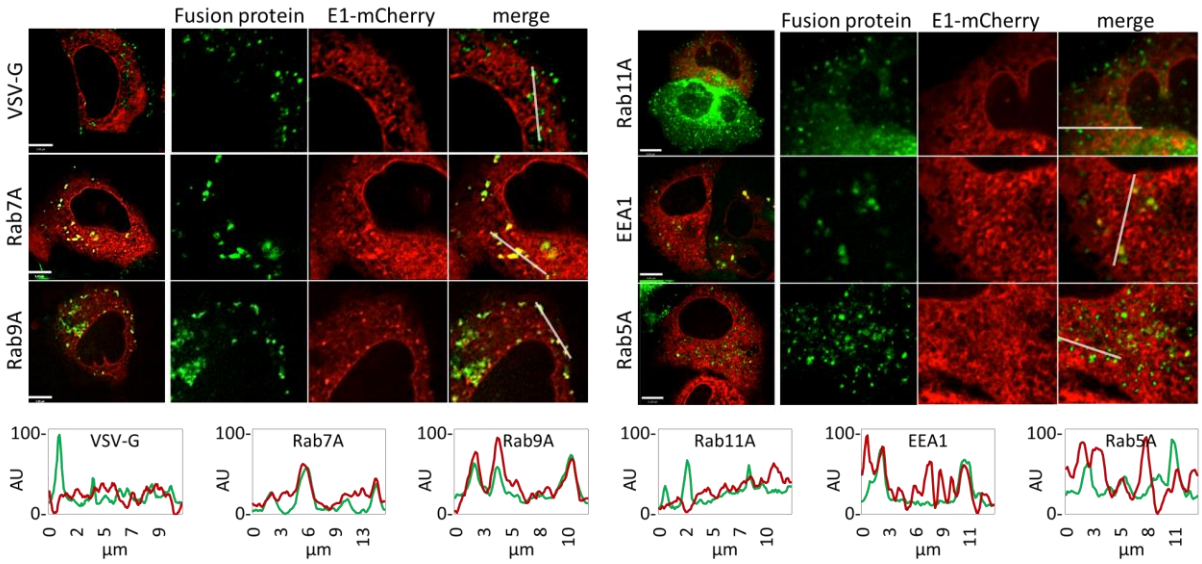

**Figure 26: HCV localizes to endosomal compartments.** Huh7.5 cells were coelectroported with JC1-E1-mCherry RNA and the DNA of the indicated fusion proteins. Representative pictures of live cell imaging 48 h pEP are shown. Bar: 11µm, and in magnification (4 µm) (B) Fluorescence profiles of lined areas are depicted. The intensity is in arbitrary fluorescence units (AU). E1-mCherry is depicted in red, the other fusion proteins in green.

### 5.3.4 E1-mCherry moves with late endosomal marker protein Rab9A

To verify the observed colocalization of JC1-E1-mCherry with endosomal marker proteins, Huh7.5 cells were coelectroporated with JC1-E1-mCherry RNA and a DNA plasmid with Rab9A-CFP (4.1.12, 4.2.3) and then analyzed by live cell microscopy (4.5.1) as well as in a FRAP study (4.5.3).

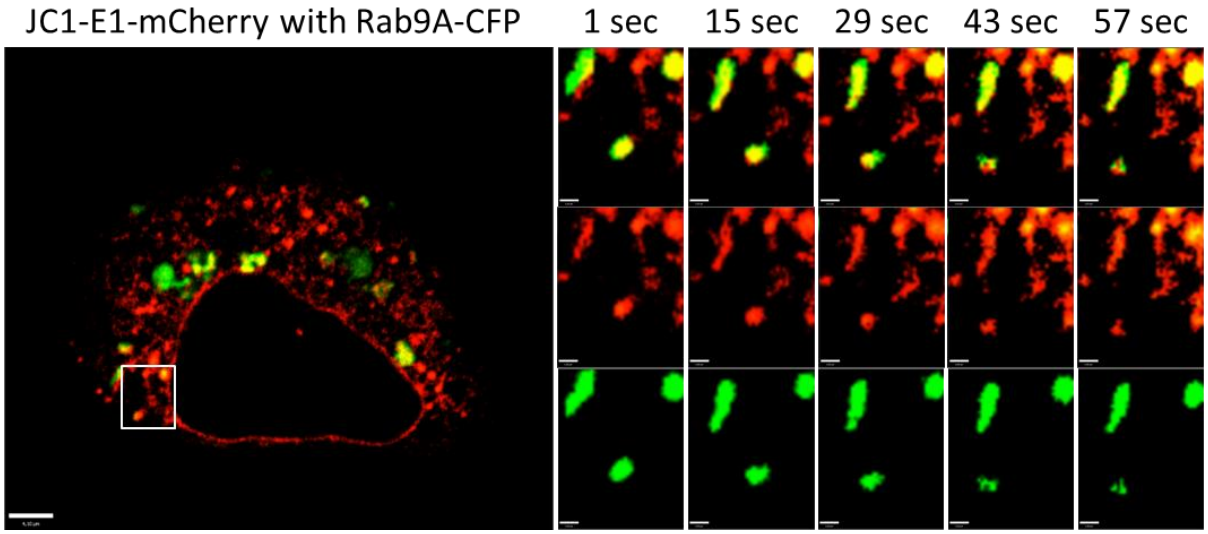


**Figure 27: E1-mCherry movement with Rab9A positive compartment.** Huh7.5 cells were coelectroported with the JC1-E1-mCherry RNA genome and a DNA plasmid of Rab9A-CFP. 53 h pEP cells were recorded in fluorescence microscopy. Slides of a video sequence over 300 sec of live-cell imaging are shown. Bar: 11µm. The white square depicts the area of magnification. Bar: 4 µm. Video S4 on supplementary CD, Bar: 3.2 µm.

A 300 second video was recorded to analyze the movement of E1-mCherry and Rab9A-GFP. Shown in Figure 27, the video sequence revealed a co-movement of E1 and Rab9A-positive compartments within a one minute timeframe (Fig. 27, Video S4).

Moreover, the discrimination of translational sites and viral trafficking, already described in chapter 5.2.5, was reconfirmed by FRAP (4.5.3). An E1-mCherry and Rab9A-positive compartment was subjected to photobleaching and then compared to an E1-mCherry-only site (Fig. 28A). FRAP for the mCherry fluorescence was conducted at second 12. Fluorescence only recovered in the E1-mCherry-only site up to 60%, whereas the transport compartment remained under 20% E1-mCherry fluorescence (Fig. 28A,B, Video S5). Only the nuclear-surrounding fluorescence recovered in this latter compartment. Taken together, these results highlight the late endosomal compartment as a

transport route for HCV release. Since the JC1-E1-mCherry virus is not infectious (refer chapter 5.1.8), it can be assumed that these findings did not occur as a result of incoming viral particles.

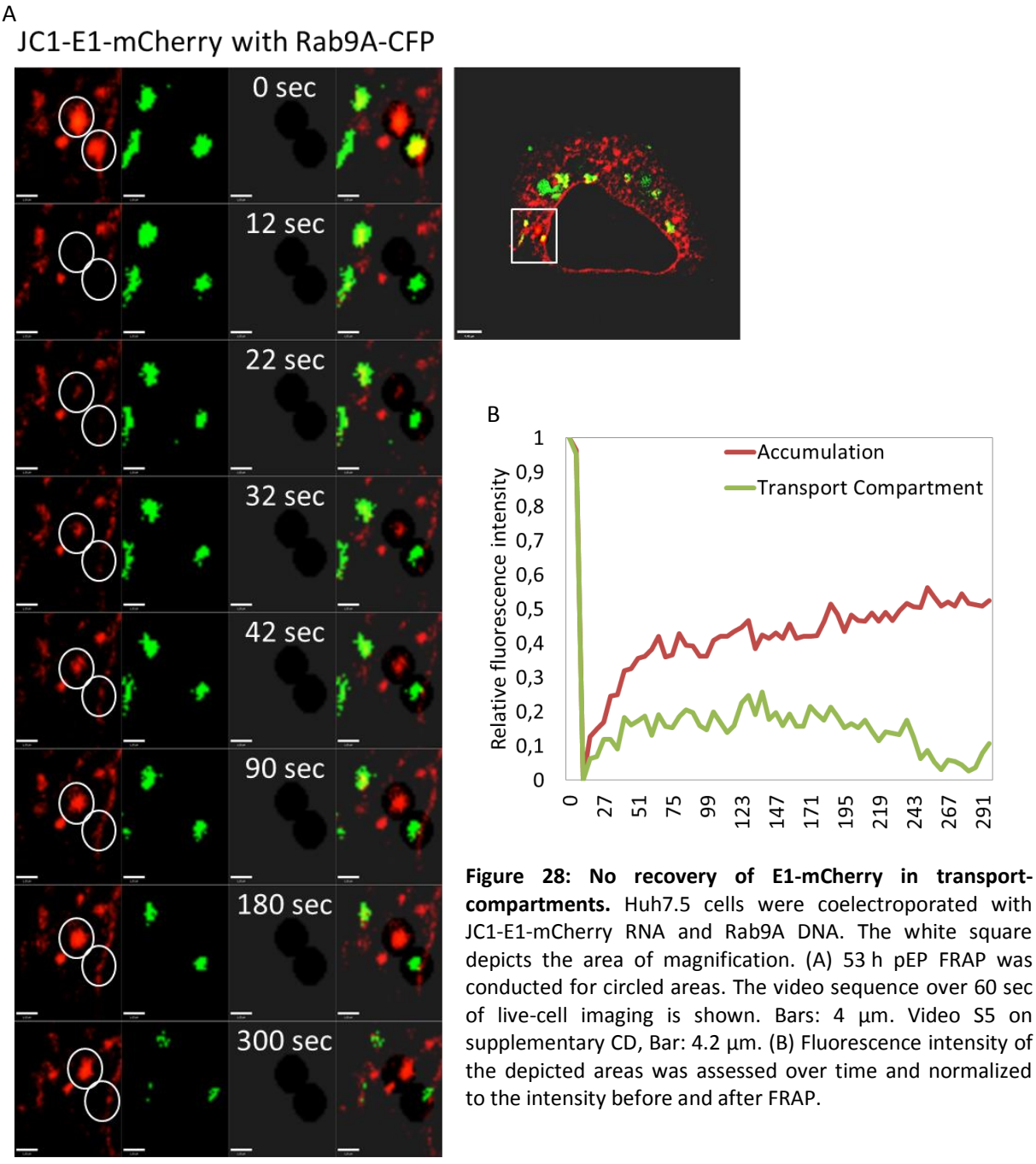


**Figure 28: No recovery of E1-mCherry in transport-compartments.** Huh7.5 cells were coelectroporated with JC1-E1-mCherry RNA and Rab9A DNA. The white square depicts the area of magnification. (A) 53 h pEP FRAP was conducted for circled areas. The video sequence over 60 sec of live-cell imaging is shown. Bars: 4 µm. Video S5 on supplementary CD, Bar: 4.2 µm. (B) Fluorescence intensity of the depicted areas was assessed over time and normalized to the intensity before and after FRAP.

In summary, E1-mCherry was neither detectable within the Golgi-compartment nor were complex glycosylations observed on the surface proteins E1 or E2 of infectious HCV. Both E1 and E2 glycoproteins are EndoH-sensitive and therefore, could not have been processed within the Golgi. Furthermore, colocalization analysis of different cellular reporter proteins with E1-mCherry indicates that HCV uses late endosomal compartments for its release.

# 6 Discussion

For this thesis, HCV genomes coding for fluorescently-labeled proteins were comprehensively characterized in order to elucidate intracellular trafficking and release of HCV. The advantage of this system is that no further treatment, fixation or staining of the cells is necessary. In other systems, like the tetracystein tag (Coller et al. 2012), cells have to be treated with a biarsenical dye and washed with 2,3-dimercapto-1-propanol, whereas in our system cells can be directly assessed in live-cell imaging. In this way, cellular stress pathways and altered protein localization can be avoided.

Studies were conducted based on the JC1-E1-mCherry genome, where the gene of the mCherry-fluorescent protein was inserted upstream of the transmembrane domain of the JC1 E1 protein (Banning, 2011). The structural protein E1 is a major player and critically involved in HCV particle assembly. In interacting with E2, E1 is incorporated into the lipid bilayer of viral particles, enveloping the capsid protein Core and the RNA. Furthermore, it plays a crucial role in virus attachment (Flint, Quinn, and Levy 2001) and probably contributes to the fusion of viral and endosomal membranes (Drummer, Boo, and Poumbourios 2007). The visualization and tracking of this structural protein allowed us to study the time-dependent organization, localization, viral morphogenesis and likely the transport of assembled viral particles.

## 6.1 HCV genomes expressing mCherry-labeled E1 are useful tools to study HCV particle assembly and release

Post introduction of the mCherry protein in the extracellular domain of E1 prior to the transmembrane region stable expression of the E1-mCherry fusion protein, as well as all other structural proteins was demonstrated, leading to the conclusion that the whole polyprotein was processed correctly. However, a faster migrating protein band appeared below E1-mCherry at around 35 kDa after staining with the E1-A4-ab. This band was not a degradation product caused by mCherry insertion, since it was also detectable at 17 kDa when untagged E1 was expressed in the JC1 backbone. Therefore, the lower E1-specific band occurs independently of the mCherry-tag. It is possible that this band is an alternatively-spliced or post-translationally processed form or may originate due to a shift within the ORF, which could still be recognized by the A4-ab. This is already known for other HCV proteins. For instance, it was reported that the Core protein is expressed in three different lengths depending on the genotype of the virus (P21, P19, P16). Synthesis of P16 was due to a single nucleotide substitution at position 9 (Argenin to Lysin) (Lo et al. 1995, Lo et al. 1994).

Furthermore, in the context of HCV JC1 expressing E1-mCherry, the intracellular distribution of the structural proteins Core and E2, as well as the non-structural protein 5A, was assessed by immunofluorescence, revealing their typical localization pattern as already described in literature (Barba et al. 1997, Duvet et al. 1998, Masaki et al. 2008, Miyanari et al. 2007, Rouillé et al. 2006). Similar to E1 from JFH1 (Rouillé et al. 2006), JC1 E1 is distributed within the cell in an E2-like pattern – namely, in perinuclear ER-like structures and this localization was not disrupted or altered by the mCherry tag. In addition, it was investigated if interaction of E1 with E2 is maintained, which might be essential for viral assembly (Dubuisson et al. 1994, Duvet et al. 1998). As validated by immunofluorescence microscopy, coimmunoprecipitation and proximity ligation assay (PLA), E1-mCherry does not disrupt the complex or the interaction with E2. Furthermore, the biophysical performance of the JC1-E1-mCherry viruses was similar to that of unlabeled viruses. In a time-course, comparable kinetics of viral accumulation in cell culture, protein production within single cells and their release into the supernatant were shown. However, electroporation efficiencies of JC1-mCherry variants were frequently lower than that of unlabeled JC1. These differences may be a consequence of RNA transcript length or base-pair composition that could lead to a different secondary or tertiary structure. Nevertheless, RNA production kinetics within the cells were stable at every time point for all expressed genomes. Additionally, efficient release of viral particles into the supernatant was detected, however slightly reduced in comparison to JC1(A4) but similar to JC1(A4)-NS5A-GFP.

Infectivity of JC1-E1-mCherry was highly attenuated, which is not surprising given that E1 plays a role in viral attachment and internalization (Drummer, Boo, and Poumbourios 2007, Flint, Quinn, and Levy 2001). Thus, introduction of mCherry into E1 could hinder the ability of E1-attachment or alter viral fusion-capability. Since HCV JC1 E1-mCherry was intended as a tool to investigate HCV morphogenesis, the altered infectivity is not an issue. In contrast, it was very important to prove proper assembly of viral particles. Thus, density gradient centrifugation was employed, revealing that all structural proteins are enriched within the same density-fraction together with viral RNA and the lipoprotein ApoE, which are known to associate with one another (Merz et al. 2011). Thus, it was shown that virus particles are readily assembled with E1-mCherry incorporated into the lipid bilayer. Moreover, these virions had the already described density of 1.11-1.14 g/mL, which is typical for infectious cell-culture-derived particles (Jammart et al. 2013, Lindenbach et al. 2005). In sum, the JC1 mCherry-labeled genomes proved to be a valuable tool for assessing questions about HCV particle assembly and release. Since the virus is not infectious in a cell-free approach, reinfection and internalization by endocytosis are most likely not compromising imaging results aiming to shed light on viral assembly and morphogenesis.

## 6.2 Expression of HCV structural and non-structural proteins is tempo-spatially organized

Immediately following HCV RNA electroporation (EP), IRES-dependent ribosomal translation is initiated. The polyprotein is cleaved into all ten HCV proteins, which are further processed in the ER. The non-structural proteins quickly start to reorganize ER-derived membranes to the membranous web, where RNA-transcription takes place in membranous cavities. It is believed that upon excess of proteins and viral positive-strand RNA, viral assembly is initiated by a protein-interaction cascade. This leads to the redistribution of replication sites, placing structural proteins and lipid droplets in close proximity with each other. Then, budding into ER membranes might be triggered and viral particles will be subsequently released.

By using the HCV JC1 E1-mCherry genome which is also labeled with NS5A GFP the dynamics of viral structural and non-structural protein expression and movement could be assessed. Early after EP, many replication/translation complexes developed within the cell, as was depicted by NS5A-GFP accumulations. In line with this, RNA and protein production showed a strong increase from 24 to 40 hours pEP. However, NS5A-GFP accumulations decreased at later time-points and RNA as well as protein production became nearly stable, reaching a plateau phase. This is in concordance with the literature, describing the RNA plateau at 24 to 48 h post infection (Keum et al. 2012). Looking at the structural proteins, it was demonstrated that E1 accumulations were built and increased over time. This observation supports the hypothesis that translation is stabilized early after EP and expanded to gain fast viral protein abundance, followed by RNA synthesis. In theory, at later time points structural proteins will be recruited together with viral RNA for the assembly of viral particles. This idea is also supported experimentally by PLA data indicating that the interactions of E1 and E2 as well as E1 and Core increased from 24 to 96 h pEP. This is in line with cumulating evidence suggesting a functional role of E1/E2 heterodimers which are found on infectious viral particles (Fraser et al. 2011, Helle et al. 2010, Vieyres et al. 2010).

Further, our data revealed that NS5A-GFP and E1-mCherry colocalize and move together 48 h pEP, implying that they are in the same cellular compartment where translation could take place. At 72 and 96 h pEP these two components separate from each other and move independently. Thus, at that time point, the E1-mCherry structural protein accumulations may represent transport vesicles containing viral particles. This is particularly plausible because distal E1-mCherry accumulations did not recover after photobleaching, which supports the idea of an E1-mCherry containing transport-compartment. In contrast, the perinuclear compartment maintains a direct communication with the ER, allowing rapid protein diffusion and transport post bleaching.

The aforementioned data together with the observation of completely assembled virions in the supernatant of HCV-expressing cells, strongly suggests that punctate E1-mCherry accumulations from 48 hour pEP onwards represent heterodimers with E2, which are incorporated into viral particles.

## 6.3 HCV might be released in a Golgi-independent manner

Different virus species differ in their budding compartment. Some well investigated viruses like HIV-1 bud from the plasma membrane of infected CD4+ T cells, others use intracellular compartments as budding platform. Rotavirus for example buds into the ER, coronaviruses utilize the ERGIC (ER-Golgi intermediate compartment) and bunyaviruses use the Golgi apparatus for their membrane envelopment. Prior to budding assembly has to take place and viral structural proteins and the genome have to accumulate in a well-organized manner, either simultaneously at the same cellular compartment or in a sequential manner. Therefore, viral proteins contain specific signals that trigger their retention in the appropriate compartment (summarized in (Griffiths and Rottier 1992, Pettersson 1991)). In case of HCV, all ten viral proteins are associated with ER-derived intracellular membranes and are enwrapped by the membranous web, which suggests that they might interact and form active complexes in this cellular compartment. In line with this, the E1/E2 heterodimer contains an ER retention signal sequence within the E2 transmembrane domain (Cocquerel et al. 1999, Cocquerel et al. 1998).

Our live-cell and colocalization studies of replicating HCV JC1 E1-mCherry with GalT-CFP revealed no E1-mCherry protein within the *trans*-Golgi compartment. By contrast, positive controls were used, i.e. the small surface protein of HBV and the Gaussia-luciferase which clearly colocalized with GalT. Both are secreted from the cell, the first being processed in an EndoH-resistant fashion (Badr et al. 2007, Patzer, Nakamura, and Yaffe 1984). As additional control, the MHCII chaperon CD74(Ii), which is located in the ER, travels through the Golgi and has an endosomal targeting sequence (Cresswell 1994), was used. As expected, with such a manifold localization in a variety of cellular compartments, a pronounced fraction of E1-mCherry colocalized with CD74(Ii). ApoE is a lipoprotein which is involved in the biogenesis and stabilization of VLDL- and analog particles. Furthermore, it is secreted from the cell to capture lipoparticles within the plasma, then reinternalized by endocytosis, separated from the lipids in lysosomes and has been described to recycle again towards the plasma membrane. But the detailed route for this recycling remain to be elucidated (recapitulated by (Fazio et al. 1999, Fazio, Linton, and Swift 2000)). ApoE was described to be associated with HCV particles and crucial for infectivity (Chang et al. 2007, Merz et al. 2011), but it is unclear whether association occurs in the ER or in a post-ER compartment and whether the direct interaction with E1 or NS5A is important in this step (Benga et al. 2010). As expected, we were able to detect E1-mCherry

accumulations colocalizing with ApoE in punctate vesicle-resembling structures, which may thus be transport compartments.

Other groups have either reported strict ER retention of the structural viral proteins (Duvet et al. 1998, Rouillé et al. 2006) or at least no further transport after the ERGIC (ER-Golgi intermediate compartment) and *cis*-Golgi (Martire et al. 2001). In contrast, different studies using the pseudo particle system (HCVpp) described the transport of HCV envelope proteins through the Golgi complex and therewith, the addition of complex glycans. To some extent due to CD81 expression leading to combined secretion in exosomes (Masciopinto et al. 2004, Op De Beeck et al. 2004, Voisset and Dubuisson 2004). These observations could be due to the utilized system in which HCV envelope proteins are incorporated in HIV-1 particles in post-Golgi compartments probably not mimicking the *in vivo* situation or the HCVcc system. Here it is important to note that HCVcc particle production takes place in ER-derived compartments and might assemble at the surface of lipid droplets (Miyanari et al. 2007). In line with this and since viral structural proteins did neither traffic nor colocalize with the Golgi, the theory was postulated that HCV might assemble in a compartment close to the ER, ERGIC or *cis*-Golgi and transport and release of assembled particles does not involve the Golgi-*cisternae*.

The established view of cellular protein release is the classical secretory route. Proteins are translated and processed within the ER. Afterwards, secretory and membrane proteins are packaged into COPII-coated vesicles and are transported to the *cis*-Golgi. The vesicle fuses and the cargo traffics through the Golgi *cisternae*, passing the *medial*- and *trans*-Golgi. *Cisternea*-specific enzymes gain access to the proteins and further modifications take place. Glycosylation is the most common alteration. Glycoproteins are therefore processed with several complex saccharides, becoming EndoH-resistant. Thereafter, they are packed again into transport vesicles and traffic to their destinations, e.g. endosomes, lysosomes or the plasma membrane (summarized in (Tveit et al. 2009)). In agreement with this, the main route for release of most flaviviruses has been shown to be the secretory pathway, where some acquire complex glycans (summarized in (Griffiths and Rottier 1992, Pettersson 1991)). Other flaviviruses, e.g. dengue virus and bovine viral diarrhea virus are transported through the Golgi apparatus (Chambers et al. 1990, Weiskircher et al. 2009, Welsch et al. 2009). Thus, the same route was postulated for HCV.

N-glycosylation plays an important role in several cellular and viral proteins. It has influence on protein conformation, functionality and antigenicity. With regard to viruses, N-glycosylation can also modulate virus-cell adhesion by interacting with members of the carbohydrate-binding lectin family. In the case of HCV and HIV-1, it has been shown that prior to infection the viral particles bind to DC-SIGN, a lectin with high affinity to high-mannose moieties (Geijtenbeek et al. 2000, Lozach et al.

2004). HCV E1 and E2 proteins are both modified by N-glycans. Depending on the cell line and the genotype, between 4 and 6 residues are processed in E1 and all 11 in E2 (Meunier et al. 1999, Zhang et al. 2004). In agreement with the fluorescence microscopy studies conducted within this thesis, several studies on intracellular E1/E2 proteins indicate that only high-mannose type oligosaccharides were attached to the surface proteins. These are usually removed and replaced by complex glycans by Golgi passage, indicating the exclusion of the Golgi during E1 and E2 trafficking (Dubuisson et al. 1994, Rouillé et al. 2006, Tani et al. 2007). Some groups, however, reported slight fractions of E2 within the ERGIC and *cis*-Golgi after transfection, which could also be due to the overexpression of proteins or the absence of virus assembly in these systems (Dubuisson et al. 1994, Martire et al. 2001). In addition, HPLC (high performance liquid chromatography) analysis of E1/E2 revealed only $Man_{(7\text{-}9)}GlcNAc_2$ oligosaccaride modifications, which indicate that the heterodimer is neither processed by *cis*-Golgi residing mannosidase trimming enzymes nor by *medial*- and *trans*-Golgi residing complex glycan adding enzymes (Duvet et al. 1998). Since these results were all obtained using artificial overexpression systems that could lead to protein mistargeting, the glycosylation pattern of E1 and E2 was reinvestigated with fully replicating and infectious HCV in Huh7.5 cells. Supporting the hypothesis of E1 and E2 processing and trafficking without involvement of the Golgi, cell associated E1 and E2 were fully sensitive to EndoH treatment.

Despite these findings, it was speculated that only small amounts of E1/E2, which are associated with assembled virions, move through the Golgi and are therefore difficult to visualize by fluorescence microscopy. In favour of this theory, Sato et al. showed complex N-linked glycans on mature virions derived from patient serum. However, these were not shown to be directly associated with E1 and E2 (Sato et al. 1993). Furthermore, particles released from the HCVpp system have complex oligosaccharides attached to E2 (Flint et al. 2004, Op De Beeck et al. 2004) and the surface expressed E2 was also found to be EndoH-resistant (Drummer, Maerz, and Poumbourios 2003). In this context it has to be noted, that in the HCVpp system the assembly site is dictated by the retroviral capsid, and therefore most likely occurs at the plasma membrane and at a post-Golgi compartment (Sandrin et al. 2005). In contrast, HCVcc particle production and assembly takes place in ER-derived compartments at the surface of lipid droplets (Miyanari et al. 2007). Thus, the sites of viral assembly might lead to incorporation of E1 and E2 glycoproteins that have either been modified through Golgi passage or are incorporated into viral particles without modification by Golgi residing enzymes. This is in agreement with the differential glycosylation pattern of E1 and E2 when produced from the HCVpp versus HCVcc system (Op De Beeck et al. 2004, Rouillé et al. 2006).

Overall, it is important to note that E1 and E2 are not generally resistant to Golgi-enzyme modifications, excluding the possibility that they can pass through the Golgi without being processed.

Within this thesis, for the first time, HCV virions released from Huh7.5 hepatocytes were purified, separated by density gradient centrifugation and biochemically investigated. E1 and E2 within the fractions associated with high infectivity were fully EndoH sensitive. At first, our data seems at odds with a single study utilizing the HCVcc system and suggesting partial EndoH resistance of E2 (Vieyres et al. 2010). Noteworthy, the authors report signal interference with BSA at the size of E2, which led to disturbance of the migration profile of E2 and complicated interpretation of the data. We never struggled with detection or avoided it automatically by gradient centrifugation prior to analysis. This problematic interpretation of E2-glycosylation could explain, at least in part, the discrepancy to our results. Interestingly, we found a slight band of EndoH-resistant E2 protein in fraction 3 and 4, which comprises non-infectious secreted viral particles. This finding suggests that marginal amounts of E2 may be processed by the Golgi-residing enzymes to complex-type glycoproteins and these are associated with low or non-infectious HCV particles. Thus, the unclear glycosylation pattern of E2 reported by Vieyres et al could also be the result of different mixed viral populations in the supernatant which have either been secreted through the Golgi or not. Overall, it is clearly shown that E1 and E2 glycoproteins associated with highly infectious HCV is EndoH sensitive and therefore most likely has not been secreted by the Golgi apparatus.

The possibility that assembled viral particles are transported through the Golgi, with their surface proteins totally shielded from the Golgi-enzymes by the associated lipoproteins cannot be fully excluded. But with respect to the cholesterol esters and neutral lipids in close proximity to a charged lipid bilayer, it is very unlikely that the whole viral particle is enwrapped by lipoparticles. At this point, it is important to mention that an inhibitor study conducted in our lab (unpublished data) using monensin A to block the intra-Golgi transport (Tartakoff, Vassalli, and Détraz 1978) had only little effect on the release of infectious HCV particles. Thus, the different lines of evidence collected in this thesis and previous work done in the lab supports the hypothesis that the Golgi is not involved in HCV particle release.

## 6.4 HCV travels through endosomal compartments

Several routes are known that can lead to the secretion of proteins. Since HCV structural proteins are absent on the plasma membrane of infected cells and are only found associated with intracellular ER-derived membranes, exocytosis - that is, budding of the PM - can be excluded for HCV release. It seems reasonable that HCV assembles at the surface of lipid droplets and subsequently buds into ER-derived membranes (Miyanari et al. 2007). However, the subsequent steps are largely unknown. The virus is associated with lipoproteins and ApoE (Merz et al. 2011), thus HCV might be transported via

the VLDL-secretory pathway. On the other hand, the cumulated data presented here argues against HCV secretion through the Golgi-compartment.

Besides the aforementioned pathways, there is the possibility of direct release, for a route utilized by cholesterol for example. Excessive intracellular cholesterol leads to cholesterol efflux which subsequently binds to ApoAI or ApoE and triggers the formation of HDL particle in the plasma. However, it is important to note that although HCV is highly associated with lipoproteins and especially with ApoE (Chang et al. 2007) and infection leads to high cholesterol within the cells (Nakamuta et al. 2009), it is unlikely that viral particles with a size of approximately 60-80 nm (Gastaminza et al. 2010, He et al. 1987, Merz et al. 2011) are capable of using the cholesterol-transporter ABCA1 in the plasma membrane to trigger its direct release.

To shed light on intracellular HCV trafficking colocalization and comovement experiments of vesicular E1-mCherry with different marker proteins for cellular pathways were employed in this thesis. Among them the Rab proteins are involved in the regulation of directed-intracellular vesicle trafficking and are compartmentalized in specific intracellular organelles, defining their identities (Grosshans, Ortiz, and Novick 2006). As an additional control, E1-mCherry association with VSV-G-GFP was assessed, which is known to be transported through the Golgi and thus acquires complex oligosaccharides (Bergmann, Tokuyasu, and Singer 1981, Zilberstein et al. 1980). In line with the results using GalT-CFP as Golgi marker, E1-mCherry neither colocalized nor trafficked together with VSV-G. The same was true for Rab11A, a marker for recycling endosomes Recycling endosomes are. known to transport their cargo back to the PM. On the other hand, marker proteins for late endosmal compartments (Rab 9A and Rab7A) showed several double positive vesicle-like structures with E1-mCherry. These compartments are described to be involved in the transport of cargo from early endosomes to lysosomes, the Golgi or retrodirected. A slight colocalization was observed for the early endosomal marker Rab5A and its effector EEA1, which are involed in cargo uptake from the PM. Based on these results, we hypothesized that after viral assembly and budding in ER-derived membranes, HCV uses endosomes for its release. The already mentioned inhibitor studies from our lab also included an inhibitor against late endosomal trafficking (U18666A), which confirmed the involvement of endosomes upon HCV release. Moreover, another experimental approach in which early endosomes were biochemically fixed strongly diminished HCV release (Banning, 2011). In concordance with our data, it was recently reported that HCV particles are associated with Tip47 (tail interacting protein), which is involved in the maturation of LDs and is involved in vesicle trafficking. Further knock-down of Rab9-positive late endosomal compartments decreased HCV release (Ploen et al. 2013).

Studies by the Lai lab are also in line with the results obtained here showing the importance of early and late endosomes for HCV release and microtubule-dependent Core motility (Lai et al. 2010). In addition, Counihan et al. showed microtubule-dependent transport of Core-positive puncta, which separated from lipid droplet sites (Counihan, Rawlinson, and Lindenbach 2011). Furthermore, exosomes and the ESCRT-complex (endosomal sorting complex required for transport) have been implicated in HCV release (Ariumi et al. 2011, Corless et al. 2010, Tamai et al. 2012). The ESCRT is an intracellular protein sorting machinery that mediates vesicle formation (e.g. late endosomes and multi vesicular buddies), vesicular transport and their attachment to the plasma membrane, thereby mediating exocytosis via SNARE (soluble N-ethylmaleimide-sensitive fusion protein (NSF) attachment protein receptors)-mediated membrane fusion. Moreover, it is involved in vesicle transfer from the Golgi to the PM (Brown and Pfeffer 2010, Hsu et al. 2004, Liu and Parpura 2010, van Niel et al. 2006). Exosomes were further described to mediate virus particle-independent propagation of HCV RNA together with Core protein to establish a full infection of inoculated cells (Ramakrishnaiah et al. 2013).

In contrast to the data of this thesis and the findings from other groups described above, a large siRNA screen combining intra- and extracellular virus infectivity with live-cell imaging provided evidence that a sub-population of TC-labeled Core travels through the classical secretory pathway. Therein, Golgi-specific proteins, some from the TGN and others from recycling endosomes, were described as important factors and confirmed by either immunofluorescence or live cell imaging (Coller et al. 2012). Intriguingly, Core was present in Rab11a vesicles and silencing of Rab11a lead to a partial colocalization of Core with Golgi markers. Since no assessment of Core in these compartments with E1 and/or E2 was done it remains completely unclear, if the described accumulations represent pre- or post-assembly compartments. And it could well be that Core is trafficking through the Golgi before it is redirected to lipid droplets for assembly. In addition, it appears obvious that some components important for HCV budding, transport and secretion, like VLDLs, associated lipids, ApoE and other influencing factors, might require transport through the secretory pathway. For example, the sphingolipid synthesis mediated by the ceramide transfer protein (CERT) and the oxysterol-binding protein (OSBP) takes place within the Golgi (Amako, Syed, and Siddiqui 2011). Therefore, the knock-down of single components important for Golgi-function may lead to an overall loss of factors involved in HCV release. More recent studies in the HCVcc system have suggested a critical role of PI4KIIIα and its interaction with NS5A in the generation of an ER-pool of PI4P (phosphatidylinositol 4-phosphate), which is crucial for membrane remodeling and replication (Reiss et al. 2011, Tai and Salloum 2011). PI4KIIIα normally localizes in the Golgi and is involved in secretory functions by recruiting different effector proteins like CERT and OSBP that are important for sphingolipid synthesis (D'Angelo et al. 2008). Additional studies have shown that both

PI4P depletion specifically from the TGN and PI4KIIIα knock-down did not affect replication, but rather, decreased HCV secretion. Instead, intracellularly-assembled viral particles increased. These observations could be due to the aforementioned side effects of depleting Golgi function. But at the same time, these studies demonstrated that a PI4P interaction partner, the GOLPH3, is important for HCV release by utilizing a silencing approach. The protein interacts with myosin MYO18A that binds to F-actin and therewith connects the Golgi to the actin network. This leads to the maintenance of the tensile force on the Golgi required for vesicle budding. The authors stated that this supports the theory of a secretory pathway for HCV release (Bishé et al. 2012, Bishé, Syed, and Siddiqui 2012, Reiss et al. 2013). Again, it should be mentioned that siRNA may show multiple side effects as well as Golgi depletion. But it should also be considered that after budding in the ER and transport in a Golgi-independent manner towards the PM, HCV could also fuse again with post Golgi compartments or the TGN to take advantage of its secretory machinery.

How HCV is transported to its release compartment is highly controversial. HCV proteins participate in a great variety of interactions with cellular proteins, lipids and microtubules. In this context, it is interesting to speculate that these may assist in a direct or vesicle-mediated transport. Furthermore, it has been reported that some cytoplasmic proteins like the galectin 10 are translocated by an unknown mechanism from the cytoplasm to CD63-positive storage vesicle and released by exocytosis following cellular activation (Hughes 1999). Thus, HCV may also mediate this form of envelopment.

The association of HCV with lipoproteins is an important step for viral infectivity (Chang et al. 2007). Since ApoE uses the secretory pathway for secretion but can also be internalized and recycled (Fazio et al. 1999, Fazio, Linton, and Swift 2000), it would be interesting to analyze whether the newly synthesized ApoE or exclusively the mature reinternalized form of ApoE is associated with HCV particles. In line with this, whether the ApoE interacting with NS5A within the membranous web (Benga et al. 2010) is the one to be associated with the viral particle should also be investigated. In serum, ApoE is bound to lipoproteins like HDLs, VLDLs and LDLs and is internalized by the cell via binding to HSPG, the LDLR and the LDL receptor-related protein (LRP). The complex then passes through early endosomes, late endosomes and while lipids are degraded in the lysosome, ApoE shuttles back to late endosomal compartments and is supposed to exit the cell again via TGN-derived export vesicles (Fazio et al. 1999, Fazio, Linton, and Swift 2000). Another group has theorized that ApoE binds to an inducible cellular receptor that mediates lipid transfer to ApoE and the subsequent release out of the cell in the context of cholesterol efflux (Basu, Goldstein, and Brown 1983, Smith et al. 1996). Investigations of the VLDL pathway and ApoE in HCV expressing cells may shed light on the site of VLDL and HCV-particle fusion and their shared transport pathway. Importantly, these questions could be addressed with JC1-E1-mCherry.

A highly controversial issue is the theory of an alternative secretion route, which bypasses the Golgi. The existence of such a pathway is further supported by the data presented in this thesis, since HCV might use a secretory transit route independent of the Golgi. Experiments in different cell systems have lent credence to the notion of a nonclassical secretion mechanism. After blocking the secretory route in MDCK cells, Tveit and colleagues first proved that Golgi-residing enzymes were still functional (Tveit et al. 2009). Then they observed a lower but persistent secretion of reporter proteins and proteoglycans that lack any subsequent Golgi-modifications. The same has been seen with a protein using an ER-retrieval signal, instead of inhibitor treatment. With low inhibitor concentrations, it was even possible to detect EndoH-sensitivity of apically-transported reporters, while basolateral-arriving cargos were still fully processed. Taken together, these observations lead to a theory postulating different routes for apical and basolateral sorting that segregate prior to meeting the Golgi enzymes. Till now, it was not clear whether this happens in the ER, the ERGIC or in *cis*-Golgi *cisternae* (Tveit et al. 2009). Regarding the ERGIC, evidence that it is flexible in size and function, in a bidirectional manner was shown. Vesicles budding from the ER are transported in a microtubule-dependent manner to the *cis*-Golgi or transit directly via tubulo-vesicular carriers. Therefore, the ERGIC expands upon secretion arrest or high amount of protein; moreover, it is strongly developed in professional secretory cells. It is composed of COPI, p58 (the rat homologue to ERGIC-53 receptor) and Rab1-tubular structures (summarized in (Sannerud et al. 2006)). In rat neuroendocrine cells, it was observed that ERGIC-like structures expand upon induction of neurite-like processes. The formation of tubules reaching from the ER-near region to the plasma membrane was triggered. Rab1 was found to be the only characteristic protein, originally from ERGIC. These structures also showed an association with the centrosome and direct connections with the endosomal system (Marie et al. 2008, Sannerud et al. 2006). A similar centrifugal route was found in nonpolarized rat kidney and human epithelial cells. The Rab1-containing ERGIC tubules led to the assumption that the observed nonclassical Golgi bypass has the advantage of fast plasma membrane remodeling. Moreover, it functions in cholesterol transport (Sannerud et al. 2006). Supporting data have been provided by Urbani and Simoni who independently found cholesterol to be a candidate for the nonclassical route (Urbani and Simoni 1990). Alternative pathways for trafficking from the ER and bypassing the Golgi have also been reported for other proteins, factors and a virus: for example, the Ras protein K-ras which is involved in regulating cell growth and differentiation (Apolloni et al. 2000), as well as the rotavirus. Beside its lytical release, rotavirus has been found in small smooth vesicles and could never be stained within the Golgi (Jourdan et al. 1997). Additionally, the aforementioned exosomes/multivesicular bodies were examined in this context (van Niel et al. 2006). It is also important to mention EDEM1 (ER degradation-enhancing mannosidase-like 1), a regulatory protein for ER transition of proteins that targets misfolded proteins to degradation. It is naturally turned over

by transport to late endosomes/lysosomes. But its exit out of the ER revealed an unconventional COPII-independent route, elucidating distinct export sites along ER *cisternae*, which are spatially segregated from the classical ones (Calì et al. 2008, Zuber et al. 2007).

Physiological roles of a nonsecretory route that bypasses the Golgi could be the fast transport of cargo or remodeling of membranes (Marie et al. 2008). Furthermore, there is the possibility that some proteins need to circumvent the Golgi and its enzymes to remain functional. Some post-translational modifications could interfere with the activity or the fate of certain proteins, like the inhibition of receptor tyrosin phosphatase β (RPTPβ) by glycosylation (Abbott, Matthews, and Pierce 2008). Moreover, inappropriate proteolysis could occur. Also the protein transit by itself, e.g. from ion channels or the EDEM1, may harm the Golgi-environmental pH or proteins therein by glycan cleavage. To date, only two factors were shown to be critical for this alternative transport route, the late endosomal target-SNARE syntaxin 13 that was found to trigger the bypass of the early secretory route in hamster cells (BHK, CHO) and, unexpectedly, the Golgi-protein dGRASP in Drosophila (Schotman, Karhinen, and Rabouille 2008) (summarized by (Grieve and Rabouille 2011, Tveit et al. 2009)).

It remains to be elucidated whether these pathways are transferable to the transport mechanism of HCV. Thus, HCV may bud into the ER or a post-ER compartment, where it could associate with lipoproteins and be released from this by vesicle fission. As opposed to classical export, HCV delivery mediated by Rab1 positive compartments could be targeted to endosomes. Joining with lipoparticles may also occur during vesicular delivery. Transfer of HCV particles to late and early endosomal compartments could bring the vesicles to a post-Golgi compartment, from where they use the secretory machinery, or directly in close proximity to the plasma membrane. Afterwards, the ESCRT machinery may play a role in plasma membrane attachment and fusion, triggering HCV release out of hepatocytes.

While further work must be done on the topic of HCV trafficking, this thesis has helped enlighten late stages of HCV life cycle. Overall, we conclude from our data that HCV viral particles are not transported through the Golgi. Not only did we demonstrate a lack of E1-mCherry in *trans*-Golgi compartments by microscopy, but we also proved the EndoH-sensitivity of both structural proteins E1 and E2 in released viral particles. Instead, late and early endosomal compartments were found to transport possible HCV viral particles.

Since Huh7.5 cells are partially impaired in their VLDL-pathway (Meex et al. 2011), it would be interesting to use a system with primary hepatocytes to investigate particle assembly and release with high infectious specificity. Furthermore, by combining of different tools and techniques like a

TC-Core and our E1-mCherry construct, it would be possible to discriminate between protein aggregation and viral assembly sites in live cell microscopy. Furthermore, both interplaying structural proteins could be tracked to investigate the transport route. The future may also shed light on the possible existence of an alternative secretion route. The regulators and key enzymes, cargos and mechanism have to be elucidated. This would give new targets for studying host-virus interactions and transition routes. With research techniques like advanced electron microscopy and super-resolution fluorescence microscopy, it could be possible to unravel direct ER to PM passage of groups of proteins or viral particles. The characterized JC1-E1-mCherry construct could serve as a basic module in this regard. It gives the opportunity for using advanced techniques, like stimulated emission depletion (STED) microscopy, stochastic optical reconstruction microscopy (STORM) or photoactivated localization microscopy (PALM). Therefore, a compatible photo-switchable tag, like mEOS, could be introduced instead of mCherry to gain resolutions of about 20 nm to investigate assembly sites and trafficking (Fernández-Suárez and Ting 2008, Huang, Babcock, and Zhuang 2010).

# 7 References


K. L. Abbott, R. T. Matthews, and M. Pierce. 2008. Receptor tyrosine phosphatase beta (rptpbeta) activity and signaling are attenuated by glycosylation and subsequent cell surface galectin-1 binding. *J Biol Chem* 283, no. 48: 33026-35.

H. Aizaki, K. Morikawa, M. Fukasawa, H. Hara, Y. Inoue, H. Tani, K. Saito, M. Nishijima, K. Hanada, Y. Matsuura, M. M. Lai, T. Miyamura, T. Wakita, and T. Suzuki. 2008. Critical role of virion-associated cholesterol and sphingolipid in hepatitis c virus infection. *J Virol* 82, no. 12: 5715-24.

A. Albecka, S. Belouzard, A. Op de Beeck, V. Descamps, L. Goueslain, J. Bertrand-Michel, F. Tercé, G. Duverlie, Y. Rouillé, and J. Dubuisson. 2012. Role of low-density lipoprotein receptor in the hepatitis c virus life cycle. *Hepatology* 55, no. 4: 998-1007.

H. J. Alter, P. V. Holland, A. G. Morrow, R. H. Purcell, S. M. Feinstone, and Y. Moritsugu. 1975. Clinical and serological analysis of transfusion-associated hepatitis. *Lancet* 2, no. 7940: 838-41.

H. J. Alter, R. H. Purcell, P. V. Holland, and H. Popper. 1978. Transmissible agent in non-a, non-b hepatitis. *Lancet* 1, no. 8062: 459-63.

Y. Amako, G. H. Syed, and A. Siddiqui. 2011. Protein kinase d negatively regulates hepatitis c virus secretion through phosphorylation of oxysterol-binding protein and ceramide transfer protein. *J Biol Chem* 286, no. 13: 11265-74.

P. Andre. 2002. Characterization of low- and very-low-density hepatitis c virus rna-containing particles. *HIV Clin Trials* 76, no. 14: 6919-28.

A. Andriulli, A. Mangia, A. Iacobellis, A. Ippolito, G. Leandro, and S. Zeuzem. 2008. Meta-analysis: The outcome of anti-viral therapy in hcv genotype 2 and genotype 3 infected patients with chronic hepatitis. *Aliment Pharmacol Ther* 28, no. 4: 397-404.

P. André, F. Komurian-Pradel, S. Deforges, M. Perret, J. L. Berland, M. Sodoyer, S. Pol, C. Bréchot, G. Paranhos-Baccalà, and V. Lotteau. 2002. Characterization of low- and very-low-density hepatitis c virus rna-containing particles. *J Virol* 76, no. 14: 6919-28.

A. Apolloni, I. A. Prior, M. Lindsay, R. G. Parton, and J. F. Hancock. 2000. H-ras but not k-ras traffics to the plasma membrane through the exocytic pathway. *Mol Cell Biol* 20, no. 7: 2475-87.

N. Appel, M. Zayas, S. Miller, J. Krijnse-Locker, T. Schaller, P. Friebe, S. Kallis, U. Engel, and R. Bartenschlager. 2008. Essential role of domain iii of nonstructural protein 5a for hepatitis c virus infectious particle assembly. *PLoS Pathog* 4, no. 3: e1000035.

Y. Ariumi, M. Kuroki, M. Maki, M. Ikeda, H. Dansako, T. Wakita, and N. Kato. 2011. The escrt system is required for hepatitis c virus production. *PLoS One* 6, no. 1: e14517.

C. E. Badr, J. W. Hewett, X. O. Breakefield, and B. A. Tannous. 2007. A highly sensitive assay for monitoring the secretory pathway and er stress. *PLoS One* 2, no. 6: e571.

G. Barba, F. Harper, T. Harada, M. Kohara, S. Goulinet, Y. Matsuura, G. Eder, Z. Schaff, M. J. Chapman, T. Miyamura, and C. Bréchot. 1997. Hepatitis c virus core protein shows a cytoplasmic localization and associates to cellular lipid storage droplets. *Proc Natl Acad Sci U S A* 94, no. 4: 1200-5.

P. Barbero, L. Bittova, and S. R. Pfeffer. 2002. Visualization of rab9-mediated vesicle transport from endosomes to the trans-golgi in living cells. *J Cell Biol* 156, no. 3: 511-8.

R. Bartenschlager, V. Lohmann, T. Wilkinson, and J. O. Koch. 1995. Complex formation between the ns3 serine-type proteinase of the hepatitis c virus and ns4a and its importance for polyprotein maturation. *J Virol* 69, no. 12: 7519-28.

R. Bartenschlager, F. Penin, V. Lohmann, and P. André. 2011. Assembly of infectious hepatitis c virus particles. *Trends Microbiol* 19, no. 2: 95-103.

H. Barth, E. K. Schnober, F. Zhang, R. J. Linhardt, E. Depla, B. Boson, F. L. Cosset, A. H. Patel, H. E. Blum, and T. F. Baumert. 2006. Viral and cellular determinants of the hepatitis c virus envelope-heparan sulfate interaction. *J Virol* 80, no. 21: 10579-90.

B. Bartosch, J. Dubuisson, and F. L. Cosset. 2003. Infectious hepatitis c virus pseudo-particles containing functional e1-e2 envelope protein complexes. *J Exp Med* 197, no. 5: 633-42.

S. K. Basu, J. L. Goldstein, and M. S. Brown. 1983. Independent pathways for secretion of cholesterol and apolipoprotein e by macrophages. *Science* 219, no. 4586: 871-3.

S. E. Behrens, L. Tomei, and R. De Francesco. 1996. Identification and properties of the rna-dependent rna polymerase of hepatitis c virus. *EMBO J* 15, no. 1: 12-22.

I. Benedicto, F. Molina-Jiménez, B. Bartosch, F. L. Cosset, D. Lavillette, J. Prieto, R. Moreno-Otero, A. Valenzuela-Fernández, R. Aldabe, M. López-Cabrera, and P. L. Majano. 2009. The tight junction-associated protein occludin is required for a postbinding step in hepatitis c virus entry and infection. *J Virol* 83, no. 16: 8012-20.

W. J. Benga, S. E. Krieger, M. Dimitrova, M. B. Zeisel, M. Parnot, J. Lupberger, E. Hildt, G. Luo, J. McLauchlan, T. F. Baumert, and C. Schuster. 2010. Apolipoprotein e interacts with hepatitis c virus nonstructural protein 5a and determines assembly of infectious particles. *Hepatology* 51, no. 1: 43-53.

J. E. Bergmann, K. T. Tokuyasu, and S. J. Singer. 1981. Passage of an integral membrane protein, the vesicular stomatitis virus glycoprotein, through the golgi apparatus en route to the plasma membrane. *Proc Natl Acad Sci U S A* 78, no. 3: 1746-50.

C. B. Bigger, B. Guerra, K. M. Brasky, G. Hubbard, M. R. Beard, B. A. Luxon, S. M. Lemon, and R. E. Lanford. 2004. Intrahepatic gene expression during chronic hepatitis c virus infection in chimpanzees. *J Virol* 78, no. 24: 13779-92.

H. C. Birnboim and J. Doly. 1979. A rapid alkaline extraction procedure for screening recombinant plasmid dna. *Nucleic Acids Res* 7, no. 6: 1513-23.

B. Bishé, G. H. Syed, S. J. Field, and A. Siddiqui. 2012. Role of phosphatidylinositol 4-phosphate (pi4p) and its binding protein golph3 in hepatitis c virus secretion. *J Biol Chem* 287, no. 33: 27637-47.

B. Bishé, G. Syed, and A. Siddiqui. 2012. Phosphoinositides in the hepatitis c virus life cycle. *Viruses* 4, no. 10: 2340-58.

K. D. Bissig, S. F. Wieland, P. Tran, M. Isogawa, T. T. Le, F. V. Chisari, and I. M. Verma. 2010. Human liver chimeric mice provide a model for hepatitis b and c virus infection and treatment. *J Clin Invest* 120, no. 3: 924-30.

J. Bitzegeio, D. Bankwitz, K. Hueging, S. Haid, C. Brohm, M. B. Zeisel, E. Herrmann, M. Iken, M. Ott, T. F. Baumert, and T. Pietschmann. 2010. Adaptation of hepatitis c virus to mouse cd81 permits infection of mouse cells in the absence of human entry factors. *PLoS Pathog* 6: e1000978.

E. Blanchard, S. Belouzard, L. Goueslain, T. Wakita, J. Dubuisson, C. Wychowski, and Y. Rouillé. 2006. Hepatitis c virus entry depends on clathrin-mediated endocytosis. *J Virol* 80, no. 14: 6964-72.

K. J. Blight, J. A. McKeating, and C. M. Rice. 2002. Highly permissive cell lines for subgenomic and genomic hepatitis c virus rna replication. *J Virol* 76, no. 24: 13001-14.

S. Boulant, C. Vanbelle, C. Ebel, F. Penin, and J. P. Lavergne. 2005. Hepatitis c virus core protein is a dimeric alpha-helical protein exhibiting membrane protein features. *J Virol* 79, no. 17: 11353-65.

E. D. Brenndörfer, J. Karthe, L. Frelin, P. Cebula, A. Erhardt, J. Schulte am Esch, H. Hengel, R. Bartenschlager, M. Sällberg, D. Häussinger, and J. G. Bode. 2009. Nonstructural 3/4a protease of hepatitis c virus activates epithelial growth factor-induced signal transduction by cleavage of the t-cell protein tyrosine phosphatase. *Hepatology* 49, no. 6: 1810-20.

C. L. Brimacombe, J. Grove, L. W. Meredith, K. Hu, A. J. Syder, M. V. Flores, J. M. Timpe, S. E. Krieger, T. F. Baumert, T. L. Tellinghuisen, F. Wong-Staal, P. Balfe, and J. A. McKeating. 2011. Neutralizing antibody-resistant hepatitis c virus cell-to-cell transmission. *J Virol* 85, no. 1: 596-605.

F. C. Brown and S. R. Pfeffer. 2010. An update on transport vesicle tethering. *Mol Membr Biol* 27, no. 8: 457-61.

P. D. Bryson, N. J. Cho, S. Einav, C. Lee, V. Tai, J. Bechtel, M. Sivaraja, C. Roberts, U. Schmitz, and J. S. Glenn. 2010. A small molecule inhibits hcv replication and alters ns4b's subcellular distribution. *Antiviral Res* 87, no. 1: 1-8.

J. Bukh. 2004. A critical role for the chimpanzee model in the study of hepatitis c. *Hepatology* 39, no. 6: 1469-75.

J. Bukh, R. H. Miller, and R. H. Purcell. 1995. Genetic heterogeneity of hepatitis c virus: Quasispecies and genotypes. *Semin Liver Dis* 15, no. 1: 41-63.

E. Buratti, S. Tisminetzky, M. Zotti, and F. E. Baralle. 1998. Functional analysis of the interaction between hcv 5'utr and putative subunits of eukaryotic translation initiation factor eif3. *Nucleic Acids Res* 26, no. 13: 3179-87.

P. D. Burbelo, E. J. Dubovi, P. Simmonds, J. L. Medina, J. A. Henriquez, N. Mishra, J. Wagner, R. Tokarz, J. M. Cullen, M. J. Iadarola, C. M. Rice, W. I. Lipkin, and A. Kapoor. 2012. Serology-enabled discovery of genetically diverse hepaciviruses in a new host. *J Virol* 86, no. 11: 6171-8.

Z. Cai, C. Zhang, K. S. Chang, J. Jiang, B. C. Ahn, T. Wakita, T. J. Liang, and G. Luo. 2005. Robust production of infectious hepatitis c virus (hcv) from stably hcv cdna-transfected human hepatoma cells. *J Virol* 79, no. 22: 13963-73.

T. Calì, C. Galli, S. Olivari, and M. Molinari. 2008. Segregation and rapid turnover of edem1 by an autophagy-like mechanism modulates standard erad and folding activities. *Biochem Biophys Res Commun* 371, no. 3: 405-10.

M. T. Catanese, K. Uryu, M. Kopp, T. J. Edwards, L. Andrus, W. J. Rice, M. Silvestry, R. J. Kuhn, and C. M. Rice. 2013. Ultrastructural analysis of hepatitis c virus particles. *Proc Natl Acad Sci U S A* 110, no. 23: 9505-10.

T. J. Chambers, C. S. Hahn, R. Galler, and C. M. Rice. 1990. Flavivirus genome organization, expression, and replication. *Annu Rev Microbiol* 44: 649-88.

K. S. Chang, Z. Cai, C. Zhang, G. C. Sen, B. R. Williams, and G. Luo. 2006. Replication of hepatitis c virus (hcv) rna in mouse embryonic fibroblasts: Protein kinase r (pkr)-dependent and pkr-independent mechanisms for controlling hcv rna replication and mediating interferon activities. *J Virol* 80, no. 15: 7364-74.

K. S. Chang, J. Jiang, Z. Cai, and G. Luo. 2007. Human apolipoprotein e is required for infectivity and production of hepatitis c virus in cell culture. *J Virol* 81, no. 24: 13783-93.

K. Chayama, S. Takahashi, J. Toyota, Y. Karino, K. Ikeda, H. Ishikawa, H. Watanabe, F. McPhee, E. Hughes, and H. Kumada. 2012. Dual therapy with the nonstructural protein 5a inhibitor, daclatasvir, and the nonstructural protein 3 protease inhibitor, asunaprevir, in hepatitis c virus genotype 1b-infected null responders. *Hepatology* 55, no. 3: 742-8.

A. A. Chen, D. K. Thomas, L. L. Ong, R. E. Schwartz, T. R. Golub, and S. N. Bhatia. 2011. Humanized mice with ectopic artificial liver tissues. *Proc Natl Acad Sci U S A* 108, no. 29: 11842-7.

Q. L. Choo, G. Kuo, A. J. Weiner, L. R. Overby, D. W. Bradley, and M. Houghton. 1989. Isolation of a cdna clone derived from a blood-borne non-a, non-b viral hepatitis genome. *Science* 244, no. 4902: 359-62.

L. Cocquerel, S. Duvet, J. C. Meunier, A. Pillez, R. Cacan, C. Wychowski, and J. Dubuisson. 1999. The transmembrane domain of hepatitis c virus glycoprotein e1 is a signal for static retention in the endoplasmic reticulum. *J Virol* 73, no. 4: 2641-9.

L. Cocquerel, J. C. Meunier, A. Pillez, C. Wychowski, and J. Dubuisson. 1998. A retention signal necessary and sufficient for endoplasmic reticulum localization maps to the transmembrane domain of hepatitis c virus glycoprotein e2. *J Virol* 72, no. 3: 2183-91.

L. Cocquerel, A. Op de Beeck, M. Lambot, J. Roussel, D. Delgrange, A. Pillez, C. Wychowski, F. Penin, and J. Dubuisson. 2002. Topological changes in the transmembrane domains of hepatitis c virus envelope glycoproteins. *EMBO J* 21, no. 12: 2893-902.

L. Coelmont, S. Kaptein, J. Paeshuyse, I. Vliegen, J. M. Dumont, G. Vuagniaux, and J. Neyts. 2009. Debio 025, a cyclophilin binding molecule, is highly efficient in clearing hepatitis c virus (hcv) replicon-containing cells when used alone or in combination with specifically targeted antiviral therapy for hcv (stat-c) inhibitors. *Antimicrob Agents Chemother* 53, no. 3: 967-76.

K. E. Coller, K. L. Berger, N. S. Heaton, J. D. Cooper, R. Yoon, and G. Randall. 2009. Rna interference and single particle tracking analysis of hepatitis c virus endocytosis. *PLoS Pathog* 5, no. 12: e1000702.

K. E. Coller, N. S. Heaton, K. L. Berger, J. D. Cooper, J. L. Saunders, and G. Randall. 2012. Molecular determinants and dynamics of hepatitis c virus secretion. *PLoS Pathog* 8, no. 1: e1002466.

L. Corless, C. M. Crump, S. D. Griffin, and M. Harris. 2010. Vps4 and the escrt-iii complex are required for the release of infectious hepatitis c virus particles. *J Gen Virol* 91, no. Pt 2: 362-72.

N. A. Counihan, S. M. Rawlinson, and B. D. Lindenbach. 2011. Trafficking of hepatitis c virus core protein during virus particle assembly. *PLoS Pathog* 7, no. 10: e1002302.

P. Cresswell. 1994. Assembly, transport, and function of mhc class ii molecules. *Annu Rev Immunol* 12: 259-93.

G. D'Angelo, M. Vicinanza, A. Di Campli, and M. A. De Matteis. 2008. The multiple roles of ptdins(4)p -- not just the precursor of ptdins(4,5)p2. *J Cell Sci* 121, no. Pt 12: 1955-63.

R. D'Souza, C. A. Sabin, and G. R. Foster. 2005. Insulin resistance plays a significant role in liver fibrosis in chronic hepatitis c and in the response to antiviral therapy. *Am J Gastroenterol* 100, no. 7: 1509-15.

V. L. Dao Thi, C. Granier, M. B. Zeisel, M. Guérin, J. Mancip, O. Granio, F. Penin, D. Lavillette, R. Bartenschlager, T. F. Baumert, F. L. Cosset, and M. Dreux. 2012. Characterization of hepatitis c virus particle subpopulations reveals multiple usage of the scavenger receptor bi for entry steps. *J Biol Chem* 287, no. 37: 31242-57.

T. Date, T. Kato, M. Miyamoto, Z. Zhao, K. Yasui, M. Mizokami, and T. Wakita. 2004. Genotype 2a hepatitis c virus subgenomic replicon can replicate in hepg2 and imy-n9 cells. *J Biol Chem* 279, no. 21: 22371-6.

B. de Chassey, V. Navratil, L. Tafforeau, M. S. Hiet, A. Aublin-Gex, S. Agaugué, G. Meiffren, F. Pradezynski, B. F. Faria, T. Chantier, M. Le Breton, J. Pellet, N. Davoust, P. E. Mangeot, A. Chaboud, F. Penin, Y. Jacob, P. O. Vidalain, M. Vidal, P. André, C. Rabourdin-Combe, and V. Lotteau. 2008. Hepatitis c virus infection protein network. *Mol Syst Biol* 4: 230.

J. A. den Boon and P. Ahlquist. 2010. Organelle-like membrane compartmentalization of positive-strand rna virus replication factories. *Annu Rev Microbiol* 64: 241-56.

L. Deng, T. Adachi, K. Kitayama, Y. Bungyoku, S. Kitazawa, S. Ishido, I. Shoji, and H. Hotta. 2008. Hepatitis c virus infection induces apoptosis through a bax-triggered, mitochondrion-mediated, caspase 3-dependent pathway. *J Virol* 82, no. 21: 10375-85.

D. L. Diamond, A. J. Syder, J. M. Jacobs, C. M. Sorensen, K. A. Walters, S. C. Proll, J. E. McDermott, M. A. Gritsenko, Q. Zhang, R. Zhao, T. O. Metz, D. G. Camp, K. M. Waters, R. D. Smith, C. M. Rice, and M. G. Katze. 2010. Temporal proteome and lipidome profiles reveal hepatitis c virus-associated reprogramming of hepatocellular metabolism and bioenergetics. *PLoS Pathog* 6, no. 1: e1000719.

M. Dorner, J. A. Horwitz, J. B. Robbins, W. T. Barry, Q. Feng, K. Mu, C. T. Jones, J. W. Schoggins, M. T. Catanese, D. R. Burton, M. Law, C. M. Rice, and A. Ploss. 2011. A genetically humanized mouse model for hepatitis c virus infection. *Nature* 474, no. 7350: 208-11.

E. Drucker, P. G. Alcabes, and P. A. Marx. 2001. The injection century: Massive unsterile injections and the emergence of human pathogens. *Lancet* 358, no. 9297: 1989-92.

H. E. Drummer, I. Boo, and P. Poumbourios. 2007. Mutagenesis of a conserved fusion peptide-like motif and membrane-proximal heptad-repeat region of hepatitis c virus glycoprotein e1. *J Gen Virol* 88, no. Pt 4: 1144-8.

H. E. Drummer, A. Maerz, and P. Poumbourios. 2003. Cell surface expression of functional hepatitis c virus e1 and e2 glycoproteins. *FEBS Lett* 546, no. 2-3: 385-90.

J. Dubuisson, H. H. Hsu, R. C. Cheung, H. B. Greenberg, D. G. Russell, and C. M. Rice. 1994. Formation and intracellular localization of hepatitis c virus envelope glycoprotein complexes expressed by recombinant vaccinia and sindbis viruses. *J Virol* 68, no. 10: 6147-60.

S. Duvet, L. Cocquerel, A. Pillez, R. Cacan, A. Verbert, D. Moradpour, C. Wychowski, and J. Dubuisson. 1998. Hepatitis c virus glycoprotein complex localization in the endoplasmic reticulum involves a determinant for retention and not retrieval. *J Biol Chem* 273, no. 48: 32088-95.

D. Egger, B. Wölk, R. Gosert, L. Bianchi, H. E. Blum, D. Moradpour, and K. Bienz. 2002. Expression of hepatitis c virus proteins induces distinct membrane alterations including a candidate viral replication complex. *J Virol* 76, no. 12: 5974-84.

S. Einav, M. Elazar, T. Danieli, and J. S. Glenn. 2004. A nucleotide binding motif in hepatitis c virus (hcv) ns4b mediates hcv rna replication. *J Virol* 78, no. 20: 11288-95.

S. Einav, D. Gerber, P. D. Bryson, E. H. Sklan, M. Elazar, S. J. Maerkl, J. S. Glenn, and S. R. Quake. 2008. Discovery of a hepatitis c target and its pharmacological inhibitors by microfluidic affinity analysis. *Nat Biotechnol* 26, no. 9: 1019-27.

M. J. Evans, C. M. Rice, and S. P. Goff. 2004. Phosphorylation of hepatitis c virus nonstructural protein 5a modulates its protein interactions and viral rna replication. *Proc Natl Acad Sci U S A* 101, no. 35: 13038-43.

M. J. Evans, T. von Hahn, D. M. Tscherne, A. J. Syder, M. Panis, B. Wölk, T. Hatziioannou, J. A. McKeating, P. D. Bieniasz, and C. M. Rice. 2007. Claudin-1 is a hepatitis c virus co-receptor required for a late step in entry. *Nature* 446, no. 7137: 801-5.

M. R. Fabian, N. Sonenberg, and W. Filipowicz. 2010. Regulation of mrna translation and stability by microrнas. *Annu Rev Biochem* 79: 351-79.

M. J. Farquhar, H. J. Harris, M. Diskar, S. Jones, C. J. Mee, S. U. Nielsen, C. L. Brimacombe, S. Molina, G. L. Toms, P. Maurel, J. Howl, F. W. Herberg, S. C. van Ijzendoorn, P. Balfe, and J. A. McKeating. 2008. Protein kinase a-dependent step(s) in hepatitis c virus entry and infectivity. *J Virol* 82, no. 17: 8797-811.

M. J. Farquhar, K. Hu, H. J. Harris, C. Davis, C. L. Brimacombe, S. J. Fletcher, T. F. Baumert, J. Z. Rappoport, P. Balfe, and J. A. McKeating. 2012. Hepatitis c virus induces cd81 and claudin-1 endocytosis. *J Virol* 86, no. 8: 4305-16.

S. Fazio, M. F. Linton, A. H. Hasty, and L. L. Swift. 1999. Recycling of apolipoprotein e in mouse liver. *J Biol Chem* 274, no. 12: 8247-53.

S. Fazio, M. F. Linton, and L. L. Swift. 2000. The cell biology and physiologic relevance of apoe recycling. *Trends Cardiovasc Med* 10, no. 1: 23-30.

S. M. Feinstone, A. Z. Kapikian, R. H. Purcell, H. J. Alter, and P. V. Holland. 1975. Transfusion-associated hepatitis not due to viral hepatitis type a or b. *N Engl J Med* 292, no. 15: 767-70.

M. Fernández-Suárez and A. Y. Ting. 2008. Fluorescent probes for super-resolution imaging in living cells. *Nat Rev Mol Cell Biol* 9, no. 12: 929-43.

E. Ferrari, Z. He, R. E. Palermo, and H. C. Huang. 2008. Hepatitis c virus ns5b polymerase exhibits distinct nucleotide requirements for initiation and elongation. *J Biol Chem* 283, no. 49: 33893-901.

N. F. Fletcher, G. K. Wilson, J. Murray, K. Hu, A. Lewis, G. M. Reynolds, Z. Stamataki, L. W. Meredith, I. A. Rowe, G. Luo, M. A. Lopez-Ramirez, T. F. Baumert, B. Weksler, P. O. Couraud, K. S. Kim, I. A. Romero, C. Jopling, S. Morgello, P. Balfe, and J. A. McKeating. 2012. Hepatitis c virus infects the endothelial cells of the blood-brain barrier. *Gastroenterology* 142, no. 3: 634-43.e6.

M. Flint, C. Logvinoff, C. M. Rice, and J. A. McKeating. 2004. Characterization of infectious retroviral pseudotype particles bearing hepatitis c virus glycoproteins. *J Virol* 78, no. 13: 6875-82.

M. Flint, E. R. Quinn, and S. Levy. 2001. In search of hepatitis c virus receptor(s). *Clin Liver Dis* 5, no. 4: 873-93.

H. Fontaine and S. Pol. 2011. Antiviral activity of telaprevir and boceprevir for the treatment of hepatitis c virus infection in treatment-experienced patients. *Clin Res Hepatol Gastroenterol* 35 Suppl 2: S59-63.

J. Fraser, I. Boo, P. Poumbourios, and H. E. Drummer. 2011. Hepatitis c virus (hcv) envelope glycoproteins e1 and e2 contain reduced cysteine residues essential for virus entry. *J Biol Chem* 286, no. 37: 31984-92.

P. Friebe and R. Bartenschlager. 2002. Genetic analysis of sequences in the 3' nontranslated region of hepatitis c virus that are important for rna replication. *J Virol* 76, no. 11: 5326-38.

P. Friebe, J. Boudet, J. P. Simorre, and R. Bartenschlager. 2005. Kissing-loop interaction in the 3' end of the hepatitis c virus genome essential for rna replication. *J Virol* 79, no. 1: 380-92.

N. Fujita, R. Sugimoto, N. Ma, H. Tanaka, M. Iwasa, Y. Kobayashi, S. Kawanishi, S. Watanabe, M. Kaito, and Y. Takei. 2008. Comparison of hepatic oxidative dna damage in patients with chronic hepatitis b and c. *J Viral Hepat* 15, no. 7: 498-507.

E. J. Gane, C. A. Stedman, R. H. Hyland, X. Ding, E. Svarovskaia, W. T. Symonds, R. G. Hindes, and M. M. Berrey. 2013. Nucleotide polymerase inhibitor sofosbuvir plus ribavirin for hepatitis c. *N Engl J Med* 368, no. 1: 34-44.

L. Gao, H. Aizaki, J. W. He, and M. M. Lai. 2004. Interactions between viral nonstructural proteins and host protein hvap-33 mediate the formation of hepatitis c virus rna replication complex on lipid raft. *J Virol* 78, no. 7: 3480-8.

P. Gastaminza, K. A. Dryden, B. Boyd, M. R. Wood, M. Law, M. Yeager, and F. V. Chisari. 2010. Ultrastructural and biophysical characterization of hepatitis c virus particles produced in cell culture. *J Virol* 84, no. 21: 10999-1009.

T. B. Geijtenbeek, D. S. Kwon, R. Torensma, S. J. van Vliet, G. C. van Duijnhoven, J. Middel, I. L. Cornelissen, H. S. Nottet, V. N. KewalRamani, D. R. Littman, C. G. Figdor, and Y. van Kooyk. 2000. Dc-sign, a dendritic cell-specific hiv-1-binding protein that enhances trans-infection of t cells. *Cell* 100, no. 5: 587-97.

S. Gitto, L. Micco, F. Conti, P. Andreone, and M. Bernardi. 2009. Alcohol and viral hepatitis: A mini-review. *Dig Liver Dis* 41, no. 1: 67-70.

A. Goffard, N. Callens, B. Bartosch, C. Wychowski, F. L. Cosset, C. Montpellier, and J. Dubuisson. 2005. Role of n-linked glycans in the functions of hepatitis c virus envelope glycoproteins. *J Virol* 79, no. 13: 8400-9.

A. Goffard and J. Dubuisson. 2003. Glycosylation of hepatitis c virus envelope proteins. *Biochimie* 85, no. 3-4: 295-301.

J. Gouttenoire, F. Penin, and D. Moradpour. 2010. Hepatitis c virus nonstructural protein 4b: A journey into unexplored territory. *Rev Med Virol* 20, no. 2: 117-29.

A. G. Grieve and C. Rabouille. 2011. Golgi bypass: Skirting around the heart of classical secretion. *Cold Spring Harb Perspect Biol* 3, no. 4.

S. D. Griffin, L. P. Beales, D. S. Clarke, O. Worsfold, S. D. Evans, J. Jaeger, M. P. Harris, and D. J. Rowlands. 2003. The p7 protein of hepatitis c virus forms an ion channel that is blocked by the antiviral drug, amantadine. *FEBS Lett* 535, no. 1-3: 34-8.

G. Griffiths and P. Rottier. 1992. Cell biology of viruses that assemble along the biosynthetic pathway. *Semin Cell Biol* 3, no. 5: 367-81.

B. L. Grosshans, D. Ortiz, and P. Novick. 2006. Rabs and their effectors: Achieving specificity in membrane traffic. *Proc Natl Acad Sci U S A* 103, no. 32: 11821-7.

V. Gusarova, J. L. Brodsky, and E. A. Fisher. 2003. Apolipoprotein b100 exit from the endoplasmic reticulum (er) is copii-dependent, and its lipidation to very low density lipoprotein occurs post-er. *J Biol Chem* 278, no. 48: 48051-8.

V. Gusarova, J. Seo, M. L. Sullivan, S. C. Watkins, J. L. Brodsky, and E. A. Fisher. 2007. Golgi-associated maturation of very low density lipoproteins involves conformational changes in apolipoprotein b, but is not dependent on apolipoprotein e. *J Biol Chem* 282, no. 27: 19453-62.

N. Hagen, K. Bayer, K. Roesch, and M. Schindler. 2014. The intra viral protein interaction network of hepatitis c virus. *Mol Cell Proteomics*.

L. F. He, D. Alling, T. Popkin, M. Shapiro, H. J. Alter, and R. H. Purcell. 1987. Determining the size of non-a, non-b hepatitis virus by filtration. *J Infect Dis* 156, no. 4: 636-40.

F. Helle, G. Vieyres, L. Elkrief, C. I. Popescu, C. Wychowski, V. Descamps, S. Castelain, P. Roingeard, G. Duverlie, and J. Dubuisson. 2010. Role of n-linked glycans in the functions of hepatitis c virus envelope proteins incorporated into infectious virions. *J Virol* 84, no. 22: 11905-15.

J. I. Henke, D. Goergen, J. Zheng, Y. Song, C. G. Schüttler, C. Fehr, C. Jünemann, and M. Niepmann. 2008. Microrna-122 stimulates translation of hepatitis c virus rna. *EMBO J* 27, no. 24: 3300-10.

V. Hernandez-Gea and S. L. Friedman. 2011. Pathogenesis of liver fibrosis. *Annu Rev Pathol* 6: 425-56.

M. Hijikata, Y. K. Shimizu, H. Kato, A. Iwamoto, J. W. Shih, H. J. Alter, R. H. Purcell, and H. Yoshikura. 1993. Equilibrium centrifugation studies of hepatitis c virus: Evidence for circulating immune complexes. *J Virol* 67, no. 4: 1953-8.

K. Hikosaka, H. Noritake, W. Kimura, N. Sultana, M. T. Sharkar, Y. Tagawa, T. Uezato, Y. Kobayashi, T. Wakita, and N. Miura. 2011. Expression of human factors cd81, claudin-1, scavenger receptor, and occludin in mouse hepatocytes does not confer susceptibility to hcv entry. *Biomed Res* 32, no. 2: 143-50.

J. H. Hoofnagle. 2002. Persistent and transient replication of full-length hepatitis c virus genomes in cell culture. *Hepatology* 76, no. 8: 4008-21.

R. G. Hope and J. McLauchlan. 2000. Sequence motifs required for lipid droplet association and protein stability are unique to the hepatitis c virus core protein. *J Gen Virol* 81, no. Pt 8: 1913-25.

S. C. Hsu, D. TerBush, M. Abraham, and W. Guo. 2004. The exocyst complex in polarized exocytosis. *Int Rev Cytol* 233: 243-65.

B. Huang, H. Babcock, and X. Zhuang. 2010. Breaking the diffraction barrier: Super-resolution imaging of cells. *Cell* 143, no. 7: 1047-58.

L. Huang, J. Hwang, S. D. Sharma, M. R. Hargittai, Y. Chen, J. J. Arnold, K. D. Raney, and C. E. Cameron. 2005. Hepatitis c virus nonstructural protein 5a (ns5a) is an rna-binding protein. *J Biol Chem* 280, no. 43: 36417-28.

R. C. Hughes. 1999. Secretion of the galectin family of mammalian carbohydrate-binding proteins. *Biochim Biophys Acta* 1473, no. 1: 172-85.

O. Isken, M. Baroth, C. W. Grassmann, S. Weinlich, D. H. Ostareck, A. Ostareck-Lederer, and S. E. Behrens. 2007. Nuclear factors are involved in hepatitis c virus rna replication. *RNA* 13, no. 10: 1675-92.

H. Jamil, C. H. Chu, J. K. Dickson, Y. Chen, M. Yan, S. A. Biller, R. E. Gregg, J. R. Wetterau, and D. A. Gordon. 1998. Evidence that microsomal triglyceride transfer protein is limiting in the production of apolipoprotein b-containing lipoproteins in hepatic cells. *J Lipid Res* 39, no. 7: 1448-54.

B. Jammart, M. Michelet, E. I. Pécheur, R. Parent, B. Bartosch, F. Zoulim, and D. Durantel. 2013. Very-low-density lipoprotein (vldl)-producing and hepatitis c virus-replicating hepg2 cells secrete no more lipoviroparticles than vldl-deficient huh7.5 cells. *J Virol* 87, no. 9: 5065-80.

H. L. Janssen, J. T. Brouwer, R. C. van der Mast, and S. W. Schalm. 1994. Suicide associated with alfa-interferon therapy for chronic viral hepatitis. *J Hepatol* 21, no. 2: 241-3.

H. L. Janssen, H. W. Reesink, E. J. Lawitz, S. Zeuzem, M. Rodriguez-Torres, K. Patel, A. J. van der Meer, A. K. Patick, A. Chen, Y. Zhou, R. Persson, B. D. King, S. Kauppinen, A. A. Levin, and M. R. Hodges. 2013. Treatment of hcv infection by targeting microrna. *N Engl J Med* 368, no. 18: 1685-94.

J. Jiang and G. Luo. 2009. Apolipoprotein e but not b is required for the formation of infectious hepatitis c virus particles. *J Virol* 83, no. 24: 12680-91.

C. T. Jones, M. T. Catanese, L. M. Law, S. R. Khetani, A. J. Syder, A. Ploss, T. S. Oh, J. W. Schoggins, M. R. MacDonald, S. N. Bhatia, and C. M. Rice. 2010. Real-time imaging of hepatitis c virus infection using a fluorescent cell-based reporter system. *Nat Biotechnol* 28, no. 2: 167-71.

D. M. Jones, A. M. Atoom, X. Zhang, S. Kottilil, and R. S. Russell. 2011. A genetic interaction between the core and ns3 proteins of hepatitis c virus is essential for production of infectious virus. *J Virol* 85, no. 23: 12351-61.

D. M. Jones, A. H. Patel, P. Targett-Adams, and J. McLauchlan. 2009. The hepatitis c virus ns4b protein can trans-complement viral rna replication and modulates production of infectious virus. *J Virol* 83, no. 5: 2163-77.

C. L. Jopling, M. Yi, A. M. Lancaster, S. M. Lemon, and P. Sarnow. 2005. Modulation of hepatitis c virus rna abundance by a liver-specific microrna. *Science* 309, no. 5740: 1577-81.

N. Jourdan, M. Maurice, D. Delautier, A. M. Quero, A. L. Servin, and G. Trugnan. 1997. Rotavirus is released from the apical surface of cultured human intestinal cells through nonconventional vesicular transport that bypasses the golgi apparatus. *J Virol* 71, no. 11: 8268-78.

T. Kanto, N. Hayashi, T. Takehara, H. Hagiwara, E. Mita, M. Naito, A. Kasahara, H. Fusamoto, and T. Kamada. 1994. Buoyant density of hepatitis c virus recovered from infected hosts: Two different features in sucrose equilibrium density-gradient centrifugation related to degree of liver inflammation. *Hepatology* 19, no. 2: 296-302.

A. Kapoor, P. Simmonds, G. Gerold, N. Qaisar, K. Jain, J. A. Henriquez, C. Firth, D. L. Hirschberg, C. M. Rice, S. Shields, and W. I. Lipkin. 2011. Characterization of a canine homolog of hepatitis c virus. *Proc Natl Acad Sci U S A* 108, no. 28: 11608-13.

T. Kato, T. Date, M. Miyamoto, A. Furusaka, K. Tokushige, M. Mizokami, and T. Wakita. 2003. Efficient replication of the genotype 2a hepatitis c virus subgenomic replicon. *Gastroenterology* 125, no. 6: 1808-17.

T. Kato, T. Date, A. Murayama, K. Morikawa, D. Akazawa, and T. Wakita. 2006. Cell culture and infection system for hepatitis c virus. *Nat Protoc* 1, no. 5: 2334-9.

S. J. Keum, S. M. Park, J. H. Park, J. H. Jung, E. J. Shin, and S. K. Jang. 2012. The specific infectivity of hepatitis c virus changes through its life cycle. *Virology* 433, no. 2: 462-70.

D. W. Kim, Y. Gwack, J. H. Han, and J. Choe. 1995. C-terminal domain of the hepatitis c virus ns3 protein contains an rna helicase activity. *Biochem Biophys Res Commun* 215, no. 1: 160-6.

M. Kobayashi, M. C. Bennett, T. Bercot, and I. R. Singh. 2006. Functional analysis of hepatitis c virus envelope proteins, using a cell-cell fusion assay. *J Virol* 80, no. 4: 1817-25.

A. A. Kolykhalov, E. V. Agapov, K. J. Blight, K. Mihalik, S. M. Feinstone, and C. M. Rice. 1997. Transmission of hepatitis c by intrahepatic inoculation with transcribed rna. *Science* 277, no. 5325: 570-4.

A. A. Kolykhalov, K. Mihalik, S. M. Feinstone, and C. M. Rice. 2000. Hepatitis c virus-encoded enzymatic activities and conserved rna elements in the 3' nontranslated region are essential for virus replication in vivo. *J Virol* 74, no. 4: 2046-51.

G. Koutsoudakis, A. Kaul, E. Steinmann, S. Kallis, V. Lohmann, T. Pietschmann, and R. Bartenschlager. 2006. Characterization of the early steps of hepatitis c virus infection by using luciferase reporter viruses. *J Virol* 80, no. 11: 5308-20.

D. Kremsdorf and N. Brezillon. 2007. New animal models for hepatitis c viral infection and pathogenesis studies. *World J Gastroenterol* 13, no. 17: 2427-35.

S. Lagaye, H. Shen, B. Saunier, M. Nascimbeni, J. Gaston, P. Bourdoncle, L. Hannoun, P. P. Massault, A. Vallet-Pichard, V. Mallet, and S. Pol. 2012. Efficient replication of primary or culture hepatitis c virus isolates in human liver slices: A relevant ex vivo model of liver infection. *Hepatology* 56, no. 3: 861-72.

C. K. Lai, K. S. Jeng, K. Machida, and M. M. Lai. 2010. Hepatitis c virus egress and release depend on endosomal trafficking of core protein. *J Virol* 84, no. 21: 11590-8.

D. Lavanchy. 2011. Evolving epidemiology of hepatitis c virus. *Clin Microbiol Infect* 17, no. 2: 107-15.

E. Lawitz, F. F. Poordad, P. S. Pang, R. H. Hyland, X. Ding, H. Mo, W. T. Symonds, J. G. McHutchison, and F. E. Membreno. 2014. Sofosbuvir and ledipasvir fixed-dose combination with and without ribavirin in treatment-naive and previously treated patients with genotype 1 hepatitis c virus infection (lonestar): An open-label, randomised, phase 2 trial. *Lancet* 383, no. 9916: 515-23.

X. D. Li, L. Sun, R. B. Seth, G. Pineda, and Z. J. Chen. 2005. Hepatitis c virus protease ns3/4a cleaves mitochondrial antiviral signaling protein off the mitochondria to evade innate immunity. *Proc Natl Acad Sci U S A* 102, no. 49: 17717-22.

B. D. Lindenbach. 2013. Virion assembly and release. *Curr Top Microbiol Immunol* 369: 199-218.

B. D. Lindenbach, M. J. Evans, A. J. Syder, B. Wölk, T. L. Tellinghuisen, C. C. Liu, T. Maruyama, R. O. Hynes, D. R. Burton, J. A. McKeating, and C. M. Rice. 2005. Complete replication of hepatitis c virus in cell culture. *Science* 309, no. 5734: 623-6.

B. D. Lindenbach, P. Meuleman, A. Ploss, T. Vanwolleghem, A. J. Syder, J. A. McKeating, R. E. Lanford, S. M. Feinstone, M. E. Major, G. Leroux-Roels, and C. M. Rice. 2006. Cell culture-grown hepatitis c virus is infectious in vivo and can be recultured in vitro. *Proc Natl Acad Sci U S A* 103, no. 10: 3805-9.

W. Liu and V. Parpura. 2010. Snares: Could they be the answer to an energy landscape riddle in exocytosis? *ScientificWorldJournal* 10: 1258-68.

J. Llopis, J. M. McCaffery, A. Miyawaki, M. G. Farquhar, and R. Y. Tsien. 1998. Measurement of cytosolic, mitochondrial, and golgi ph in single living cells with green fluorescent proteins. *Proc Natl Acad Sci U S A* 95, no. 12: 6803-8.

S. Y. Lo, F. Masiarz, S. B. Hwang, M. M. Lai, and J. H. Ou. 1995. Differential subcellular localization of hepatitis c virus core gene products. *Virology* 213, no. 2: 455-61.

S. Y. Lo, M. Selby, M. Tong, and J. H. Ou. 1994. Comparative studies of the core gene products of two different hepatitis c virus isolates: Two alternative forms determined by a single amino acid substitution. *Virology* 199, no. 1: 124-31.

V. Lohmann, F. Körner, A. Dobierzewska, and R. Bartenschlager. 2001. Mutations in hepatitis c virus rnas conferring cell culture adaptation. *J Virol* 75, no. 3: 1437-49.

V. Lohmann, F. Körner, U. Herian, and R. Bartenschlager. 1997. Biochemical properties of hepatitis c virus ns5b rna-dependent rna polymerase and identification of amino acid sequence motifs essential for enzymatic activity. *J Virol* 71, no. 11: 8416-28.

V. Lohmann, F. Körner, J. Koch, U. Herian, L. Theilmann, and R. Bartenschlager. 1999. Replication of subgenomic hepatitis c virus rnas in a hepatoma cell line. *Science* 285, no. 5424: 110-3.

P. Y. Lozach, A. Amara, B. Bartosch, J. L. Virelizier, F. Arenzana-Seisdedos, F. L. Cosset, and R. Altmeyer. 2004. C-type lectins l-sign and dc-sign capture and transmit infectious hepatitis c virus pseudotype particles. *J Biol Chem* 279, no. 31: 32035-45.

J. Lupberger, M. B. Zeisel, F. Xiao, C. Thumann, I. Fofana, L. Zona, C. Davis, C. J. Mee, M. Turek, S. Gorke, C. Royer, B. Fischer, M. N. Zahid, D. Lavillette, J. Fresquet, F. L. Cosset, S. M. Rothenberg, T. Pietschmann, A. H. Patel, P. Pessaux, M. Doffoël, W. Raffelsberger, O. Poch, J. A. McKeating, L. Brino, and T. F. Baumert. 2011. Egfr and epha2 are host factors for hepatitis c virus entry and possible targets for antiviral therapy. *Nat Med* 17, no. 5: 589-95.

Y. Ma, M. Anantpadma, J. M. Timpe, S. Shanmugam, S. M. Singh, S. M. Lemon, and M. Yi. 2011. Hepatitis c virus ns2 protein serves as a scaffold for virus assembly by interacting with both structural and nonstructural proteins. *J Virol* 85, no. 1: 86-97.

M. P. Manns and T. von Hahn. 2013. Novel therapies for hepatitis c - one pill fits all? *Nat Rev Drug Discov* 12, no. 8: 595-610.

M. Marie, R. Sannerud, H. Avsnes Dale, and J. Saraste. 2008. Take the 'a' train: On fast tracks to the cell surface. *Cell Mol Life Sci* 65, no. 18: 2859-74.

G. Martire, A. Viola, L. Iodice, L. V. Lotti, R. Gradini, and S. Bonatti. 2001. Hepatitis c virus structural proteins reside in the endoplasmic reticulum as well as in the intermediate compartment/cis-golgi complex region of stably transfected cells. *Virology* 280, no. 2: 176-82.

T. Masaki, R. Suzuki, K. Murakami, H. Aizaki, K. Ishii, A. Murayama, T. Date, Y. Matsuura, T. Miyamura, T. Wakita, and T. Suzuki. 2008. Interaction of hepatitis c virus nonstructural protein 5a with core protein is critical for the production of infectious virus particles. *J Virol* 82, no. 16: 7964-76.

F. Masciopinto, C. Giovani, S. Campagnoli, L. Galli-Stampino, P. Colombatto, M. Brunetto, T. S. Yen, M. Houghton, P. Pileri, and S. Abrignani. 2004. Association of hepatitis c virus envelope proteins with exosomes. *Eur J Immunol* 34, no. 10: 2834-42.

B. Mazumdar, A. Banerjee, K. Meyer, and R. Ray. 2011. Hepatitis c virus e1 envelope glycoprotein interacts with apolipoproteins in facilitating entry into hepatocytes. *Hepatology* 54, no. 4: 1149-56.

H. M. McBride, V. Rybin, C. Murphy, A. Giner, R. Teasdale, and M. Zerial. 1999. Oligomeric complexes link rab5 effectors with nsf and drive membrane fusion via interactions between eea1 and syntaxin 13. *Cell* 98, no. 3: 377-86.

D. R. McGivern and S. M. Lemon. 2009. Tumor suppressors, chromosomal instability, and hepatitis c virus-associated liver cancer. *Annu Rev Pathol* 4: 399-415.

J. McLauchlan, M. K. Lemberg, G. Hope, and B. Martoglio. 2002. Intramembrane proteolysis promotes trafficking of hepatitis c virus core protein to lipid droplets. *EMBO J* 21, no. 15: 3980-8.

C. J. Mee, M. J. Farquhar, H. J. Harris, K. Hu, W. Ramma, A. Ahmed, P. Maurel, R. Bicknell, P. Balfe, and J. A. McKeating. 2010. Hepatitis c virus infection reduces hepatocellular polarity in a vascular endothelial growth factor-dependent manner. *Gastroenterology* 138, no. 3: 1134-42.

C. J. Mee, H. J. Harris, M. J. Farquhar, G. Wilson, G. Reynolds, C. Davis, S. C. van IJzendoorn, P. Balfe, and J. A. McKeating. 2009. Polarization restricts hepatitis c virus entry into hepg2 hepatoma cells. *J Virol* 83, no. 12: 6211-21.

S. J. Meex, U. Andreo, J. D. Sparks, and E. A. Fisher. 2011. Huh-7 or hepg2 cells: Which is the better model for studying human apolipoprotein-b100 assembly and secretion? *J Lipid Res* 52, no. 1: 152-8.

N. Menzel, W. Fischl, K. Hueging, D. Bankwitz, A. Frentzen, S. Haid, J. Gentzsch, L. Kaderali, R. Bartenschlager, and T. Pietschmann. 2012. Map-kinase regulated cytosolic phospholipase a2 activity is essential for production of infectious hepatitis c virus particles. *PLoS Pathog* 8, no. 7: e1002829.

D. F. Mercer, D. E. Schiller, J. F. Elliott, D. N. Douglas, C. Hao, A. Rinfret, W. R. Addison, K. P. Fischer, T. A. Churchill, J. R. Lakey, D. L. Tyrrell, and N. M. Kneteman. 2001. Hepatitis c virus replication in mice with chimeric human livers. *Nat Med* 7, no. 8: 927-33.

A. Merz, G. Long, M. S. Hiet, B. Brügger, P. Chlanda, P. Andre, F. Wieland, J. Krijnse-Locker, and R. Bartenschlager. 2011. Biochemical and morphological properties of hepatitis c virus particles and determination of their lipidome. *J Biol Chem* 286, no. 4: 3018-32.

J. C. Meunier, A. Fournillier, A. Choukhi, A. Cahour, L. Cocquerel, J. Dubuisson, and C. Wychowski. 1999. Analysis of the glycosylation sites of hepatitis c virus (hcv) glycoprotein e1 and the influence of e1 glycans on the formation of the hcv glycoprotein complex. *J Gen Virol* 80 ( Pt 4): 887-96.

J. C. Meunier, R. S. Russell, R. E. Engle, K. N. Faulk, R. H. Purcell, and S. U. Emerson. 2008. Apolipoprotein c1 association with hepatitis c virus. *J Virol* 82, no. 19: 9647-56.

E. Meylan, J. Curran, K. Hofmann, D. Moradpour, M. Binder, R. Bartenschlager, and J. Tschopp. 2005. Cardif is an adaptor protein in the rig-i antiviral pathway and is targeted by hepatitis c virus. *Nature* 437, no. 7062: 1167-72.

S. Miller and J. Krijnse-Locker. 2008. Modification of intracellular membrane structures for virus replication. *Nat Rev Microbiol* 6, no. 5: 363-74.

H. Miyamoto, H. Okamoto, K. Sato, T. Tanaka, and S. Mishiro. 1992. Extraordinarily low density of hepatitis c virus estimated by sucrose density gradient centrifugation and the polymerase chain reaction. *J Gen Virol* 73 ( Pt 3): 715-8.

Y. Miyanari, K. Atsuzawa, N. Usuda, K. Watashi, T. Hishiki, M. Zayas, R. Bartenschlager, T. Wakita, M. Hijikata, and K. Shimotohno. 2007. The lipid droplet is an important organelle for hepatitis c virus production. *Nat Cell Biol* 9, no. 9: 1089-97.

M. Monazahian, I. Böhme, S. Bonk, A. Koch, C. Scholz, S. Grethe, and R. Thomssen. 1999. Low density lipoprotein receptor as a candidate receptor for hepatitis c virus. *J Med Virol* 57, no. 3: 223-9.

D. Moradpour, V. Brass, E. Bieck, P. Friebe, R. Gosert, H. E. Blum, R. Bartenschlager, F. Penin, and V. Lohmann. 2004. Membrane association of the rna-dependent rna polymerase is essential for hepatitis c virus rna replication. *J Virol* 78, no. 23: 13278-84.

Y. Nahmias, J. Goldwasser, M. Casali, D. van Poll, T. Wakita, R. T. Chung, and M. L. Yarmush. 2008. Apolipoprotein b-dependent hepatitis c virus secretion is inhibited by the grapefruit flavonoid naringenin. *Hepatology* 47, no. 5: 1437-45.

M. Nakamuta, R. Yada, T. Fujino, M. Yada, N. Higuchi, M. Tanaka, M. Miyazaki, M. Kohjima, M. Kato, T. Yoshimoto, N. Harada, A. Taketomi, Y. Maehara, M. Koga, T. Nishinakagawa, M. Nakashima, K. Kotoh, and M. Enjoji. 2009. Changes in the expression of cholesterol metabolism-associated genes in hcv-infected liver: A novel target for therapy? *Int J Mol Med* 24, no. 6: 825-8.

C. M. Narbus, B. Israelow, M. Sourisseau, M. L. Michta, S. E. Hopcraft, G. M. Zeiner, and M. J. Evans. 2011. Hepg2 cells expressing microrna mir-122 support the entire hepatitis c virus life cycle. *J Virol* 85, no. 22: 12087-92.

P. K. Nelson, B. M. Mathers, B. Cowie, H. Hagan, D. Des Jarlais, D. Horyniak, and L. Degenhardt. 2011. Global epidemiology of hepatitis b and hepatitis c in people who inject drugs: Results of systematic reviews. *Lancet* 378, no. 9791: 571-83.

E. Ohara, N. Hiraga, M. Imamura, E. Iwao, N. Kamiya, I. Yamada, T. Kono, M. Onishi, D. Hirata, F. Mitsui, T. Kawaoka, M. Tsuge, S. Takahashi, H. Abe, C. N. Hayes, H. Ochi, C. Tateno, K. Yoshizato, S. Tanaka, and K. Chayama. 2011. Elimination of hepatitis c virus by short term ns3-4a and ns5b inhibitor combination therapy in human hepatocyte chimeric mice. *J Hepatol* 54, no. 5: 872-8.

K. Ohata, K. Hamasaki, K. Toriyama, K. Matsumoto, A. Saeki, K. Yanagi, S. Abiru, Y. Nakagawa, M. Shigeno, S. Miyazoe, T. Ichikawa, H. Ishikawa, K. Nakao, and K. Eguchi. 2003. Hepatic steatosis is a risk factor for hepatocellular carcinoma in patients with chronic hepatitis c virus infection. *Cancer* 97, no. 12: 3036-43.

D. B. Olsen, M. E. Davies, L. Handt, K. Koeplinger, N. R. Zhang, S. W. Ludmerer, D. Graham, N. Liverton, M. MacCoss, D. Hazuda, and S. S. Carroll. 2011. Sustained viral response in a hepatitis c virus-infected chimpanzee via a combination of direct-acting antiviral agents. *Antimicrob Agents Chemother* 55, no. 2: 937-9.

A. Op De Beeck, C. Voisset, B. Bartosch, Y. Ciczora, L. Cocquerel, Z. Keck, S. Foung, F. L. Cosset, and J. Dubuisson. 2004. Characterization of functional hepatitis c virus envelope glycoproteins. *J Virol* 78, no. 6: 2994-3002.

J. Patel, A. H. Patel, and J. McLauchlan. 2001. The transmembrane domain of the hepatitis c virus e2 glycoprotein is required for correct folding of the e1 glycoprotein and native complex formation. *Virology* 279, no. 1: 58-68.

E. J. Patzer, G. R. Nakamura, and A. Yaffe. 1984. Intracellular transport and secretion of hepatitis b surface antigen in mammalian cells. *J Virol* 51, no. 2: 346-53.

J. F. Perz, G. L. Armstrong, L. A. Farrington, Y. J. Hutin, and B. P. Bell. 2006. The contributions of hepatitis b virus and hepatitis c virus infections to cirrhosis and primary liver cancer worldwide. *J Hepatol* 45, no. 4: 529-38.

T. V. Pestova, I. N. Shatsky, S. P. Fletcher, R. J. Jackson, and C. U. Hellen. 1998. A prokaryotic-like mode of cytoplasmic eukaryotic ribosome binding to the initiation codon during internal translation initiation of hepatitis c and classical swine fever virus rnas. *Genes Dev* 12, no. 1: 67-83.

R. F. Pettersson. 1991. Protein localization and virus assembly at intracellular membranes. *Curr Top Microbiol Immunol* 170: 67-106.

S. Piccininni, A. Varaklioti, M. Nardelli, B. Dave, K. D. Raney, and J. E. McCarthy. 2002. Modulation of the hepatitis c virus rna-dependent rna polymerase activity by the non-structural (ns) 3 helicase and the ns4b membrane protein. *J Biol Chem* 277, no. 47: 45670-9.

T. Pietschmann, A. Kaul, G. Koutsoudakis, A. Shavinskaya, S. Kallis, E. Steinmann, K. Abid, F. Negro, M. Dreux, F. L. Cosset, and R. Bartenschlager. 2006. Construction and characterization of

infectious intragenotypic and intergenotypic hepatitis c virus chimeras. *Proc Natl Acad Sci U S A* 103, no. 19: 7408-13.

P. Pileri, Y. Uematsu, S. Campagnoli, G. Galli, F. Falugi, R. Petracca, A. J. Weiner, M. Houghton, D. Rosa, G. Grandi, and S. Abrignani. 1998. Binding of hepatitis c virus to cd81. *Science* 282, no. 5390: 938-41.

D. Ploen, M. L. Hafirassou, K. Himmelsbach, S. A. Schille, M. L. Biniossek, T. F. Baumert, C. Schuster, and E. Hildt. 2013. Tip47 is associated with the hepatitis c virus and its interaction with rab9 is required for release of viral particles. *Eur J Cell Biol* 92, no. 12: 374-82.

A. Ploss, M. J. Evans, V. A. Gaysinskaya, M. Panis, H. You, Y. P. de Jong, and C. M. Rice. 2009. Human occludin is a hepatitis c virus entry factor required for infection of mouse cells. *Nature* 457, no. 7231: 882-6.

P. Podevin, A. Carpentier, V. Pène, L. Aoudjehane, M. Carrière, S. Zaïdi, C. Hernandez, V. Calle, J. F. Méritet, O. Scatton, M. Dreux, F. L. Cosset, T. Wakita, R. Bartenschlager, S. Demignot, F. Conti, A. R. Rosenberg, and Y. Calmus. 2010. Production of infectious hepatitis c virus in primary cultures of human adult hepatocytes. *Gastroenterology* 139, no. 4: 1355-64.

C. I. Popescu, N. Callens, D. Trinel, P. Roingeard, D. Moradpour, V. Descamps, G. Duverlie, F. Penin, L. Héliot, Y. Rouillé, and J. Dubuisson. 2011. Ns2 protein of hepatitis c virus interacts with structural and non-structural proteins towards virus assembly. *PLoS Pathog* 7, no. 2: e1001278.

M. H. Powdrill, E. P. Tchesnokov, R. A. Kozak, R. S. Russell, R. Martin, E. S. Svarovskaia, H. Mo, R. D. Kouyos, and M. Götte. 2011. Contribution of a mutational bias in hepatitis c virus replication to the genetic barrier in the development of drug resistance. *Proc Natl Acad Sci U S A* 108, no. 51: 20509-13.

A. Premkumar, L. Wilson, G. D. Ewart, and P. W. Gage. 2004. Cation-selective ion channels formed by p7 of hepatitis c virus are blocked by hexamethylene amiloride. *FEBS Lett* 557, no. 1-3: 99-103.

E. M. Quezada and C. M. Kane. 2009. The hepatitis c virus ns5a stimulates ns5b during in vitro rna synthesis in a template specific manner. *Open Biochem J* 3: 39-48.

D. Quinkert, R. Bartenschlager, and V. Lohmann. 2005. Quantitative analysis of the hepatitis c virus replication complex. *J Virol* 79, no. 21: 13594-605.

V. Ramakrishnaiah, C. Thumann, I. Fofana, F. Habersetzer, Q. Pan, P. E. de Ruiter, R. Willemsen, J. A. Demmers, V. Stalin Raj, G. Jenster, J. Kwekkeboom, H. W. Tilanus, B. L. Haagmans, T. F. Baumert, and L. J. van der Laan. 2013. Exosome-mediated transmission of hepatitis c virus between human hepatoma huh7.5 cells. *Proc Natl Acad Sci U S A* 110, no. 32: 13109-13.

K. D. Raney, S. D. Sharma, I. M. Moustafa, and C. E. Cameron. 2010. Hepatitis c virus non-structural protein 3 (hcv ns3): A multifunctional antiviral target. *J Biol Chem* 285, no. 30: 22725-31.

K. R. Reddy, M. L. Shiffman, T. R. Morgan, S. Zeuzem, S. Hadziyannis, F. M. Hamzeh, T. L. Wright, and M. Fried. 2007. Impact of ribavirin dose reductions in hepatitis c virus genotype 1 patients completing peginterferon alfa-2a/ribavirin treatment. *Clin Gastroenterol Hepatol* 5, no. 1: 124-9.

S. Reigadas, M. Ventura, L. Sarih-Cottin, M. Castroviejo, S. Litvak, and T. Astier-Gin. 2001. Hcv rna-dependent rna polymerase replicates in vitro the 3' terminal region of the minus-strand viral rna more efficiently than the 3' terminal region of the plus rna. *Eur J Biochem* 268, no. 22: 5857-67.

S. Reiss, C. Harak, I. Romero-Brey, D. Radujkovic, R. Klein, A. Ruggieri, I. Rebhan, R. Bartenschlager, and V. Lohmann. 2013. The lipid kinase phosphatidylinositol-4 kinase iii alpha regulates the phosphorylation status of hepatitis c virus ns5a. *PLoS Pathog* 9, no. 5: e1003359.

S. Reiss, I. Rebhan, P. Backes, I. Romero-Brey, H. Erfle, P. Matula, L. Kaderali, M. Poenisch, H. Blankenburg, M. S. Hiet, T. Longerich, S. Diehl, F. Ramirez, T. Balla, K. Rohr, A. Kaul, S. Bühler, R. Pepperkok, T. Lengauer, M. Albrecht, R. Eils, P. Schirmacher, V. Lohmann, and R. Bartenschlager. 2011. Recruitment and activation of a lipid kinase by hepatitis c virus ns5a is

essential for integrity of the membranous replication compartment. *Cell Host Microbe* 9, no. 1: 32-45.

B. Roche and D. Samuel. 2012. Hepatitis c virus treatment pre- and post-liver transplantation. *Liver Int* 32 Suppl 1: 120-8.

O. Rocks, M. Gerauer, N. Vartak, S. Koch, Z. P. Huang, M. Pechlivanis, J. Kuhlmann, L. Brunsveld, A. Chandra, B. Ellinger, H. Waldmann, and P. I. Bastiaens. 2010. The palmitoylation machinery is a spatially organizing system for peripheral membrane proteins. *Cell* 141, no. 3: 458-71.

P. Roelandt, S. Obeid, J. Paeshuyse, J. Vanhove, A. Van Lommel, Y. Nahmias, F. Nevens, J. Neyts, and C. M. Verfaillie. 2012. Human pluripotent stem cell-derived hepatocytes support complete replication of hepatitis c virus. *J Hepatol* 57, no. 2: 246-51.

I. Romero-Brey, A. Merz, A. Chiramel, J. Y. Lee, P. Chlanda, U. Haselman, R. Santarella-Mellwig, A. Habermann, S. Hoppe, S. Kallis, P. Walther, C. Antony, J. Krijnse-Locker, and R. Bartenschlager. 2012. Three-dimensional architecture and biogenesis of membrane structures associated with hepatitis c virus replication. *PLoS Pathog* 8, no. 12: e1003056.

C. Romero-López, A. Barroso-Deljesus, A. García-Sacristán, C. Briones, and A. Berzal-Herranz. 2012. The folding of the hepatitis c virus internal ribosome entry site depends on the 3'-end of the viral genome. *Nucleic Acids Res* 40, no. 22: 11697-713.

Y. Rouillé, F. Helle, D. Delgrange, P. Roingeard, C. Voisset, E. Blanchard, S. Belouzard, J. McKeating, A. H. Patel, G. Maertens, T. Wakita, C. Wychowski, and J. Dubuisson. 2006. Subcellular localization of hepatitis c virus structural proteins in a cell culture system that efficiently replicates the virus. *J Virol* 80, no. 6: 2832-41.

M. Rubino, M. Miaczynska, R. Lippé, and M. Zerial. 2000. Selective membrane recruitment of eea1 suggests a role in directional transport of clathrin-coated vesicles to early endosomes. *J Biol Chem* 275, no. 6: 3745-8.

S. Rustaeus, P. Stillemark, K. Lindberg, D. Gordon, and S. O. Olofsson. 1998. The microsomal triglyceride transfer protein catalyzes the post-translational assembly of apolipoprotein b-100 very low density lipoprotein in mca-rh7777 cells. *J Biol Chem* 273, no. 9: 5196-203.

B. Sainz, N. Barretto, D. N. Martin, N. Hiraga, M. Imamura, S. Hussain, K. A. Marsh, X. Yu, K. Chayama, W. A. Alrefai, and S. L. Uprichard. 2012. Identification of the niemann-pick c1-like 1 cholesterol absorption receptor as a new hepatitis c virus entry factor. *Nat Med* 18, no. 2: 281-5.

B. Sainz and F. V. Chisari. 2006. Production of infectious hepatitis c virus by well-differentiated, growth-arrested human hepatoma-derived cells. *J Virol* 80, no. 20: 10253-7.

T. Saito, D. M. Owen, F. Jiang, J. Marcotrigiano, and M. Gale. 2008. Innate immunity induced by composition-dependent rig-i recognition of hepatitis c virus rna. *Nature* 454, no. 7203: 523-7.

V. Sandrin, P. Boulanger, F. Penin, C. Granier, F. L. Cosset, and B. Bartosch. 2005. Assembly of functional hepatitis c virus glycoproteins on infectious pseudoparticles occurs intracellularly and requires concomitant incorporation of e1 and e2 glycoproteins. *J Gen Virol* 86, no. Pt 12: 3189-99.

R. Sannerud, M. Marie, C. Nizak, H. A. Dale, K. Pernet-Gallay, F. Perez, B. Goud, and J. Saraste. 2006. Rab1 defines a novel pathway connecting the pre-golgi intermediate compartment with the cell periphery. *Mol Biol Cell* 17, no. 4: 1514-26.

E. Santolini, L. Pacini, C. Fipaldini, G. Migliaccio, and N. Monica. 1995. The ns2 protein of hepatitis c virus is a transmembrane polypeptide. *J Virol* 69, no. 12: 7461-71.

K. Sato, H. Okamoto, S. Aihara, Y. Hoshi, T. Tanaka, and S. Mishiro. 1993. Demonstration of sugar moiety on the surface of hepatitis c virions recovered from the circulation of infected humans. *Virology* 196, no. 1: 354-7.

Y. Sato, J. Kato, R. Takimoto, K. Takada, Y. Kawano, K. Miyanishi, M. Kobune, T. Takayama, T. Matunaga, and Y. Niitsu. 2006. Hepatitis c virus core protein promotes proliferation of human hepatoma cells through enhancement of transforming growth factor alpha expression via activation of nuclear factor-kappab. *Gut* 55, no. 12: 1801-8.

E. Scarselli, H. Ansuini, R. Cerino, R. M. Roccasecca, S. Acali, G. Filocamo, C. Traboni, A. Nicosia, R. Cortese, and A. Vitelli. 2002. The human scavenger receptor class b type i is a novel candidate receptor for the hepatitis c virus. *EMBO J* 21, no. 19: 5017-25.

T. Schaller, N. Appel, G. Koutsoudakis, S. Kallis, V. Lohmann, T. Pietschmann, and R. Bartenschlager. 2007. Analysis of hepatitis c virus superinfection exclusion by using novel fluorochrome gene-tagged viral genomes. *J Virol* 81, no. 9: 4591-603.

H. Schotman, L. Karhinen, and C. Rabouille. 2008. Dgrasp-mediated noncanonical integrin secretion is required for drosophila epithelial remodeling. *Dev Cell* 14, no. 2: 171-82.

V. Schregel, S. Jacobi, F. Penin, and N. Tautz. 2009. Hepatitis c virus ns2 is a protease stimulated by cofactor domains in ns3. *Proc Natl Acad Sci U S A* 106, no. 13: 5342-7.

R. E. Schwartz, K. Trehan, L. Andrus, T. P. Sheahan, A. Ploss, S. A. Duncan, C. M. Rice, and S. N. Bhatia. 2012. Modeling hepatitis c virus infection using human induced pluripotent stem cells. *Proc Natl Acad Sci U S A* 109, no. 7: 2544-8.

C. W. Shepard, L. Finelli, and M. J. Alter. 2005. Global epidemiology of hepatitis c virus infection. *Lancet Infect Dis* 5, no. 9: 558-67.

T. Shimakami, D. Yamane, R. K. Jangra, B. J. Kempf, C. Spaniel, D. J. Barton, and S. M. Lemon. 2012. Stabilization of hepatitis c virus rna by an ago2-mir-122 complex. *Proc Natl Acad Sci U S A* 109, no. 3: 941-6.

Y. Shirota, H. Luo, W. Qin, S. Kaneko, T. Yamashita, K. Kobayashi, and S. Murakami. 2002. Hepatitis c virus (hcv) ns5a binds rna-dependent rna polymerase (rdrp) ns5b and modulates rna-dependent rna polymerase activity. *J Biol Chem* 277, no. 13: 11149-55.

P. Simister, M. Schmitt, M. Geitmann, O. Wicht, U. H. Danielson, R. Klein, S. Bressanelli, and V. Lohmann. 2009. Structural and functional analysis of hepatitis c virus strain jfh1 polymerase. *J Virol* 83, no. 22: 11926-39.

P. Simmonds. 2013. The origin of hepatitis c virus. *Curr Top Microbiol Immunol* 369: 1-15.

P. Simmonds, E. C. Holmes, T. A. Cha, S. W. Chan, F. McOmish, B. Irvine, E. Beall, P. L. Yap, J. Kolberg, and M. S. Urdea. 1993. Classification of hepatitis c virus into six major genotypes and a series of subtypes by phylogenetic analysis of the ns-5 region. *J Gen Virol* 74 ( Pt 11): 2391-9.

D. B. Smith, J. Bukh, C. Kuiken, A. S. Muerhoff, C. M. Rice, J. T. Stapleton, and P. Simmonds. 2014. Expanded classification of hepatitis c virus into 7 genotypes and 67 subtypes: Updated criteria and genotype assignment web resource. *Hepatology* 59, no. 1: 318-27.

J. D. Smith, M. Miyata, M. Ginsberg, C. Grigaux, E. Shmookler, and A. S. Plump. 1996. Cyclic amp induces apolipoprotein e binding activity and promotes cholesterol efflux from a macrophage cell line to apolipoprotein acceptors. *J Biol Chem* 271, no. 48: 30647-55.

M. J. Sofia, D. Bao, W. Chang, J. Du, D. Nagarathnam, S. Rachakonda, P. G. Reddy, B. S. Ross, P. Wang, H. R. Zhang, S. Bansal, C. Espiritu, M. Keilman, A. M. Lam, H. M. Steuer, C. Niu, M. J. Otto, and P. A. Furman. 2010. Discovery of a β-d-2'-deoxy-2'-α-fluoro-2'-β-c-methyluridine nucleotide prodrug (psi-7977) for the treatment of hepatitis c virus. *J Med Chem* 53, no. 19: 7202-18.

K. A. Stapleford and B. D. Lindenbach. 2011. Hepatitis c virus ns2 coordinates virus particle assembly through physical interactions with the e1-e2 glycoprotein and ns3-ns4a enzyme complexes. *J Virol* 85, no. 4: 1706-17.

E. Steinmann, C. Brohm, S. Kallis, R. Bartenschlager, and T. Pietschmann. 2008. Efficient trans-encapsidation of hepatitis c virus rnas into infectious virus-like particles. *J Virol* 82, no. 14: 7034-46.

E. Steinmann, F. Penin, S. Kallis, A. H. Patel, R. Bartenschlager, and T. Pietschmann. 2007. Hepatitis c virus p7 protein is crucial for assembly and release of infectious virions. *PLoS Pathog* 3, no. 7: e103.

A. I. Su, J. P. Pezacki, L. Wodicka, A. D. Brideau, L. Supekova, R. Thimme, S. Wieland, J. Bukh, R. H. Purcell, P. G. Schultz, and F. V. Chisari. 2002. Genomic analysis of the host response to hepatitis c virus infection. *Proc Natl Acad Sci U S A* 99, no. 24: 15669-74.

M. S. Sulkowski, D. F. Gardiner, M. Rodriguez-Torres, K. R. Reddy, T. Hassanein, I. Jacobson, E. Lawitz, A. S. Lok, F. Hinestrosa, P. J. Thuluvath, H. Schwartz, D. R. Nelson, G. T. Everson, T. Eley, M.

Wind-Rotolo, S. P. Huang, M. Gao, D. Hernandez, F. McPhee, D. Sherman, R. Hindes, W. Symonds, C. Pasquinelli, D. M. Grasela, and AI444040 Study Group. 2014. Daclatasvir plus sofosbuvir for previously treated or untreated chronic hcv infection. *N Engl J Med* 370, no. 3: 211-21.

B. Sönnichsen, S. De Renzis, E. Nielsen, J. Rietdorf, and M. Zerial. 2000. Distinct membrane domains on endosomes in the recycling pathway visualized by multicolor imaging of rab4, rab5, and rab11. *J Cell Biol* 149, no. 4: 901-14.

A. W. Tai and S. Salloum. 2011. The role of the phosphatidylinositol 4-kinase pi4ka in hepatitis c virus-induced host membrane rearrangement. *PLoS One* 6, no. 10: e26300.

K. Tamai, M. Shiina, N. Tanaka, T. Nakano, A. Yamamoto, Y. Kondo, E. Kakazu, J. Inoue, K. Fukushima, K. Sano, Y. Ueno, T. Shimosegawa, and K. Sugamura. 2012. Regulation of hepatitis c virus secretion by the hrs-dependent exosomal pathway. *Virology* 422, no. 2: 377-85.

H. Tani, Y. Komoda, E. Matsuo, K. Suzuki, I. Hamamoto, T. Yamashita, K. Moriishi, K. Fujiyama, T. Kanto, N. Hayashi, A. Owsianka, A. H. Patel, M. A. Whitt, and Y. Matsuura. 2007. Replication-competent recombinant vesicular stomatitis virus encoding hepatitis c virus envelope proteins. *J Virol* 81, no. 16: 8601-12.

B. A. Tannous, D. E. Kim, J. L. Fernandez, R. Weissleder, and X. O. Breakefield. 2005. Codon-optimized gaussia luciferase cdna for mammalian gene expression in culture and in vivo. *Mol Ther* 11, no. 3: 435-43.

A. Tartakoff, P. Vassalli, and M. Détraz. 1978. Comparative studies of intracellular transport of secretory proteins. *J Cell Biol* 79, no. 3: 694-707.

P. Tedbury, S. Welbourn, A. Pause, B. King, S. Griffin, and M. Harris. 2011. The subcellular localization of the hepatitis c virus non-structural protein ns2 is regulated by an ion channel-independent function of the p7 protein. *J Gen Virol* 92, no. Pt 4: 819-30.

T. L. Tellinghuisen, K. L. Foss, and J. Treadaway. 2008. Regulation of hepatitis c virion production via phosphorylation of the ns5a protein. *PLoS Pathog* 4, no. 3: e1000032.

D. L. Thomas. 2000. Hepatitis c epidemiology. *Curr Top Microbiol Immunol* 242: 25-41.

R. Thomssen, S. Bonk, and A. Thiele. 1993. Density heterogeneities of hepatitis c virus in human sera due to the binding of beta-lipoproteins and immunoglobulins. *Med Microbiol Immunol* 182, no. 6: 329-34.

J. M. Timpe, Z. Stamataki, A. Jennings, K. Hu, M. J. Farquhar, H. J. Harris, A. Schwarz, I. Desombere, G. L. Roels, P. Balfe, and J. A. McKeating. 2008. Hepatitis c virus cell-cell transmission in hepatoma cells in the presence of neutralizing antibodies. *Hepatology* 47, no. 1: 17-24.

D. M. Tscherne, C. T. Jones, M. J. Evans, B. D. Lindenbach, J. A. McKeating, and C. M. Rice. 2006. Time- and temperature-dependent activation of hepatitis c virus for low-ph-triggered entry. *J Virol* 80, no. 4: 1734-41.

H. Tveit, L. K. Akslen, G. L. Fagereng, M. A. Tranulis, and K. Prydz. 2009. A secretory golgi bypass route to the apical surface domain of epithelial mdck cells. *Traffic* 10, no. 11: 1685-95.

L. Urbani and R. D. Simoni. 1990. Cholesterol and vesicular stomatitis virus g protein take separate routes from the endoplasmic reticulum to the plasma membrane. *J Biol Chem* 265, no. 4: 1919-23.

G. van Niel, I. Porto-Carreiro, S. Simoes, and G. Raposo. 2006. Exosomes: A common pathway for a specialized function. *J Biochem* 140, no. 1: 13-21.

C. Vandelli, F. Renzo, L. Romanò, S. Tisminetzky, M. De Palma, T. Stroffolini, E. Ventura, and A. Zanetti. 2004. Lack of evidence of sexual transmission of hepatitis c among monogamous couples: Results of a 10-year prospective follow-up study. *Am J Gastroenterol* 99, no. 5: 855-9.

B. J. Veldt, W. Chen, E. J. Heathcote, H. Wedemeyer, J. Reichen, W. P. Hofmann, R. J. de Knegt, S. Zeuzem, M. P. Manns, B. E. Hansen, S. W. Schalm, and H. L. Janssen. 2008. Increased risk of hepatocellular carcinoma among patients with hepatitis c cirrhosis and diabetes mellitus. *Hepatology* 47, no. 6: 1856-62.

G. Vieyres, X. Thomas, V. Descamps, G. Duverlie, A. H. Patel, and J. Dubuisson. 2010. Characterization of the envelope glycoproteins associated with infectious hepatitis c virus. *J Virol* 84, no. 19: 10159-68.

C. Voisset and J. Dubuisson. 2004. Functional hepatitis c virus envelope glycoproteins. *Biol Cell* 96, no. 6: 413-20.

T. Wakita, T. Pietschmann, T. Kato, T. Date, M. Miyamoto, Z. Zhao, K. Murthy, A. Habermann, H. G. Kräusslich, M. Mizokami, R. Bartenschlager, and T. J. Liang. 2005. Production of infectious hepatitis c virus in tissue culture from a cloned viral genome. *Nat Med* 11, no. 7: 791-6.

H. Wang, D. Gilham, and R. Lehner. 2007. Proteomic and lipid characterization of apolipoprotein b-free luminal lipid droplets from mouse liver microsomes: Implications for very low density lipoprotein assembly. *J Biol Chem* 282, no. 45: 33218-26.

G. Waris, A. Livolsi, V. Imbert, J. F. Peyron, and A. Siddiqui. 2003. Hepatitis c virus ns5a and subgenomic replicon activate nf-kappab via tyrosine phosphorylation of ikappabalpha and its degradation by calpain protease. *J Biol Chem* 278, no. 42: 40778-87.

M. L. Washburn, M. T. Bility, L. Zhang, G. I. Kovalev, A. Buntzman, J. A. Frelinger, W. Barry, A. Ploss, C. M. Rice, and L. Su. 2011. A humanized mouse model to study hepatitis c virus infection, immune response, and liver disease. *Gastroenterology* 140, no. 4: 1334-44.

E. Weiskircher, J. Aligo, G. Ning, and K. V. Konan. 2009. Bovine viral diarrhea virus ns4b protein is an integral membrane protein associated with golgi markers and rearranged host membranes. *Virol J* 6: 185.

K. Weissenborn, A. B. Tryc, M. Heeren, H. Worthmann, H. Pflugrad, G. Berding, M. Bokemeyer, H. L. Tillmann, and A. Goldbecker. 2009. Hepatitis c virus infection and the brain. *Metab Brain Dis* 24, no. 1: 197-210.

S. Welsch, S. Miller, I. Romero-Brey, A. Merz, C. K. Bleck, P. Walther, S. D. Fuller, C. Antony, J. Krijnse-Locker, and R. Bartenschlager. 2009. Composition and three-dimensional architecture of the dengue virus replication and assembly sites. *Cell Host Microbe* 5, no. 4: 365-75.

J. Wilkinson, M. Radkowski, and T. Laskus. 2009. Hepatitis c virus neuroinvasion: Identification of infected cells. *J Virol* 83, no. 3: 1312-9.

A. L. Wozniak, S. Griffin, D. Rowlands, M. Harris, M. Yi, S. M. Lemon, and S. A. Weinman. 2010. Intracellular proton conductance of the hepatitis c virus p7 protein and its contribution to infectious virus production. *PLoS Pathog* 6, no. 9: e1001087.

B. Wölk, D. Sansonno, H. G. Kräusslich, F. Dammacco, C. M. Rice, H. E. Blum, and D. Moradpour. 2000. Subcellular localization, stability, and trans-cleavage competence of the hepatitis c virus ns3-ns4a complex expressed in tetracycline-regulated cell lines. *J Virol* 74, no. 5: 2293-304.

M. Yanagi, R. H. Purcell, S. U. Emerson, and J. Bukh. 1999. Hepatitis c virus: An infectious molecular clone of a second major genotype (2a) and lack of viability of intertypic 1a and 2a chimeras. *Virology* 262, no. 1: 250-63.

G. Y. Yu, K. J. Lee, L. Gao, and M. M. Lai. 2006. Palmitoylation and polymerization of hepatitis c virus ns4b protein. *J Virol* 80, no. 12: 6013-23.

M. Zhang, B. Gaschen, W. Blay, B. Foley, N. Haigwood, C. Kuiken, and B. Korber. 2004. Tracking global patterns of n-linked glycosylation site variation in highly variable viral glycoproteins: Hiv, siv, and hcv envelopes and influenza hemagglutinin. *Glycobiology* 14, no. 12: 1229-46.

J. Zhong, P. Gastaminza, G. Cheng, S. Kapadia, T. Kato, D. R. Burton, S. F. Wieland, S. L. Uprichard, T. Wakita, and F. V. Chisari. 2005. Robust hepatitis c virus infection in vitro. *Proc Natl Acad Sci U S A* 102, no. 26: 9294-9.

A. Zilberstein, M. D. Snider, M. Porter, and H. F. Lodish. 1980. Mutants of vesicular stomatitis virus blocked at different stages in maturation of the viral glycoprotein. *Cell* 21, no. 2: 417-27.

C. Zuber, J. H. Cormier, B. Guhl, R. Santimaria, D. N. Hebert, and J. Roth. 2007. Edem1 reveals a quality control vesicular transport pathway out of the endoplasmic reticulum not involving the copii exit sites. *Proc Natl Acad Sci U S A* 104, no. 11: 4407-12.